FUNCTIONAL STUDIES ON THE INFLUENZA A VIRUS M2 PROTEIN

BY

FINOLA MARIA GERAGHTY

A thesis submitted in partial fulfillment of the requirements of the University of London for the degree of Doctor of Philosophy.

Division of Virology
National Institute for Medical Research
Mill Hill
London
NW7 1AA

July 1996

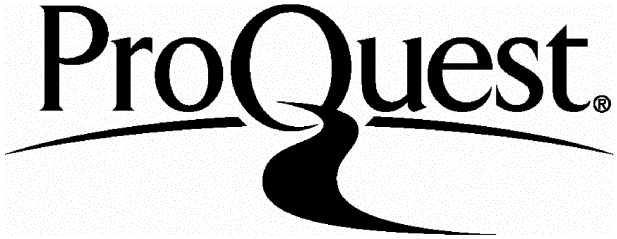

ABSTRACT

The M2 protein of influenza A viruses is a homotetramer composed of four 97 amino acid subunits which form an ion permeable channel. It plays an important role both in the process of virus uncoating and in modulating the pH of the transport pathway which is necessary for haemagglutinin (HA) maturation.

M2 was stably expressed in mouse erythroleukaemia (MEL) cells under the control of the inducible β-globin locus control region (LCR). The production of M2 peaked at 4-6 days post induction and was at a level comparable to that in virus-infected MDCK cells. The expressed M2 was structurally similar to that produced in virus-infected MDCK cells, in particular with regard to the formation and stability of the tetramer and was also phosphorylated and palmitoylated.

The function of the M2 protein expressed in MEL cells was studied using three assays, 1) co-expression of HA and M2, 2) determination of intracellular pH and 3) measurements of ion conductance. Analysis of MEL cells showed that they provided a suitable environment for the co-expression of M2 and HA. Expression of M2 resulted in a decrease in intracellular pH, indicating that the M2 protein is responsible for the decrease in cytoplasmic pH during virus infection. Voltage clamp measurements showed that the expressed M2 formed a proton-selective channel which was specifically inhibited by rimantadine. Two features of the results indicated that the current was due to a proton conductance. At zero membrane potential, both the direction and magnitude of the current were dependent on the proton gradient and secondly the reversal potential was equal to the proton equilibrium potential. Neither the reversal potential nor the amplitude of the current were influenced by the presence of other small ions, including Na^+, K^+ or Cl^-. These results are consistent with the biochemical role that M2 is perceived to play during virus infection. Structure/activity studies were also undertaken to identify residues in the transmembrane domain of the M2 protein which affected both the activation and thermal stability of the tetramer. In particular amino acid differences between the Weybridge and Rostock M2 proteins were studied.

CONTENTS

LIST OF TABLES

LIST OF FIGURES

ACKNOWLEDGEMENTS

I would like to thank Dr Alan Hay for his help, encouragement and supervision of this project. Thanks also go to Dr Michael Antoniou for his help and advice with the MEL cell expression system and to Dr's Igor Chizhmakov and David Ogden for the patch-clamping measurements.

I would also like to thank Dr Cornelia Schroeder, Dr Duncan Sparrow, Seti Grambas and Michael Bennett for technical assistance and also Jim Burt for assistance with the fluorescence microscope. Thank you also to the photo-graphics section for making the figures for this thesis.

I would also like to acknowledge Mark Prudden, Dr Graeme Esslemont, Dr Lan Bandara, Paul Donohoe and Dr Anita Skinner for their friendship and support during my time at Mill Hill, especially during the "bad times".

Finally I would like to express my gratitude to my parents for their unfailing love and support and to Arnd Hostert who gave me the support and encouragement to finish this thesis.

ABBREVIATIONS

ATP	Adenosine triphosphate
3-APTS	3-Aminopropyltriethoxysilane
BHA	Bromelain-released HA
BHK	Baby hamster kidney cells
bp	Base pairs
BSA	Bovine serum albumin
CD	Circular dichroism
cDNA	Complementary DNA
CEF	Chick embryo fibroblasts
CIP	Calf intestinal phosphatase
cRNA	Complementary RNA
CS	Calf serum
Da	Daltons
DAMP	[3-(2,4 dinitroanilino)-3-amino-N-methyl-dipropylamine]
DAR-I^{125}	Donkey anti-rabbit antibody conjugated to I^{125}
dH_2O	Distilled water
DMSO	Dimethyl sulphoxide
dNTP	Deoxy-nucleotide triphosphate
DTT	Dithiothreitol
E.coli	*Escherichia coli*
EDTA	Diaminoethanetetra-acetic acid disodium salt
EGTA	Ethylene glycol bis(β-aminoethyl ether)-N, N, N', N'- tetra acetate
ELISA	Enzyme-linked immunosorbent assay

ER	Endoplasmic reticulum
FCS	Foetal calf serum
GAM-FITC	Goat anti-mouse IgG-FITC conjugate
GAR-FITC	Goat anti-rabbit IgG-FITC conjugate
HA	Haemagglutinin
HEPES	N(2-hydroxyethyl)piperazine-N'(2-ethanesulphonic acid)
HRP	Horseradish peroxidase
IgG-FITC	Immunoglobulin G fluorescein isothiocyanate
KLH	Keyhole limpet haemocyanin
LCR	Locus control region
LMP	Low melting point
M1	Matrix protein
MDCK	Madin-Darby canine kidney cells
MEL	Mouse erythroleukaemia cells
MEM	Minimal essential medium
MES	2-(N-Morpholino)ethanesulphonic acid
m.o.i.	Multiplicity of infection
mRNA	Messenger RNA
NA	Neuraminidase
NBCS	Newborn calf serum
NMDG	N-methyl-D-glucamine
NMR	Nuclear magnetic resonance
NP	Nucleoprotein
OD	Optical density
PBS	Phosphate buffered saline
PCR	Polymerase chain reaction
p.f.u.	Plaque forming units

p.i.	Post induction
PIPES	Piperazine-N,N-bis[2-ethane-sulphonic acid]
PMSF	Phenylmethylsulphonylfluoride
RER	Rough endoplasmic reticulum
RNP	Ribonucleoprotein
RT	Room temperature
SDS	Sodium dodecyl sulphate
SDS-PAGE	SDS polyacrylamide gel electrophoresis
SFV	Semliki Forest virus
SNARF-1-AM	Seminaphthorhodafluor-1-acetoxymethyl ester
TGN	*Trans*-Golgi network
TMB	Tetramethyl benzidine dihydrochloride
vRNA	Viral RNA
WHO	World Health Organization

INTRODUCTION

INTRODUCTION

Influenza viruses are responsible for much of the respiratory disease encountered by mankind and as yet there is no vaccine available to provide long term immunity. Currently the anti-viral compound amantadine and its structural analogue rimantadine are the only effective anti-influenza prophylactic drugs. Worldwide influenza pandemics and epidemics have been responsible for considerable human morbidity and mortality, but fortunately in most individuals the disease is usually mild and it is mainly the elderly and immunocompromised who are most at risk from complications. Due to the ability of the virus to reassort, new pandemic strains have emerged, as for example in 1957 and 1968, which pose a considerable risk to the human population at large. For example the "Spanish flu" outbreak in 1918, claimed more lives than the First World War. These cases exemplify the need for an efficient method of treatment.

1.1 VIRUS CLASSIFICATION

Influenza virus is a negative strand enveloped RNA virus with a segmented genome. The group of viruses responsible for influenza collectively form a group known as Orthomyxoviruses. The viruses are divided into three types A, B and C, based on the antigenicity of their nucleoproteins (NP) and matrix (M1) proteins. Type A viruses are further classified into subtypes on the basis of antigenic differences in the haemagglutinin (HA) and neuraminidase (NA) glycoproteins. Currently fourteen HA and nine NA subtypes have been identified.

1.2 VIRION STRUCTURE

Influenza virions, except filamentous forms found in freshwater isolates, are roughly spherical in shape with a diameter of approximately 80-120nm (Figure I). The ribonucleoprotein (RNP) core is located inside the virus particle and can be visualized by disruption of the virus (Hoyle and Davies, 1961). The RNP core is composed of eight different RNA segments of negative polarity that form a complex with the arginine-rich, positively charged NP (Pons, 1975). The RNP is thought to form a double helix which then folds back on itself with a loop at one end (Schulze, 1970; Compans *et al.*, 1972; Murti *et al.*, 1988). NP also plays a part in viral RNA (vRNA) replication. Studies *in vitro* have shown that NP is required for the production of complete transcripts of the viral RNA segments during vRNA synthesis (Beaton and Krug, 1986; Shapiro and Krug 1988). Murti *et al.*, (1988) showed that there was a binding site for an RNA-dependent RNA polymerase associated with the end of each RNA segment. This enzyme is composed of three polypeptides, two of which are basic (PB1 and PB2) and one which is acidic (PA) (Horisberger, 1980).

FIGURE I: **A SCHEMATIC REPRESENTATION OF THE INFLUENZA VIRUS**

The viral core is composed of eight segments of RNA in association with NP and the three polymerase proteins, PB1, PB2 and PA. The M1 protein surrounds the RNA core and is in close association with the viral envelope. The two major viral glycoproteins HA and NA are located within the viral envelope as "spike" and "mushroom" structures respectively. Also found embedded within the viral membrane is the M2 protein.

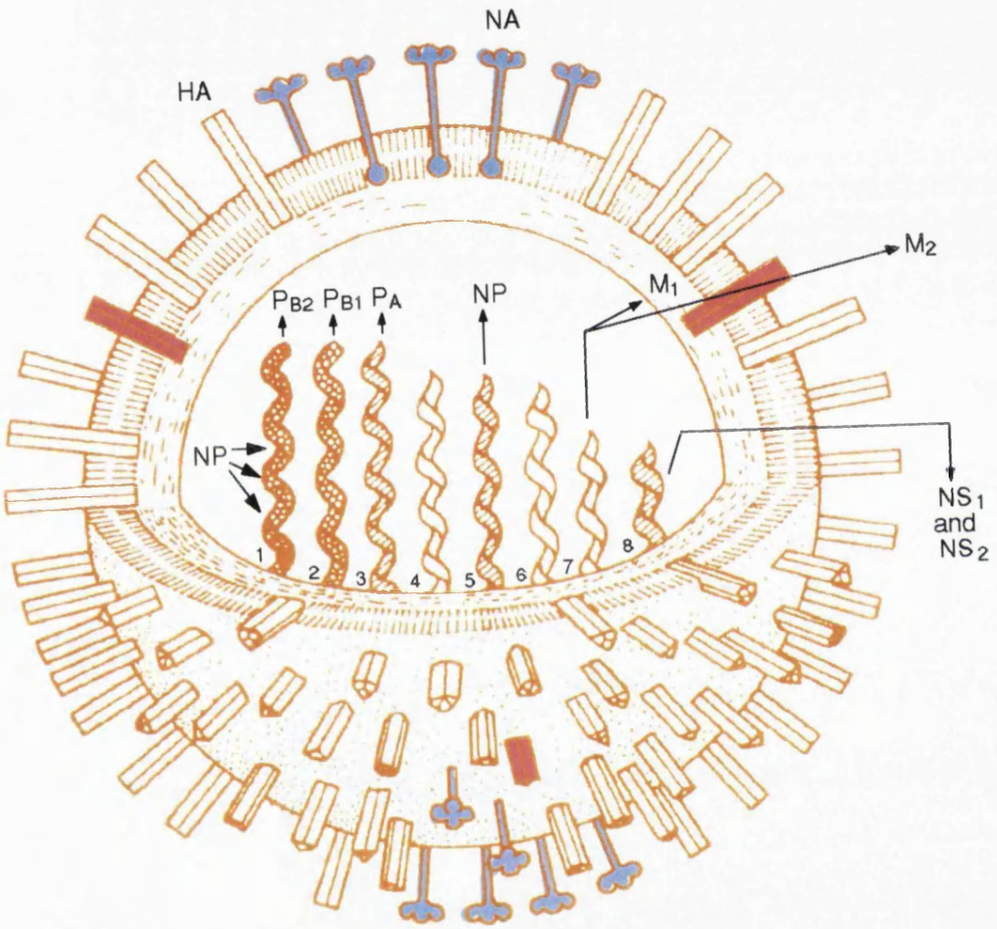
NA
HA
M2
M1
PB2 PB1 PA
NP
NP
NS1
and
NS2
1
2
3
4
5
6
7
8

The M1 protein is the most abundant protein found within the virus (Compans *et al.*, 1970; Haslam *et al.*, 1970; Skehel and Schild, 1971) and it surrounds and closely associates with the RNP core. M1 is involved in maintaining the structural integrity of the virus and can be visualized as an electron dense layer located below the lipid bilayer (Apostolov and Flewett, 1969; Compans and Dimmock, 1969). Functions of the M1 protein include a role in the regulation of transcription (Ye *et al.*, 1987; Hankins *et al.*, 1990) and nuclear-cytoplasmic transport of negative-sense vRNA segments, before their assembly into mature virus particles (Martin and Helenius, 1991b; Enami *et al.*, 1993).

The influenza virion is encapsulated in a lipid envelope derived from the infected cell. The viral envelope is composed of host cell lipids, but contains only viral proteins. Two major viral glycoproteins are embedded in the envelope, namely, HA and NA. Electron micrographs have revealed these glycoproteins to have a "spike" and "mushroom" shaped structure respectively and they are present in a ratio of approximately 5:1 (Laver and Valentine, 1969; Wrigley *et al.*, 1977). The HA glycoprotein binds to sialic acid containing receptors on the cell surface, thus allowing viral attachment and internalization of the virus particle into the host cell cytoplasm by a HA-mediated fusion event (see 1.5, pp18-19).

The HA glycoprotein is a trimeric molecule with a molecular mass of 224,640 Daltons (Da) (Wiley *et al.*, 1977; reviewed by Wiley and Skehel, 1987). Each HA monomer is synthesized as a precursor polypeptide chain, known as HA0, in the rough endoplasmic reticulum (RER). During its transport to the Golgi apparatus, the HA0 molecule is modified by glycosylation, the number of glycosylation sites varying with subtype and the signal peptide is also removed. The HA0 precursor is then cleaved to form two disulphide-linked polypeptides known as HA1 (328 residues) and HA2

(221 residues) (Wiley *et al.*, 1977). This post-translational cleavage event allows HA to undergo a pH-mediated fusion event (Wiley and Skehel, 1987) and is necessary for infectivity of the virus. However, uncleaved HA is still capable of binding to sialic acid-containing receptors (Lazarowitz *et al.*, 1973; Klenk *et al.*, 1975). Information relating to the structure of the HA-sialic acid complex obtained from X-ray crystallography data (Weis *et al.*, 1988), indicated that the sialic acid binding domain was located at the distal end of the globular head of HA and formed a pocket or depression, at the bottom of which were several conserved amino acids (Wilson *et al.*, 1981). The HA glycoprotein is also the major antigen against which neutralizing antibodies are produced (Wiley and Skehel, 1987). Accordingly, changes in the antigenic structure of this molecule may result in the emergence of new epidemic strains (see section 1.3, pp12-14).

The three dimensional structure of bromelain-released HA (BHA), determined by X-ray diffraction (Wilson *et al.*, 1981; Weis *et al.*, 1990; Watowich *et al.*, 1994), showed that HA consisted of two distinct structural regions (Figure II). A coiled coil of α-helices forming a stem domain is composed primarily of the HA2 polypeptide chain. The C-terminus of HA2 is also responsible for anchoring the HA glycoprotein into the viral or infected cell membrane. The HA1 polypeptide makes some contribution to the stem structure, but is principally involved in forming a globular head domain rich in β-pleated sheets, which contains the sialic acid binding site.

The NA glycoprotein forms a homotetramer with a mass of about 220,000 Da (Varghese *et al.*, 1983) and accounts for approximately 7% of the total viral protein. NA is responsible for the cleavage of sialic acid residues and is also subject to antigenic variation. Structural studies of the NA tetramer by X-ray diffraction have shown that each monomer is composed of a box-shaped head (100Å x 100Å x 60Å) attached to a stalk

FIGURE II: **A SCHEMATIC DIAGRAM OF THE X-31 HA MONOMER**

The HA molecule is anchored into the membrane by the C-terminus of HA2. HA1 chains are blue and HA2 chains red. The α-helical stem region, denoted by coils, supports the globular head which is composed of anti-parallel β-sheets (flat arrows). This region of the molecule contains the receptor binding domain and the five main antigenic sites. The fusion peptide of HA2 is located buried deep within the trimer. During low pH-mediated fusion this peptide is extruded.

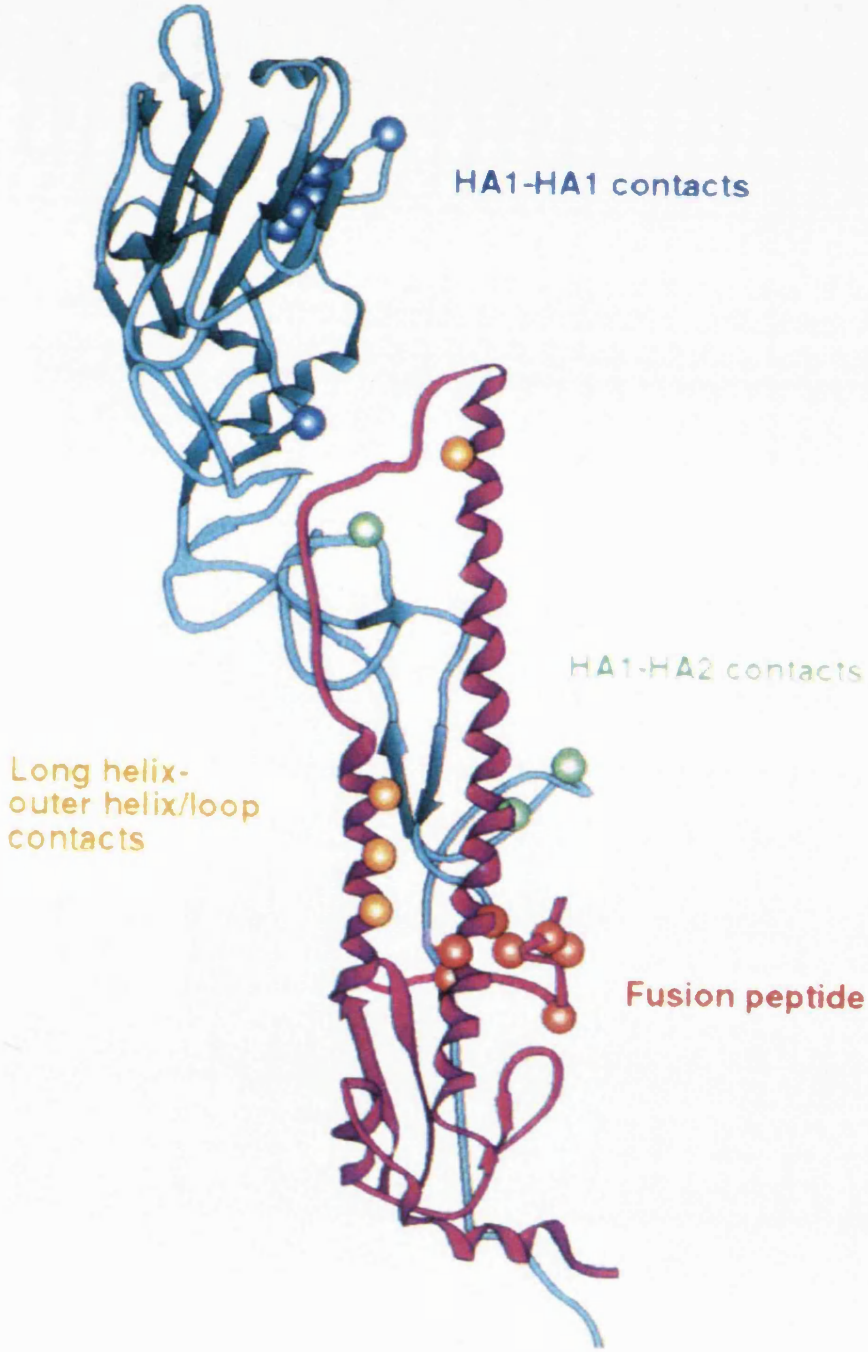
HA1-HA1 contacts
HA1-HA2 contacts
Long helix-
outer helix/loop
contacts
Fusion peptide

domain (Varghese *et al.*, 1983; Varghese and Colman, 1991). The stalk is extensively glycosylated and the stalk length has been found to vary between virus subtypes. This led to the suggestion that stalk length may influence the virus host range (Castrucci and Kawaoka, 1993). Located near the N-terminus is a hydrophobic region extending from amino acids 7 to 35 which is responsible for anchoring NA into the membrane. A cytoplasmic tail is formed by 6 amino acid residues (Fields and Winter, 1981), the sequence of which is highly conserved, unlike the amino acid composition of the hydrophobic region which tends to vary between subtypes (Blok *et al.*, 1982).

There is still much to be learned about the role of NA in the viral replication cycle. Influenza virus infects epithelial cells in the upper respiratory tract which are constantly bathed in mucosal secretions rich in sialic acid (Gottschalk, 1958; Gottschalk, 1972). It is likely that NA facilitates the transport of the virus through the respiratory tract to its target cells by the removal of sialic acid. It has also been shown that removal of sialic acid from both NA and HA is necessary to prevent self-aggregation of virions (Palese *et al.*, 1974; Griffin and Compans, 1979; Griffin *et al.*, 1983).

The M2 protein, which is the subject of this work, is the product of a spliced messenger RNA (mRNA) of the M gene, encoded by RNA segment 7 (Lamb *et al.*, 1981). The protein is a minor component of the influenza A virus envelope (Lamb *et al.*, 1985; Zebedee and Lamb, 1988), however during synthesis of progeny virus particles, large numbers of M2 molecules are produced within the infected cell. The M2 protein is a homotetramer composed of two disulphide-linked dimers held together non-covalently (Sugrue and Hay, 1991; Holsinger and Lamb, 1991). Each M2 monomer consists of a 23 amino acid N-terminal region which is located externally, a 19 amino acid transmembrane domain and an internally located C-terminal domain composed of 54 amino acids. The M2 protein of both

A/Chicken/Germany/34 ("Rostock") virus and A/Chicken/Germany/37 ("Weybridge") virus is post-translationally modified by the addition of palmitate to cysteine 50 (Sugrue *et al.*, 1990b; Veit *et al.*, 1991) and phosphate to threonine 65. However, serine 64 has recently been shown to be the main site of phosphorylation of the A/Udorn/72 virus M2 protein (Holsinger *et al.*, 1995). Some viruses also have a potential glycosylation site in the external domain of the M2 protein, but this appears to be largely unused (Zebedee *et al.*, 1985).

RNA segment 8 also encodes two proteins by differential splicing, known as NS1 and NS2, which are considered to be non-structural, although NS2 has been found within the virus particle (Richardson and Akkina 1992; Yasuda *et al.*, 1993). The function of these two proteins is still unclear, however, NS1 has been shown to inhibit the nuclear export of poly(A) mRNA (Qiu and Krug, 1994; Fortes *et al.*, 1994). It has also been suggested that NS1 may play a role in the post-transcriptional control of synthesis of late viral proteins (Hatada *et al.*, 1992).

1.3 GENETIC AND ANTIGENIC VARIATION

Influenza epidemics and pandemics occur due to the ability of the virus to undergo antigenic changes which allow it to escape host immune surveillance. Epidemics may also be caused by the re-emergence of viral strains which a significant proportion of the population have not encountered before, as occurred in 1977. New viral strains arise as a consequence of two processes known as antigenic drift and shift.

Antigenic drift

Antigenic drift is a gradual process and is the result of point mutations (additions, substitutions and deletions) which occur within the viral genome. This process of antigenic variation allows the virus to evade the host immune system. The majority of changes occur within the two surface glycoproteins, HA and NA.

The major antigen against which neutralizing antibodies are produced is the HA surface glycoprotein. Point mutations may mean that the virus can evade the host immune response and a new dominant circulating strain can arise. Mutations which confer drug resistance are also advantageous to the virus. The genes encoding the viral proteins tend to evolve at different rates, with the surface proteins evolving at the fastest rate. The HA glycoprotein undergoes greater variation than the NA molecule and most of the changes occur in the HA1 region of the protein, which contains the antigenic sites (Both and Sleigh, 1981). Antibodies raised against HA have the ability to neutralize virus infectivity, in contrast with anti-NA antibodies which inhibit the enzymic activity of the protein, preventing the release of progeny virus particles.

Under certain selective conditions, point mutations may confer a selective advantage on the virus and a new dominant strain will appear. The viral RNA polymerase proteins produce replication errors at a rate of 1 base in every 10^4 (Holland *et al.*, 1982; Steinhauer and Holland, 1987), in contrast with DNA virus polymerase proteins which produce errors of the order 1 base in every 10^9.

The internal viral proteins are subject to a slower rate of evolution. Antigenic differences have been detected in the NP within and between virus subtypes (Schild *et al.*, 1979; Van Wyke *et al.*, 1980) and it is thought the NP

may be involved in determining the host range of influenza virus (Scholtissek *et al.*, 1985; Tian *et al.*, 1985; Snyder *et al.*, 1987). From the nucleotide sequence data available the M gene appears to be reasonably conserved throughout evolution. Of interest however is the differential rate of evolution between the M1 and M2 proteins, with the M2 protein evolving at a much faster rate than the M1 protein.

Antigenic shift

Antigenic shift relates to a sudden change primarily in the HA glycoprotein and to a lesser extent, the NA glycoprotein. The process of antigenic shift generally leads to the introduction of a HA gene into a human influenza virus from another animal virus, or from an avian virus. The segmented nature of the influenza virus genome facilitates the production of new strains of virus by a process of reassortment of the RNA segments. Thus when cells undergo a mixed infection with two or more different viruses, reassortant viruses may be produced. Many new progeny viruses will contain combinations of RNA segments which are not viable, but occasionally this process of reassortment leads to the production of a new pandemic strain.

The antigenic shift which led to the Hong Kong influenza epidemic in 1968 was due to the production of a recombinant virus containing an avian H3 subtype HA gene and the remaining seven RNA segments from an "Asian" H2N2 virus that was circulating within the human population at that time (Kawaoka *et al.*, 1989). It is unusual for avian viruses to infect humans and also human viruses do not infect birds. This implies that there is a species which is susceptible to infection by viruses from both the human and avian population. Current evidence suggests that swine are permissive to infection by both human and avian strains of virus, thus acting as "mixing vessels".

Swine therefore play an important role in the emergence of new pandemic strains.

1.4 PREVENTION AND TREATMENT OF INFLUENZA

Vaccination

The phenomenon of antigenic variation means that vaccines provide limited protection against influenza virus unless they represent existing circulating strains. The two major surface proteins against which antibodies are produced are the HA and NA glycoproteins. The World Health Organization (WHO) continuously monitors current circulating strains and vaccines are produced annually to provide protection based on the recommendations of the WHO. The vaccine consists of one type B virus and two type A virus strains. Vaccination of individuals affords 70-90% protection (Meiklejohn *et al.*, 1978; Meyer, 1978; Ruben, 1987) and is recommended for persons who are at an increased risk of complications arising as a consequence of influenza virus infection. This refers mainly to the elderly and individuals suffering from chronic cardiopulmonary disorders. Fortunately in most people the disease is not life threatening.

Chemotherapy

Due to the lack of a vaccine providing long term protection, there is a need for the development of anti-influenza chemotherapeutic agents. Currently the only drugs available are the tricyclic amine amantadine (1-amino adamantane hydrochloride) and its structural analogue rimantadine (α-methyl-1-adamantane hydrochloride) (Figure III). They were discovered

FIGURE III: **THE STRUCTURE OF THE ANTI-VIRAL COMPOUNDS AMANTADINE AND RIMANTADINE**

A: Amantadine

B: Rimantadine

A

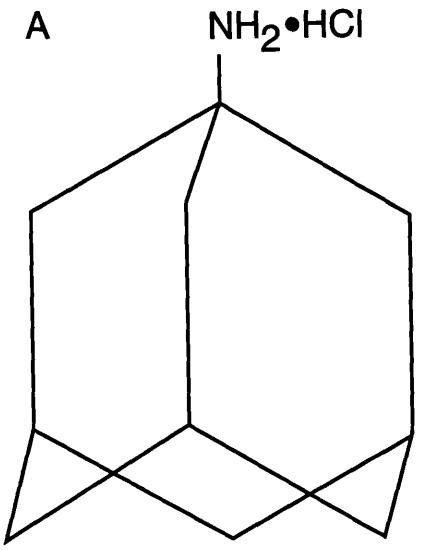

B

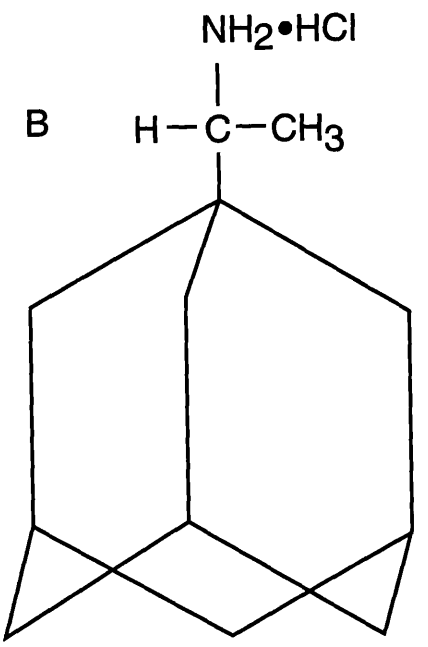

in the early 1960's and if administered to patients during the early stages of infection have some prophylactic effect. Although amantadine was licensed in 1966, its use in the USA and UK has been somewhat limited. Rimantadine was recently licensed for use in France and was also used in the former Soviet Union (Zlydnikov *et al.*, 1981). The main disadvantage of these drugs is their extreme specificity for influenza A virus infections and their ineffectiveness against influenza B viruses, which are responsible for a significant proportion of disease in the human population.

Furthermore, it is necessary to consider whether continuous long-term use of the drugs will allow drug-resistant viruses to enter the human population. After the administration of either of the anti-influenza A drugs, resistant mutant viruses can be isolated both *in vitro* and *in vivo* (Appleyard, 1977; Belshe *et al.*, 1988; Hayden *et al.*, 1989; Mast *et al.*, 1991; Houck *et al.*, 1995). Drug resistance is the result of mutations in the M gene (Lubeck *et al.*, 1978; Hay *et al.*, 1979; Belshe *et al.*, 1988). Analysis of resistant viruses has shown that mutations conferring drug resistance are mapped to the M2 protein (Hay *et al.*, 1985; Hay *et al.*, 1986). Amantadine selection however, has led to the production of a mutant virus with an acid-stable HA glycoprotein (Steinhauer *et al.*, 1991). Point mutations located in the transmembrane domain of M2 at residues 27, 30, 31 and 34 (Hay *et al.*, 1985; Bean *et al.*, 1989; Hay, 1989; Kendal and Klenk, 1991; Mast *et al.*, 1991) confer drug resistance, suggesting that it is this region with which amantadine interacts.

More recent approaches to anti-influenza therapy have involved computer-aided design of potential chemotherapeutic agents. As the neuraminidase enzyme contains a highly conserved sequence close to the active site, this represents a possible target for a sialidase inhibitor (Itzstein *et al.*, 1993). The HA glycoprotein is also a potential target for anti-viral compounds. More recently, X-ray crystallography studies of the BHA

molecule complexed with high-affinity receptor analogues, have suggested new ligands for inhibiting viral attachment and fusion activity (Watowich *et al.*, 1994), a "cocktail" of which may overcome the problems of viral resistance. The M2 protein however, still remains an attractive target for anti-viral therapy and when more information is obtained regarding its structure, computer-aided design may be beneficial in the development of new anti-influenza chemotherapeutic agents.

1.5 VIRAL REPLICATION

Attachment and entry

Influenza virus binds to a sialic acid-containing receptor in order to enter the cell. Although all influenza viruses bind to sialic acid-containing receptors, there are differences in receptor binding specificity between human, avian and swine subtypes. Different subtypes may bind preferentially to particular types of α-ketosidic linkages and this is thought to play a role in the adaptation of viruses to different hosts.

To facilitate delivery of the viral genome to the host cell cytoplasm the virus is internalized by a process of receptor-mediated endocytosis. A pH-activated fusion event then takes place between the viral envelope and the endosomal membrane, induced by the low pH encountered in the endosomal vesicle (~ pH 5.5). This results in uncoating of the virus and delivery of the RNP core to the cytoplasm.

Structural rearrangements in HA following the low pH-induced conformational change have been studied using various methods such as antibody binding (Daniels *et al.*, 1983 a and b; Webster *et al.*, 1983; Yewdell *et al.*, 1983; White and Wilson, 1987), analysis of proteolytic fragments

(Skehel *et al.*, 1982; Ruigrok *et al.*, 1988) and the production of site-specific mutations (Godley *et al.*, 1992). Recently the structure of HA in the low pH conformation has been studied in more detail (Bullough *et al.*, 1994; Wharton *et al.*, 1995). When BHA is incubated at the pH of fusion it self-aggregates due to exposure of the hydrophobic fusion peptide, however it also becomes susceptible to proteolysis. Trypsin digestion results in the release of the HA1 globular domains and after removal of the fusion peptide with thermolysin the resulting structure known as TBHA2 can be solubilized (Daniels *et al.*, 1983a; Ruigrok *et al.*, 1988) rendering it more amenable to crystallization.

Results from X-ray crystallographic studies of TBHA2 crystals indicate that major structural changes occur at both ends of the HA2 polypeptide (Bullough *et al.*, 1994). The N-terminal region of TBHA2 is displaced by 100Å, a distance which is sufficient to move the fusion peptide by at least 150Å. A structural change also occurs at the C-terminal region of the molecule which has the effect of displacing the remainder of the helix and the C-terminal regions of HA1 and HA2 associated with it by rotating it through 180°. The changes that occur at each end of the HA2 polypeptide also result in the 13 C-terminal residues becoming slightly disordered. Electron microscopy studies of TBHA2 in the fusion conformation complexed with antibody are consistent with these crystallography data (Wharton *et al.*, 1995). Projections were observed protruding from the membrane-distal end of the TBHA2 molecule and were identified as the C-terminal region which had been rotated through 180°.

Following the HA-mediated low pH fusion of the viral envelope with the endosomal membrane, the M1 protein dissociates from the RNP. This allows the RNP core to gain entry to the cell nucleus where transcription occurs. Studies of the inhibitory action of amantadine have indicated that the M2 protein plays a role in the uncoating process (Bukrinskaya *et al.*, 1982; Sugrue *et al.*, 1990a; Martin and Helenius, 1991a; Ciampor *et al.*, 1992a;

Grambas and Hay, 1992; Bron *et al.*, 1993; Wharton *et al.*, 1994). The role of M2 in the viral replication cycle will be discussed in section 1.6 pp25-31.

Gene expression and replication

After delivery of the viral genome into the host cell cytoplasm, the vRNA and associated proteins are transported to the cell nucleus. They enter the nucleus through nuclear pores and the viral polymerase associated with each of the eight RNA segments initiates transcription.

The synthesis of viral mRNA is initiated using primers from newly synthesized host cell RNA polymerase II transcripts which are capped at the 5' end and methylated (Bouloy *et al.*, 1978, 1979; Krug *et al.*, 1979; Plotch *et al.*, 1979, 1981). The PB2 protein binds to the cap structure of the host cell mRNA (Ulmanen *et al.*, 1981) and cleaves it approximately 10-13 nucleotides from the 5' end of the mRNA usually at a purine residue (Plotch *et al.*, 1981; Shi *et al.*, 1995). Transcription commences with the addition of a G residue to the resulting fragment. The PB1 protein is responsible for the elongation of the nascent mRNA (Ulmanen *et al.*, 1981; Braam *et al.*, 1983) until the termination site is reached and the poly(A) tail is added (Hay *et al.*, 1977a and b; Robertson *et al.*, 1981). As yet no specific role has been found for PA in the transcription process other than formation of the transcription complex, but it has been suggested that it may be involved in vRNA replication.

The M2 protein is derived from a spliced transcript encoded by RNA segment 7, the unspliced transcript coding for the M1 protein (Lamb *et al.*, 1981). The first nine amino acids are translated in the same reading frame as M1 and an interrupted region of 689 nucleotides which is spliced out follows. Translation then switches to a +1 reading frame relative to the unspliced transcript at nucleotide 740 in order to translate the remaining 88 amino acids

(Figure IV).

A second type of transcript known as a template or complementary, positive strand RNA (cRNA) is required for viral replication. The cRNA molecules are complete transcripts of the viral RNA and are not polyadenylated or capped (Hay *et al.*, 1977b; Hay *et al.*, 1980; Hay *et al.*, 1982). Synthesis of vRNA seems to involve protein synthesis *in vivo* (Hay *et al.*, 1982) so it is likely that the presence of a viral protein product is required. It has been suggested that NP which is not associated with the nucleocapsids may play a role in the prevention of termination of vRNA synthesis at the site of polyadenylation as well as the NS1 protein (Buonaguirio *et al.*, 1984; Beaton and Krug, 1986; Shapiro and Krug, 1988).

Viral protein synthesis, assembly and release

Synthesis of viral mRNA has been shown to correlate well with viral protein production (Hay *et al.*, 1977a; Inglis and Mahy, 1979). NP and the NS1 protein are synthesized during the early stages of infection, in contrast to NA, HA, M1 and the M2 protein which are produced preferentially during the later stages of infection (Skehel, 1972).

The assembly of mature virions involves first of all the formation of the RNP cores, which are then transported from the cell nucleus to the plasma membrane. M1 has been shown to associate with the RNP cores in the nucleus, which is necessary for their transport out into the cytoplasm (Martin and Helenius, 1991b). The RNP core is incorporated into the virus particle prior to budding from the infected cell surface and the M1 protein has been implicated in this process.

FIGURE IV: SPLICING OF THE M GENE mRNA

Three mRNA species are derived from the 1027 base pair (bp) RNA complementary to RNA segment 7, known as M1, M2 and mRNA3. The 5' and 3' non-coding regions are represented by thin lines and the coloured areas denote coding regions. Spliced regions are shown by thin V-shaped lines. The region between nucleotides 42 and 740 is excised and translation of the M2 mRNA occurs in a +1 reading frame relative to M1 from nucleotide 740-1004. Potentially mRNA3 could encode a 9 amino acid peptide which corresponds to the C-terminal region of the M1 protein, but as yet no protein has been identified. The black boxes are representative of cap sequences derived from the host cell.

(Taken from Lamb *et al.*, 1981).

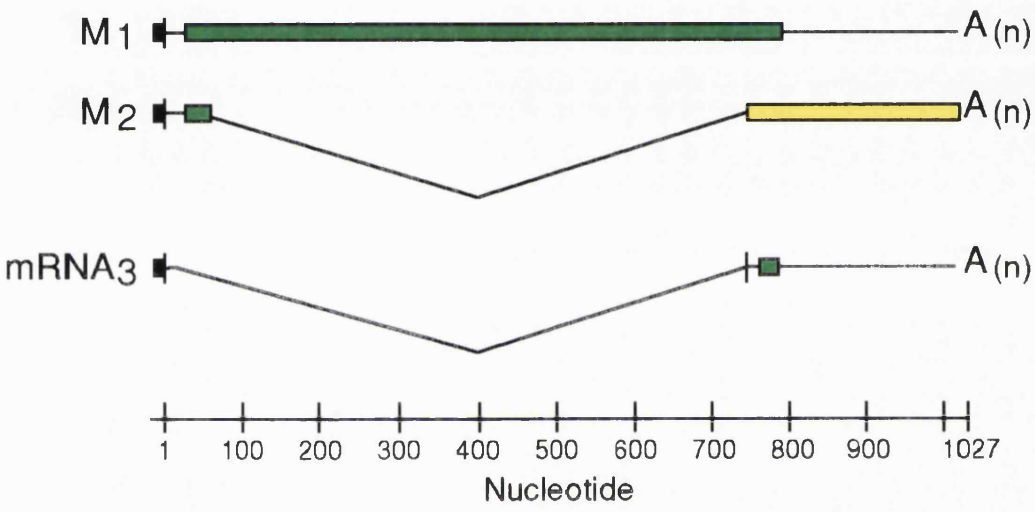
M1
A(n)
M2
A(n)
mRNA3
A(n)
1
100
200
300
400
500
600
700
800
900
1027
Nucleotide

The HA, NA and M2 proteins are transported to the cell surface for the final stage of virus assembly to occur. Signal sequences facilitate transport of the polypeptides into the endoplasmic reticulum (ER) lumen, where further modifications take place. These changes include cleavage of the signal peptide, glycosylation, and disulphide bond formation (reviewed by Roth *et al.* 1989). In the case of NA the signal sequence remains uncleaved as it is required to anchor the NA protein into the ER membrane.

The proteins enter the Golgi apparatus and the HA and M2 proteins are modified by the addition of palmitate to certain residues (Naeve and Williams, 1990; Sugrue *et al.*, 1990b; Veit *et al.*, 1990; Veit *et al.*, 1991) and the M2 protein also undergoes phosphorylation (Sugrue *et al.*, 1991; Holsinger *et al.*, 1995). The terminal mannose residues added to the HA and NA glycoproteins in the ER are further trimmed and following the movement of HA into the *trans*-Golgi cisternae, sialic acid residues are added (Basak *et al.*, 1985). It is also here in the *trans*-Golgi network (TGN) that proteolytic cleavage of HA0 into HA1 and HA2 takes place.

Before formation of a mature virion, protein sorting occurs within polarized epithelial cells, so that the viral proteins are expressed only on the apical surface of the plasma membrane (Rodriguez-Boulan and Sabatini, 1978; Rodriguez-Boulan and Prendergast, 1980; Roth and Compans 1981; Roth *et al.*, 1983). RNP cores visualized by electron microscopy, are shown to collect below a thickened patch of membrane containing the viral surface proteins, thus constituting the first stage of viral budding. Although M2 is abundantly expressed at the cell surface, it is a minor component of the virion. Therefore as M2 appears to be almost selectively excluded from the mature virus particle, it is possible that it may play a role in the assembly and budding process, but as yet this is undetermined.

1.6 THE ROLE OF M2 IN VIRUS REPLICATION

Millimolar concentrations of amantadine and rimantadine block membrane fusion and viral uncoating in an unspecific manner. At such high concentrations their basic properties result in the elevation of the endosomal pH. This has the effect of reducing the acidity of the vesicles thus preventing the low pH-induced conformational change in HA and subsequent uncoating of the virus. However, micromolar concentrations of either drug have a direct inhibitory effect on the M2 protein and studies with amantadine have identified two roles of M2 in the virus replication cycle, namely virus uncoating and virus maturation.

It has been suggested that acid conditions are required for the dissociation of the M1 protein from the RNP core after the fusion activity of HA has been activated (Gregoriades, 1973; Zhirnov, 1990). The fact that micromolar concentrations of amantadine prevent this dissociation from happening and result in the RNP core remaining trapped with the M1 protein shell within the cell cytoplasm provides evidence for the involvement of the M2 protein. It has been suggested that the low endosomal pH activates the M2 protein, so that protons are transported from the acidic endosomal vesicle to the virion interior, in order to provide the necessary acidic conditions for dissociation of the M1 protein from the RNP core (Hay, 1989; Wharton *et al.*, 1990) (Figure VA). Recent evidence suggests that inhibition of M2 function also results in a decrease in the rate of fusion between the viral and endosomal membranes (Bron *et al.*, 1993; Wharton *et al.*, 1994), without altering the extent of fusion. Studies on amantadine-sensitive viruses showed that the rate of fusion was decreased in the presence of drug, in contrast with amantadine-resistant viruses, whose rate of fusion was unaffected by the presence of drug. The proton ionophore monensin which would act in a similar manner to M2 by promoting acidification of the virion interior was found

FIGURE V: **THE PERCEIVED ROLE OF THE M2 PROTEIN IN INFLUENZA A VIRUS REPLICATION**

A: This represents the role of the M2 protein in the low pH-induced uncoating of influenza virus. It is proposed that the M2 protein allows protons to enter the virion interior from the late endosome. This facilitates the dissociation of the M1 protein from the RNP core, allowing transport of the viral RNA to the cell nucleus to occur.

B: M2 is known to be involved in the maturation of HA. Evidence indicates that M2 colocalized with HA in transport vesicles in the TGN is responsible for the removal of protons from the vesicles. This has the effect of decreasing the acidity of the TGN thus preventing the HA from undergoing a premature low pH-induced conformational change.

(Taken from Hay, 1992).

A

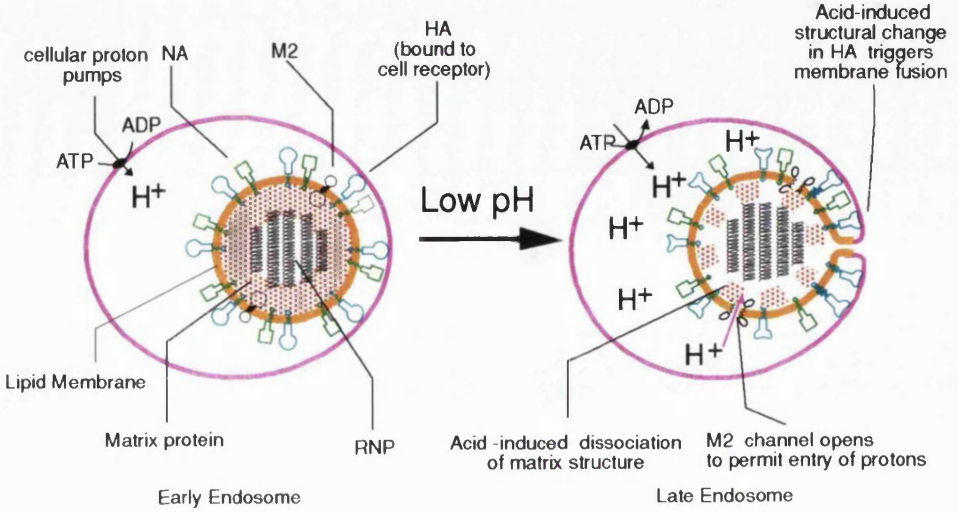
cellular proton pumps
NA
M2
HA (bound to cell receptor)
ADP
ATP
H+
Lipid Membrane
Matrix protein
RNP
Early Endosome
Low pH
Acid-induced structural change in HA triggers membrane fusion
ADP
ATP
H+
Acid -induced dissociation of matrix structure
M2 channel opens to permit entry of protons
Late Endosome

B

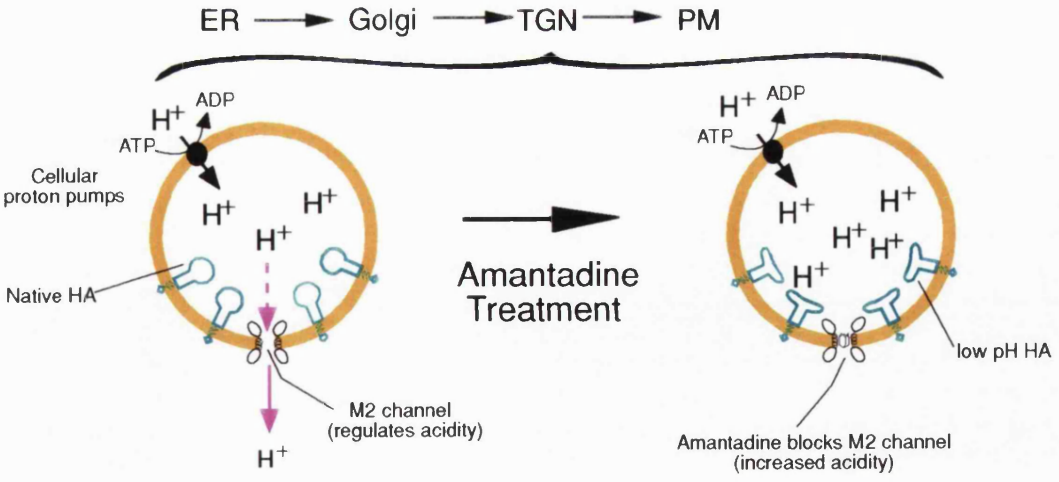
ER
Golgi
TGN
PM
ADP
ATP
H+
Cellular proton pumps
Native HA
M2 channel (regulates acidity)
Amantadine Treatment
low pH HA
Amantadine blocks M2 channel (increased acidity)

to cause a large increase in the rate of fusion of the A/Singapore/1/57 virus (Wharton *et al.*, 1994). These results provide further support for an ion channel function for the M2 protein, in particular that M2 is capable of transporting protons across the viral membrane to create the conditions necessary for virus uncoating.

A second role has also been proposed for M2. In certain H5 influenza A viruses which have HA molecules that are cleaved intracellularly, M2 plays an additional role in glycoprotein maturation. The M2 protein is involved in maintaining the structural integrity of the HA glycoprotein during its transport through the TGN to the plasma membrane. Inhibition of this function by amantadine results in HA being converted to the low pH form and the subsequent inhibition of virus release (Figure VB) (Sugrue *et al.*, 1990b; Ruigrok *et al.*, 1991).

Immunofluorescence studies have shown that M2 is co-localized with HA in transport vesicles in the TGN. Work involving the immunocytochemical pH probe [3-(2,4 dinitroanilino)-3-amino-N-methyl-dipropylamine] (DAMP) has shown the vesicles containing low pH HA to be particularly acidic (Ciampor *et al.*, 1992a). It is therefore postulated that M2 is present in the membranes of HA-containing transport vesicles and is capable of regulating the pH of the TGN and associated vesicles by counteracting the acidifying effects of vesicular proton pumps. Inhibition of the M2 protein by amantadine resulted in a decrease in vesicular pH and the conversion of native HA to its low-pH form. This is consistent with the decrease in cytoplasmic pH which is inhibitable by amantadine (Ciampor *et al.*, 1992b). Point mutations found within the transmembrane domain of amantadine-resistant M2 proteins, indicate that it is this region with which amantadine interacts (Figure VI). The transmembrane domain has the capability of forming an amphiphilic alpha helix, therefore it is thought that the hydrophilic faces of the four monomers

FIGURE VI: A REPRESENTATION OF THE PROPOSED CHANNEL STRUCTURE OF THE A/CHICKEN/GERMANY/27 ("WEYBRIDGE") M2 PROTEIN AND ITS INTERACTION WITH AMANTADINE.

The proposed structure of the transmembrane domain is shown with the two hydrophilic faces of the α-helices associating to form an ion permeable channel. The boxed residues denote sites of single amino acid changes which confer drug resistance and the interaction of amantadine within the channel is shown.

(Taken from Hay, 1992).

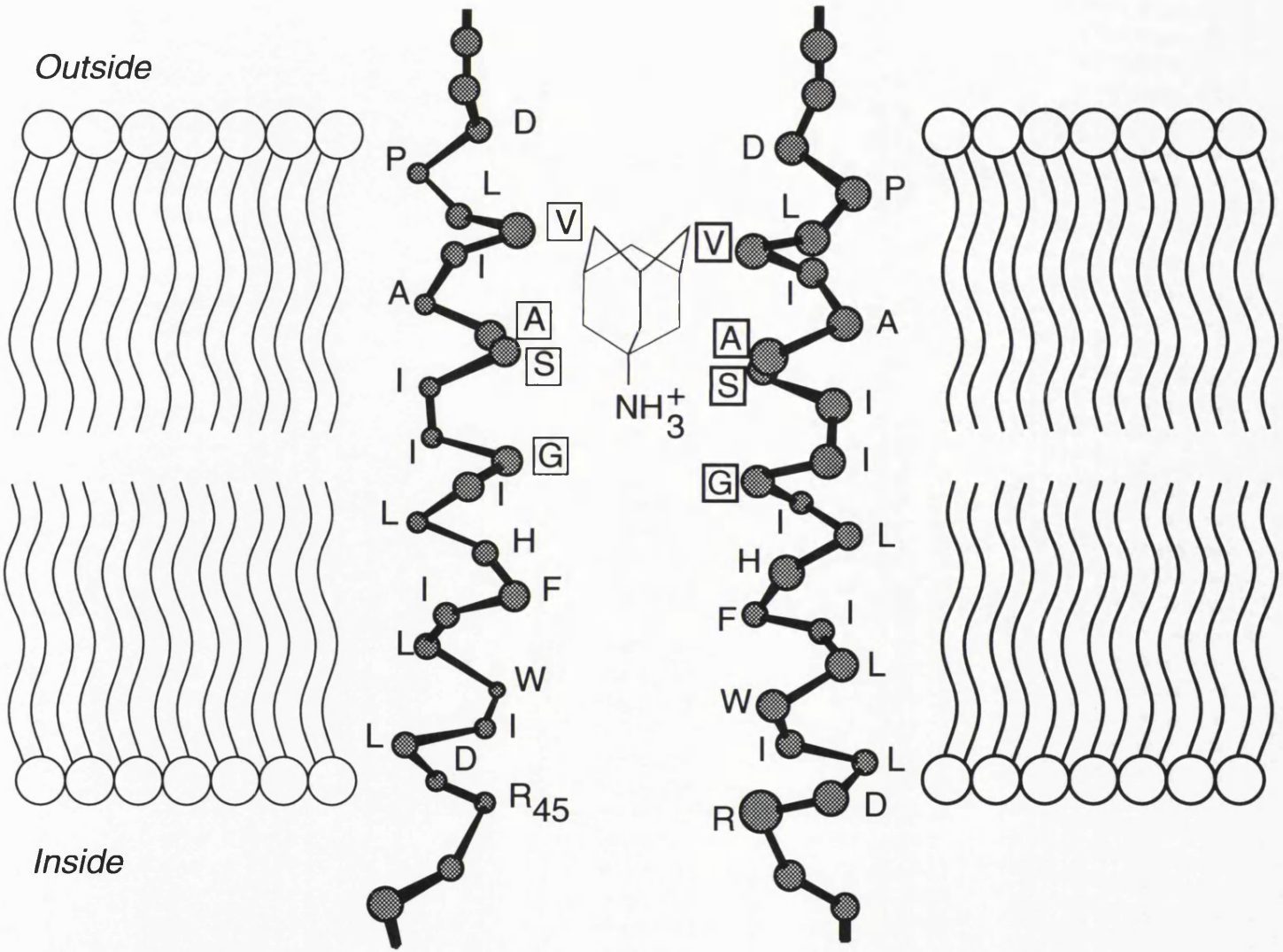
Outside
Inside
D
P
L
V
I
A
A
S
I
I
G
I
L
H
I
F
L
W
L
I
D
R45
NH3+
D
P
L
V
I
A
A
S
I
I
G
I
L
H
F
I
L
W
I
L
D
R

are arranged in such a way as to form a transmembrane ion permeable channel. The hypothesis, based on the structural and functional attributes, that M2 forms a proton channel has recently been supported by work carried out by other workers (Pinto *et al.*, 1992; Chizmahkov *et al.*, submitted).

1.7 PROJECT AIMS

The aim of this work was to set up a high level expression system to produce the M2 protein, allowing further investigation of M2 at a structural and functional level, in particular the characterization of its ion conductance properties. An expression system using MEL cells was chosen as these cells are particularly suited to the expression and study of an ion channel, due to the low level of intrinsic channel activity (Arcangeli *et al.*, 1987). The objective of this study was to further characterize the functional properties of the M2 protein by co-expression of M2 and HA and determination of intracellular pH of M2-expressing MEL cells. The ion channel function of M2 was investigated using a patch-clamp technique. Mutagenesis was also performed to try and correlate differences between structure and activity.

MATERIALS AND METHODS

MATERIALS AND METHODS

2.1 CELL CULTURE

Cells

MEL cells were cultured at 37°C (3-5% CO_2) in minimal essential medium (MEM) supplemented with 10% foetal calf serum (FCS) (GIBCO) and 2mM glutamine. Madin-Derby canine kidney (MDCK) cells were maintained as above in MEM supplemented with 5% FCS. Baby hamster kidney (BHK) cells and CV-1 cells were propagated in H-21 pyruvate medium supplemented with 5% FCS and were maintained at 37°C with 3-5% CO_2.

MEL cells were attached to 35mm tissue culture dishes for radiolabelling and Western blotting and 20mm diameter No.1 coverslips (Chance Propper Ltd) for immunofluorescence. Before attachment, coverslips and tissue culture dishes were treated with either 0.1% poly-L-lysine (Sigma Chemical Co.) in distilled water (dH_2O), or 2% 3-aminopropyltriethoxysilane (3-APTS) (Sigma Chemical Co.) in industrial methylated spirits for 10 minutes at room temperature (RT) prior to use. For enzyme-linked immunosorbent assay (ELISA) studies, MEL cells were attached to 96-well microtitre plates (MaxiSorp, NUNC, flat bottomed wells). Prior to attachment, the cells were washed twice in MEM lacking FCS (MEM-) (300g, 5 minutes, 18°C) and resuspended in MEM- at a density of ~$1x10^7$ cells/ml. Approximately $1x10^7$ cells were added to each tissue culture dish, $2x10^6$ cells to the coverslips and $5x10^5$ cells to each well of the microtitre plate. Monolayers were allowed to form over a period of 20 minutes at 37°C. Unattached cells were removed by two washes with MEM-. Confluent monolayers of CV-1, BHK and MDCK cells were grown on untreated 35mm tissue culture dishes.

Primary chick embryo fibroblasts (CEF) were prepared from 11 day old chick embryos by a method modified from Porterfield (1960). Chick embryos

with the eyes and guts removed were finely chopped and digested with trypsin (1.25g/l) for 30 minutes. After centrifugation (300g, 10 minutes, 4°C), the cells were resuspended at a density of $2x10^6$ cells/ml in Tris-buffered Gey's medium supplemented with 10% calf serum (CS) and filtered through a fine wire gauze. Approximately 24 hours prior to use, 2ml of cell suspension (~$4x10^6$ cells) were added to 35mm tissue culture dishes and incubated at 37°C.

2.2 PREPARATION OF DNA

Polymerase chain reaction (PCR)

Rostock M2 complementary DNA (cDNA) and mutant M2 cDNAs were amplified from the vectors pUTL.7p1-11 (a gift from A. Hayhurst) and using a forward primer with the sequence **5' G*GAATTC*CAAAAGCAGGTAGATAT 3'** and a reverse primer with the sequence **3 ' GA*AGATCT*TTTACTCCAGCTCTAT 5'**. The forward primer incorporated an *Eco*RI site and the reverse primer a *Bgl*II site (shown in italic and underlined). To amplify the cDNA 50µl reactions were set up, consisting of 42µl PCR "mix" (to give a final concentration of 1.5mM $MgCl_2$, 10mM Tris-HCl pH8.8, 50mM KCl, 100µg/ml Bovine serum albumin (BSA) (Sigma Chemical Co.), 250µM deoxy-nucleotide triphosphates (dNTPs) (Pharmacia) pH7.6), 100ng of each primer, 5µl DNA template (500-1000ng) and 2.5 units AmpliTaq® DNA polymerase (Perkin Elmer). One drop of mineral oil was added to each tube (Sigma Chemical Co.) and a Hybaid Thermal Cycling machine was pre-heated to 95°C prior to starting the thermocycling program. The conditions involved denaturation at 95°C for 30 seconds, annealing at 50°C for 30 seconds and extension at 72°C for 2 minutes. After 25 cycles there was a final 10 minute incubation at 72°C. Rostock HA was amplified from infected cells by an RT reaction using the reverse primer (42°C 1 hour; 95°C 10 minutes) and then a PCR reaction as above.

Cloning of M2 cDNA into pEV3

All restriction and modifying enzymes used were purchased from Boehringer Mannheim, except Calf Intestinal Phosphatase (CIP) and T4 DNA Ligase (both from New England Biolabs) and RNase A (Sigma Chemical Co.). All enzymes were used in accordance with the manufacturers instructions.

After digestion of 200-500ng of M2 cDNA and pEV3 DNA, (Needham *et al.*, 1992) reaction mixtures were resolved in 1% low melting point (LMP) agarose (SeaPlaque® GTG®, FMC) gels buffered with TAE (40mM Tris-acetate, 2mM diaminoethanetetra-acetic acid disodium salt (EDTA) pH8.0) for 90 minutes at 50V, using 1kB ladder (GIBCO) as a standard size marker. The relevant fragments were excised and heated to 65°C for 15 minutes. Gel slices containing appropriate DNA fragments were combined to give a total volume of 10µl and placed at 37°C. 10µl of an ice-cold reaction mixture containing 10x enzyme buffer, 2 units of T4 DNA Ligase and 1mM adenosine triphosphate (ATP) were added to each tube and the reactions left overnight at RT for ligation to occur. Prior to transformation of competent cells, 400µl of TCM (10mM Tris-HCl pH7.0, 10mM $CaCl_2$, 10mM $MgCl_2$) were added to each ligation mix and the tubes heated to 65°C for 15 minutes.

Preparation of competent cells

Escherichia coli (*E.coli*) DH5-α cells were made competent by a method modified from Hanahan (1983). 500ml of L-broth were inoculated with 5ml of a saturated culture of DH5-α cells and grown at 37°C in a New Brunswick orbital shaker (300rpm) to an optical density (OD) of 0.3-0.4 at 595nm. The cells were chilled on ice for 15 minutes, pelleted (400g, 10 minutes, 4°C) and resuspended in 200ml of FSB (10mM potassium acetate pH7.5, 45mM $MnCl_2.4H_2O$, 10mM $CaCl_2$, 100mM KCl, 3mM hexammine cobalt chloride, 10% glycerol). After 10 minutes on ice the cells were pelleted as above and resuspended in 40ml of ice-cold FSB. Following the addition of

140µl of dimethyl sulphoxide (DMSO), 1ml aliquots of the cells were flash-frozen by placing in a dry ice/ethanol bath and stored at -70°C.

Transformation of competent cells

Competent cells were thawed and placed on ice. Ligation mixes or vector DNA diluted with TCM were also placed on ice for 5 minutes before use. 200µl of diluted ligation reaction mixture were added to a 100µl aliquot of DH5-α competent cells and left on ice for 30 minutes. Following heat shock treatment at 42°C for 90 seconds, the cells were placed on ice for 5 minutes. 1ml of SOC medium was then added and the cells incubated at 37°C for 1 hour. After pelleting (low speed, 30 seconds, MSE microfuge) the cells were resuspended in 200µl of L-broth, plated out on L-agar plates containing 100µg/ml ampicillin (Sigma Chemical Co.) and incubated at 37°C overnight.

DNA mini-prep

2ml of L-broth containing 100µg/ml ampicillin were inoculated with a transformed colony of cells and shaken at 37°C for 5-6 hours. The cells contained in 1.5ml of culture were pelleted (full speed, 1 minute, MSE microfuge) and resuspended in 100µl of solution I (50mM glucose, 10mM EDTA, 25mM Tris-HCl pH8.0). 200µl of freshly made solution II (0.2N NaOH, 1% sodium dodecyl sulphate (SDS)) were then added and the tubes placed on ice for 10 minutes. Following the addition of 150µl of solution III (3M potassium acetate, 2M acetic acid), the tubes were placed on ice for a further 10 minutes, before the extraction of the aqueous phase with 450µl of phenol/chloroform solution (25 phenol: 24 chloroform: 1 *iso*-amyl alcohol v/v). After vigorous vortexing the phases were separated by centrifugation (full speed, 5 minutes, MSE microfuge). The aqueous phase was transferred to a clean eppendorf tube and the DNA immediately ethanol precipitated by adding 0.1 volumes of 3M sodium acetate and 2 volumes of 100% ethanol

(full speed, 15 minutes, MSE microfuge). The pellet was washed with 200µl of 70% ethanol, desiccated for 10 minutes in an Edwards Modulyo lyophilizer and then resuspended in 50µl of water containing 0.1µg/µl RNase A.

DNA maxi-prep

500ml of L-broth containing 100µg/ml ampicillin were inoculated with 5ml of an overnight culture of DH5-α cells. The flask was shaken at approximately 300rpm, overnight at 37°C. The bacteria were then pelleted (400g, 20 minutes, 4°C) and resuspended in 20ml of solution I. Following the addition of 40ml of freshly made solution II, the resulting mixture was left on ice for 10 minutes. 30ml of ice cold solution III were added and after gentle mixing the lysed bacteria were again left on ice for 10 minutes. After centrifugation (800g, 10 minutes, 0°C) the supernatant was filtered through butter muslin and 0.6 volumes of isopropanol were added. Following centrifugation (800g, 10 minutes, 0°C) the pellet was desiccated for 20-30 minutes and then resuspended in 14.70ml TE (10mM Tris-HCl pH8.0 and 1mM EDTA pH8.0). CsCl was added to a concentration of 1g/ml followed by 630µl of 10 mg/ml ethidium bromide. The tube was then left in the dark for 1 hour, before centrifugation (400g, 20 minutes, 20°C) to remove the precipitated material. The supernatant was loaded into Beckman centrifuge tubes (No. 349622) and after subsequent centrifugation (174,000g, 16 hours, 18°C) the plasmid DNA was isolated.

The lower band of plasmid DNA was extracted (approximately 0.5ml per tube) and transferred to a 15ml Falcon tube. The ethidium bromide was removed by alternate extractions with 1ml of butanol and water-saturated butanol until the aqueous phase became colourless. The DNA was precipitated by the addition of two volumes of TE , 0.1 volumes of 3M sodium acetate and three volumes of 100% ethanol (400g, 20 minutes, 20°C). After washing with 2ml of 70% ethanol, the pellet was desiccated for 10 minutes

and resuspended in water to a concentration of 1mg/ml.

Sequencing

A *fmol*™ DNA Sequencing System was used (Promega). A forward primer with the sequence **5' GGAATTCCAAAAGCAGGTAGATAT 3'** and reverse primer with the sequence **3' AAGATCTTTTACTCCAGCTCTAT 5'** were used for M2 cycle sequencing.

1µl of primer (~100ng) was end labelled with 10pmol of [γ^{33}P]-ATP (Du Pont, NEN) according to the manufacturers instructions. The kinase was then inactivated by heating the samples to 90°C for 2 minutes.

1.5µl of this reaction mixture were combined with 4µl of template DNA (~500ng) and 5µl of sequencing buffer and the volume made up to 16µl with water. After the addition of 1µl of *Taq* polymerase (sequencing grade), 4µl of this reaction mixture were added to tubes containing the appropriate deoxy/dideoxy NTP mix, followed by one drop of mineral oil. A Hybaid Thermal Cycling machine was pre-heated to 95°C prior to starting the thermocycling program (95°C for 30 seconds, 50°C for 30 seconds, 72°C for 2 minutes). After 25 cycles a final extension time of 10 minutes at 72°C was included. The resulting fragments were resolved on 6% denaturing polyacrylamide gels. After drying under vacuum, the gels were exposed to photographic film (KODAK X-OMAT AR) at RT.

2.3 PRODUCTION OF M2 EXPRESSING CELLS

Electroporation

MEL cells were seeded so that they were in log phase growth (0.5-1.0x10^6 cells/ml) on the day of transfection. Approximately 10^7 cells were pelleted for each transfection (300g, 5 minutes, 18°C). After washing twice with 50ml of phosphate buffered saline (PBS) (300g, 5 minutes, 18°C) the cells were resuspended in 0.9ml of ESB (25mM N(2-hydroxyethyl)piperazine-

N'(2-ethanesulphonic acid) (HEPES) pH7.15, 140mM NaCl, 0.7mM Na_2HPO_4). 50-100μg of pEV3 plasmid DNA (containing the appropriate M2 or HA cDNA), linearized with *Pvu*I and resuspended in 100μl of ESB, was added to the cells and mixed well 10 minutes prior to electroporation. The MEL cell/DNA mixture was transferred to an electroporation cuvette (BIO-RAD Gene Pulser® Cuvette, 0.4cm electrode gap) and a single pulse of 250V, 960μF was delivered. The cells were left in the cuvette for 10 minutes before being divided equally between two 75cm^2 tissue culture flasks containing 30ml of MEM supplemented with 10% FCS. Geneticin® (G418 sulphate) (GIBCO) was added to a concentration of 800μg/ml 24-48 hours after electroporation. An untransfected stock culture of MEL C88 cells was set up in selection media as a negative control.

After 7 days in selective media, cell death was complete and colonies of transfected drug resistant cells could be seen. When the cultures became 50% confluent the G418 concentration was reduced to 400μg/ml and at about 14 days post-selection the cultures were ready to be analyzed. Clones were obtained by plating the G418-resistant population at 1 cell/microtiitre well.

Screening of transfected cells

DMSO was added directly to MEL cells in log phase growth to a final concentration of 2%. Samples of cells were taken at various times post induction (p.i.) for further analysis.

Extraction of total RNA from MEL cells

MEL cells (~10^7 cells) were pelleted (300g, 5 minutes, 18°C) and the supernatant removed. The cell pellet was vortexed and 5ml of 3M LiCl/6M urea were added. The cell homogenate was then sonicated for 1 minute with a small-diameter probe (3mm) to shear the DNA and produce a non-viscous lysate which was stored overnight at 4°C. After centrifugation (1000g, 30

minutes, 4°C) the supernatant was removed and the resulting pellet dissolved in 1ml of 3M LiCl/6M urea and then transferred to an eppendorf tube. Following centrifugation (full speed, 5 minutes, MSE microfuge) and removal of the supernatant, the pellet was dissolved in 300µl of TES buffer (10mM Tris, 1mM EDTA, 0.5% SDS pH8.0) and sodium acetate was added to a concentration of 0.3M. The solution was extracted once with an equal volume of phenol/chloroform and the phases separated by centrifugation (full speed, 5 minutes, MSE microfuge). The aqueous phase was transferred to a clean eppendorf tube and 2.5 volumes of 100% ethanol were added. The RNA was pelleted (full speed, 5 minutes, MSE microfuge) after an overnight precipitation at -20°C. The pellet was washed with 800µl of 70% ethanol and centrifuged as above. Finally the pellet was resuspended in 100-200µl of S1 hybridization buffer (80% Formamide, 400mM NaCl, 40mM Piperazine-N,N'-bis[2-ethane-sulphonic acid] (PIPES) pH6.7, 1mM EDTA), the concentration determined and stored at -20°C.

S1 nuclease protection analysis

2µg of RNA were made up to 15µl with S1 hybridization buffer. 5µl of end-labelled probe (15ng) were added and after denaturation at 90°C for 5 minutes, hybridization was allowed to occur at 52°C overnight. Each reaction was subsequently digested with 100 units of S1 nuclease for 2 hours at 25°C. The mouse β-major probe was a *Hin*dIII-*Nco*I fragment that protected approximately 90 nucleotides of the 5' half of the second exon and the human β-globin probe was an *Eco*RI-*Pst*I fragment that protected approximately 200 nucleotides of the 3' half of the human gene (Kollias *et al.*, 1986). After extraction with phenol/chloroform the DNA/RNA hybrid molecules were ethanol precipitated and the pellet resuspended in 5µl loading buffer (7M urea, 5mM Tris borate pH8.3, 1mM EDTA, 0.1% xylene cyanol, 0.1% bromophenol blue). Protected fragments were then resolved on 6%

denaturing polyacrylamide gels which were dried under vacuum and exposed to photographic film (KODAK X-OMAT AR) in the presence of an intensifying screen at -70°C.

2.4 VIRAL INFECTION OF CELLS

Infection of cells with influenza virus

Viruses were grown in the allantoic cavity of 11 day old fertile hens eggs. Infectivity of virus stocks, as determined by plaque assay (Hay *et al.*, 1985), was found to be approximately $5x10^8$ plaque forming units (p.f.u.) per ml. The viruses used were BR02A, a reassortant containing the HA, NA and M genes from A/Chicken/Germany/34 ("Rostock") and the remaining genes from A/Bel/42, 15B which was a reassortant containing the PB1, HA and M genes from A/Chicken/Germany/37 ("Weybridge") and the remaining genes from A/Singapore/1/57 and finally 08 virus which was an amantadine resistant mutant derived from BR02A (Grambas and Hay, 1992).

MEL cells, MDCK cells and CEF were washed twice in MEM- and infected with influenza virus at a multiplicity of infection (m.o.i.) of approximately 50 p.f.u. per cell, for 30 minutes at RT. After washing twice in pre-warmed MEM- (time post-infection =0), the cells were incubated for 5-8 hours at 37°C.

Infection of cells with vaccinia virus

MEL cells attached to 35mm 3-APTS treated tissue culture dishes and confluent CV-1 monolayers grown in 35mm tissue culture dishes were infected with a recombinant vaccinia virus expressing the X-31 HA(H3N2) (Skehel and Schild 1971). The cells were infected for 1 hour at 37°C at various m.o.i. and then washed twice in pre-warmed medium and incubated for 48 hours at 37°C. The recombinant vaccinia virus was a gift from Mr David Stevens.

Infection of cells with Semliki Forest virus (SFV)

MEL cells attached to 3-APTS treated 35mm tissue culture dishes and confluent BHK cell monolayers were infected with SFV A7 (74) virus, in MEM- containing 0.2% (w/v) BSA, 10mM HEPES, and 2mM glutamine. The cells were infected for 30 minutes at 37°C at an m.o.i. of 15 p.f.u. per cell. The cells were washed twice in pre-warmed MEM- and incubated for various time intervals post-infection before metabolic labelling. The virus was a gift from Dr. John Fazakerley.

2.5 RADIOLABELLING OF CELLS

[^{35}S] labelling

MDCK or BHK cell monolayers grown on, or MEL cells attached to 35mm tissue culture dishes were washed with Tris-Gey's medium and incubated in 200µl of pre-warmed Tris-Gey's medium containing 10µCi of [^{35}S]-Cysteine/Methionine (>1000 Ci/mmol) (ICN Trans label) for 1 hour at 37°C.

[^{32}P] inorganic phosphate labelling

MEL cells attached to 3-APTS coated tissue culture dishes were incubated for 4 hours at 37°C in phosphate-free MEM-. This was replaced with 0.5ml phosphate-free MEM- containing 0.25mCi [^{32}P] orthophosphate, (Amersham; carrier free orthophosphate in dilute HCl [<0.1M]) and the cells incubated for a further 4 hours.

[^{3}H] palmitic acid labelling

MEL cells attached to 35mm tissue culture dishes were incubated at 37°C in 250µl of MEM- supplemented with 5mM sodium pyruvate and containing 250µCi of [9,10 (n) -^{3}H] palmitic acid (Amersham; 40-60Ci/mmol) for 4 hours.

2.6 IMMUNOLOGICAL METHODS

Antibodies

Rabbit antisera were previously prepared by S.Grambas against M2 peptides conjugated to keyhole limpet haemocyanin (KLH). R7-90 and R53 were raised against peptides corresponding to the N-terminal 24 amino acids and R54 to the C-terminal 16 amino acids.

Monoclonal anti-HA antibodies against whole virus (HC2 and HC58) and the low pH form of HA (H9) were previously prepared in BALB/c mice using SP20/0-Ag14 myeloma cells as described by Sugrue *et al.,* (1990a).

Immunofluorescence

MEL cell monolayers attached to poly-L-lysine coated coverslips were washed twice with PBS and fixed with 3.7% paraformaldehyde for 10 minutes at RT. The cells were then washed three times with PBS before permeabilization with 0.5% Triton X-100 in CSK buffer (100mM NaCl, 300mM sucrose, 10mM PIPES pH6.8, 3mM $MgCl_2$ and 1mM EDTA) for 10 minutes at RT. After three further washes in PBS, non-specific antibody binding was blocked by incubation for 15 minutes at RT with 3% BSA in PBS. After washing with 0.2% BSA in PBS (PBS/BSA), a 1/100 dilution of the monoclonal antibodies HC58 and H9 (as described by Sugrue *et al.,* 1990a) was applied to the infected cells and a 1/500 dilution of the rabbit antiserum R53 (Sugrue *et al.,* 1990a) was applied to the induced cells. After 1 hour at 37°C, the cells were washed 6 times with PBS/BSA before incubation with either a 1/80 dilution of goat anti-rabbit immunoglobulinG-fluorescein isothiocyanate (IgG-FITC) conjugate (Sigma Chemical Co.) (cells stained with R53), or a 1/125 dilution of goat anti-mouse IgG-FITC conjugate (cells stained with HC2/HC58/H9) for 1 hour, again at 37°C. The coverslips were washed 6 times with PBS and mounted in Uvinert (BDH). Staining was observed using a Leitz Ortholux II microscope equipped for epifluorescence.

ELISA

Influenza virus-infected MEL cells or HA-expressing MEL cells were attached to 96-well plates as described previously (section 2.1 pp31). The cells were fixed with 0.05% (w/v) glutaraldehyde in PBS for 15 minutes at RT. After blocking with 3% BSA in PBS for 1 hour, the cells were incubated with a 1/1000 dilution of monoclonal antibodies HC58 or H9 in PBS/BSA. After 1 hour at 37°C the cells were washed 3 times in PBS/BSA and incubated for a further hour with a 1/2500 dilution of protein A-horseradish peroxidase (HRP) conjugate (BIO-RAD Laboratories blotting grade) in PBS/BSA. Cells were again washed 6 times with PBS before the addition of 50µl of citrate buffer (25mM sodium citrate: 25mM citric acid 4:3 (v/v) at pH4.5) containing 0.012% (w/v) H_2O_2 and 0.03% (w/v) 3,3',5,5'- tetramethyl benzidine dihydrochloride (TMB) (Sigma Chemical Co.). After the development of a blue colouration (2-5 minutes), the reaction was stopped by the addition of 1M H_2SO_4. The absorbance was measured at 450nm using a Labsystems Multiskan Biochromatic plate reader.

Western blotting

Induced MEL cells and influenza virus-infected MDCK cells were washed twice with ice cold PBS and lysed in a minimal volume of NP-40 extraction buffer (1% NP-40, 150mM NaCl, 1mM EDTA, 2mM phenylmethylsulphonylfluoride (PMSF), 5µg/ml aprotinin, 100µg/ml soyabean trypsin inhibitor, 20mM Tris-HCl pH7.5) for 10 minutes. Equal volumes of cell lysate and 2x sample buffer (125mM Tris-HCl pH6.8, 4% SDS, 20% glycerol, 100mM dithiothreitol (DTT) and 0.002% bromophenol blue as the dye) were combined and heated for 2 minutes at 100°C. The samples were analysed by electrophoresis on 12% SDS polyacrylamide gels (Laemmli, 1970). Rainbow® protein molecular weight markers (Amersham) in the size range 200 to 14.3kDa were used to estimate the molecular weights of the separated

proteins.

The proteins were then transferred onto an Immobilon-P 45µm pore size membrane (Millipore), using a Semi-Dry Electroblotter (ANCOS). The membrane was blocked for 1 hour at RT with a 10% solution of new-born calf serum (NBCS) and 0.2% tween in PBS (PBS/NBCS). A 1/500 dilution in PBS/NBCS of the R54 rabbit antiserum was applied for 1 hour at RT. The membrane was washed 3 times with PBS and then a 1/2500 dilution of the secondary layer protein A-HRP conjugate in PBS/NBCS was applied for 1 hour at RT. The membrane was again washed 3 times with PBS, before being placed for 1 minute in a solution containing an equal mix of ECL detection reagents 1 and 2 (ECL blotting kit Amersham). Finally the membrane was exposed to photographic film (X-ograph) until a satisfactory exposure was obtained.

Immuneprecipitation

Cells were lysed with a minimal volume of ice cold NP-40 extraction buffer for 10 minutes. 100µl of cell lysate were added to 600µl of binding buffer (0.5% NP-40, 150mM NaCl, 1mM EDTA, 0.25% (w/v) BSA and 20mM Tris-HCl pH8.0) and 2µl of either R7-90 or HC2 antibodies were added and incubated at 4°C overnight. A 100µl aliquot of a 10% solution of protein A-Sepharose (Pharmacia) in binding buffer was added and the tubes incubated at 4°C for 2 hours on a rotating wheel, to isolate the immune complexes. The protein A-Sepharose pellet was then washed 6 times with high salt buffer (1% Triton X-100, 650mM NaCl, 1mM EDTA and 10mM NaH_2PO_4 pH7.0) and once with PBS. The resulting pellet was resuspended in 80µl of 2x sample buffer and heated at 100°C for 5 minutes. The samples were analysed on 12% SDS polyacrylamide gels. Gels were placed in Fix solution (10% acetic acid, 25% isopropanol and 65% water) for 20 minutes at RT followed by incubation in Amplify (Amersham) for 30 minutes at RT (^{35}S and ^{3}H labelled

and ^{3}H labelled samples only), prior to being dried under vacuum overnight. The dried gels were then exposed to pre-flashed photographic film (KODAK X-OMAT AR) in the presence of an intensifying screen at -70°C.

2.7 DETERMINATION OF INTRACELLULAR pH

MEL cells (~10^{7}) were washed twice in MEM- (300g, 5 minutes 18°C). The cells were resuspended in 2ml of MEM- and incubated for 15 minutes at 37°C with 5μM seminaphthorhodafluor-1-acetoxymethyl ester (SNARF-1-AM) (Molecular Probes). After two washes, the cell pellet was resuspended in 350μl of Gey's medium buffered with 20mM HEPES pH7.1, transferred to a quartz cuvette and maintained at 37°C. Emission spectra were obtained for SNARF-1 from 550nm to 650nm, with an excitation wavelength of 534nm at 37°C, using a Perkin Elmer LS-50 fluorescence spectrophotometer. Dilutions of amantadine and rimantadine (Sigma Chemical Co.) were added to the cuvette medium.

Standard curves were obtained by incubating cells with 10μM nigericin (Sigma Chemical Co.) in Gey's medium buffered with 20mM HEPES, adjusted to various pH values.

2.8 VOLTAGE CLAMP TECHNIQUE

Ion conductance measurements were kindly carried out by Dr. Igor Chizhmakov, N.I.M.R.(Chizhmakov *et al.*, submitted). Isolated MEL cells were clamped in the whole cell configuration. The solution in the patch pipette contained 90mM N-methyl-D-Glucamine (NMDG), 180mM HEPES, pH7.3 or 180mM 2-(N-Morpholino)ethane sulphonic acid (MES), pH6.0 and 10mM ethylene glycol bis(β-aminoethyl ether)-N,N,N',N'-tetra-acetate (EGTA) and was allowed to equilibrate with the cell interior for 5 minutes before currents were recorded at RT using a patch clamp amplifier (AXO-PATCH 200A USA). Fast perfusion of the cell exterior with solutions of different pH

was performed using the U-tube method (Krishtal and Pidoplichko 1980). Extracellular solutions were prepared by mixing two stock solutions containing 280mM NMDG, 2mM $CaCl_2$ and 280mM MES or HEPES, 2mM $CaCl_2$ to give the desired pH. Cells were allowed to re-equilibrate with the bath solution for several minutes before re-perfusion at a different pH or different membrane potential.

2.9 MATERIALS

All bacterial and cell media was obtained from the media room at N.I.M.R. SOC medium was made according to the recipe:
20g Bacto tryptone, 5g yeast extract, 0.5g NaCl, 2.5mM KCl, 10mM $MgCl_2$, 20mM glucose pH7.0/L.

HEPES, MES and PIPES were purchased from Sigma Chemical Co. All other chemicals not specified were purchased from BDH.

RESULTS

RESULTS

3.0 EXPRESSION OF THE M2 PROTEIN IN MEL CELLS

3.1.0 MEL CELL EXPRESSION SYSTEM

A mammalian expression system using MEL cells was chosen due to the low level of intrinsic channel activity which makes the cells particularly suitable for the expression and study of an ion channel (Arcangeli *et al.*, 1987). Clones with stable high level expression can be obtained 3-4 weeks after transfection, thereby facilitating characterization of mutant M2 proteins. Avian H7 Weybridge and Rostock M2 cDNAs were chosen for this study as their function in the virus life cycle had already been partly characterized (Sugrue *et al.*, 1990a; Grambas *et al.*, 1992). Expression of M2 is regulated by the human β-globin locus control region (LCR) and promoter and is stimulated on the addition of an inducer (Needham *et al.*, 1992). Expression is not dependent on gene amplification, a problem which is inherent in many mammalian expression systems and is independent of the site of integration in the genome.

3.1.1 Expression of the Weybridge M2 cDNA

The Weybridge M2 cDNA and also the Weybridge deletion mutant designated $M2\Delta_{28\text{-}31}$ were cloned into the *Bgl*II site of plasmid pEV3 (Figure 1) as *Bam*HI restriction digest fragments from the vectors pMal.pntr and pCS respectively. The Rostock cDNA and all subsequent mutants were cloned into pEV3 as PCR products amplified from the series of vectors designated pUTL.7P1-11, with a 5' terminal *Eco*RI site and a 3' terminal *Bgl*II site. The vector pEV3 containing the M2 cDNA was electroporated into MEL-C88 cells to produce two transformed G418-resistant cell populations from which approximately 50 clones were analysed. Following the addition of 2% DMSO,

FIGURE 1: **THE EXPRESSION VECTOR pEV3**

The M2 cDNA was cloned into the polylinker region under the control of the human β-globin LCR and promoter as either a *Bam*HI restriction digest fragment into the *Bgl*II site or as an *Eco*RI/*Bgl*II PCR fragment into the corresponding sites in the polylinker. Prior to electroporation the vector was linearized at the unique *Pvu*I site located in the ampicillin resistance gene.

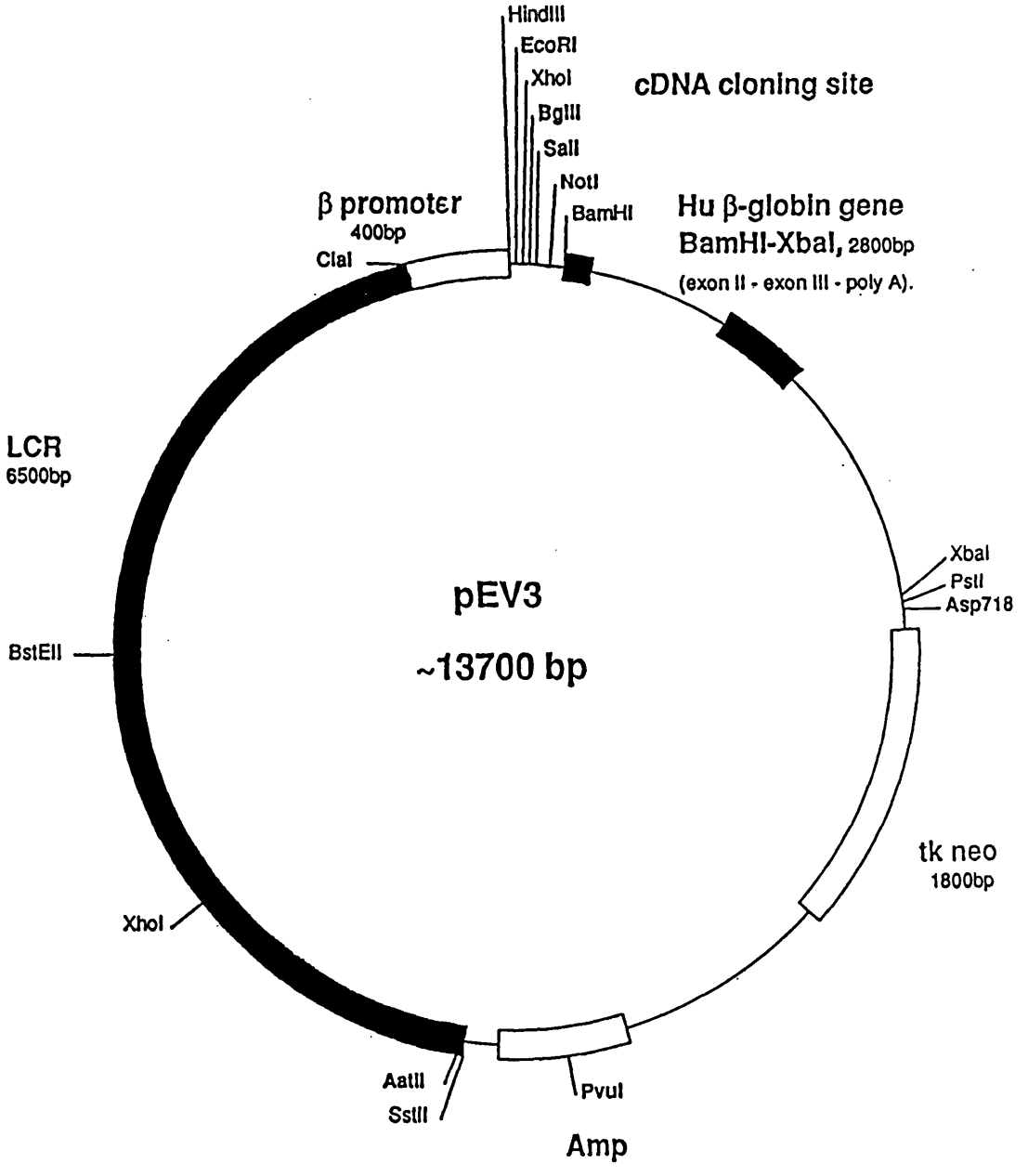
HindIII
EcoRI
XhoI
BglII
SalI
NotI
BamHI
cDNA cloning site
β promoter
400bp
ClaI
Hu β-globin gene
BamHI-XbaI, 2800bp
(exon II - exon III - poly A).
LCR
6500bp
XbaI
PstI
Asp718
pEV3
~13700 bp
BstEII
tk neo
1800bp
XhoI
AatII
SstII
PvuI
Amp

cells were harvested 4 days post induction for mRNA and protein analysis.

Analysis of mRNA production in the G418-resistant cells was performed using an S1 nuclease digestion assay. Two probes were utilized, one complementary to the 3' end of the human β-globin gene, thus probing for the M2/human β-globin chimeric mRNA, the other complementary to the murine β-major globin mRNA, providing an internal control for the efficiency of induction.

It has been noted that after a 2-3 day exposure to inducer, there is a 30-40 fold increase in levels of α and β-globin mRNA (Fraser *et al.,* 1987). Following induction there was a similar increase in the levels of chimeric M2/human β-globin mRNA in the G418-resistant cells. The transformed cells produced this chimeric mRNA at levels approximately equivalent to those of the endogenous mouse β-major globin mRNA (Figure 2A). Processing and maturation signals are provided by essential parts of the human β-globin gene and result in an increase in the stability of the hybrid mRNA (Needham *et al.,* 1992).

A comparison of uninduced and induced cells by Western blot analysis showed that there was a low level of constitutive expression in the uninduced cells of both populations which increased 3-5 fold following induction (Figure 2B). Under non-reducing conditions, both dimer and tetramer were present, indicating that the M2 protein was expressed in its native form and was able to associate into homotetramers (Sugrue *et al.,* 1991). Reducing conditions resulted in the conversion of tetramer and dimer to monomer (data not shown).

3.1.2 Selection of high expressing clones

Single cell clones were derived, in order to try and isolate high expressing clones which could then be used for functional studies of the M2 protein. Approximately 50 single cell clones were screened by protein dot

FIGURE 2: **mRNA PRODUCTION AND PROTEIN SYNTHESIS IN G418-RESISTANT MEL CELLS FOLLOWING INDUCTION**

A: After extraction of total RNA from both uninduced and 4 day induced G418-resistant MEL cell populations an S1 nuclease digestion assay was used to determine the level of M2/human β-globin mRNA. Two ^{32}-P end-labelled probes were hybridized to the RNA, one complementary to the M2/human β-globin DNA, the other complementary to the murine β-major globin RNA. The human ß-globin input probe was 700bp in length and the murine input probe was 500bp in length. After digestion with S1 nuclease, protected fragments of 212 base pairs (bp) and 96 bp were generated respectively. Left to right the lanes show induced untransformed cells (1) uninduced cell population A (2), induced population A (3), uninduced population B (4) and induced population B (5).

B: After Western blotting cell lysates made in parallel to those above, M2 was detected with the anti-M2 polyclonal serum R54 and a secondary donkey anti- rabbit antibody conjugated to I^{125} (DAR-I^{125}). The lanes are labelled in the same way as those shown above.

Increases in levels of RNA and protein were quantittated by microdensitometry.

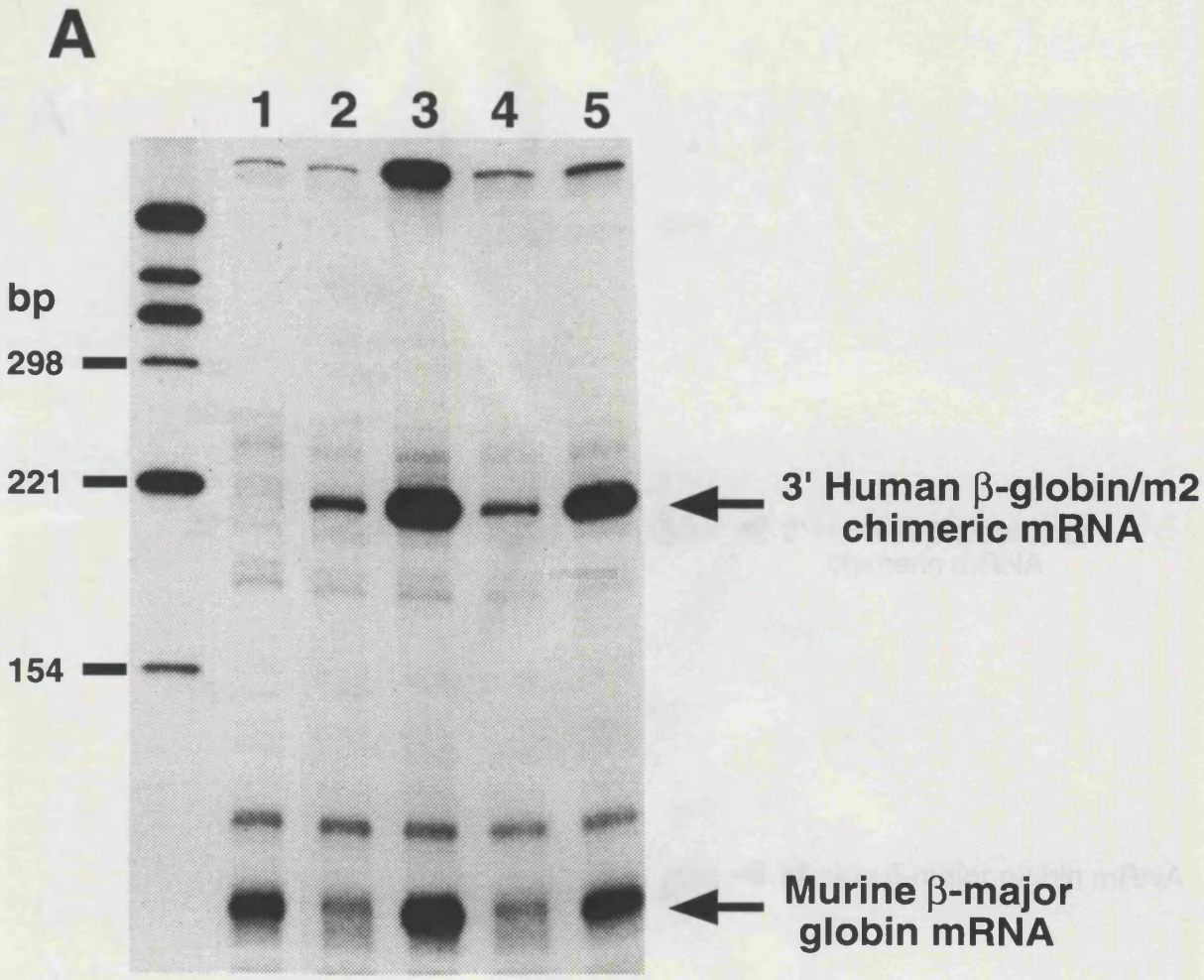
A
1 2 3 4 5
bp
298
221
154
3' Human β-globin/m2 chimeric mRNA
Murine β-major globin mRNA

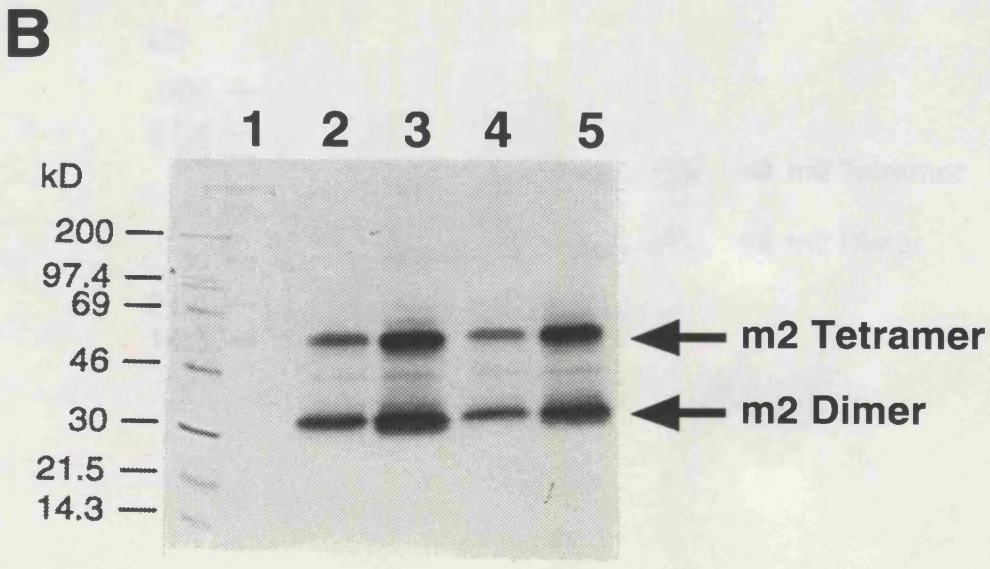
B
1 2 3 4 5
kD
200
97.4
69
46
30
21.5
14.3
m2 Tetramer
m2 Dimer

blot analysis. The results showed that only a few clones produced a larger amount of protein compared to the majority (Figure 3). A large proportion of the cells produced low amounts of the M2 protein. This is consistent with the results of immunofluorescence experiments on the transformed cell populations where only very few cells showed high levels of fluorescence. The majority of the population of M2-expressing cells showed an intermediate level of fluorescence (Figure 4).

Clones expressing different levels of M2 were selected for further analysis and the lysates compared by SDS-polyacrylamide gel electrophoresis (SDS-PAGE) and Western blotting, to assess more accurately the amount of M2 protein expressed (data not shown). One of the highest expressing clones, designated M2-39, was selected for subsequent studies.

3.1.3 Expression of the M2 protein

Following the addition of 2% DMSO, most of the morphological changes associated with differentiation occur 24-48 hours later. These changes include significant cell shrinkage, accumulation of globin mRNA, cessation of cell division and the production of haemoglobin which gives the cell pellet a characteristic red colouration. It was observed during the screening of M2-expressing clones that not all clones produced a red cell pellet following induction. However, these cells still expressed high levels of M2 and showed other morphological changes associated with induction.

Analysis of M2-39 cell lysates, showed a small level of constitutive expression which was probably due to spontaneous differentiation of the cells. This was followed by an increase in M2 protein levels, with the maximum level of M2 production occurring at approximately 3-4 days p.i.(Figure 5A[i] and [ii]). After this time the cumulative amount of M2 protein started to decline, probably due to the fact that terminal differentiation of the cells leads to cell death. Expression of high levels of M2 may also have had some deleterious

FIGURE 3: **DOT BLOT ANALYSIS OF G418-RESISTANT CELL CLONES**

Cell lysates were prepared at 4 days p.i. and 15µl of lysate was spotted onto a 45µm pore size nitrocellulose membrane. M2 was detected with the anti-M2 polyclonal serum, R54 and a secondary DAR-I^{125}. Uninduced (U) and induced (I) lysates are shown.

The M2-39 cell clone is underlined in black.

Untransformed uninduced and induced MEL-C88 control cells are shown underlined in red.

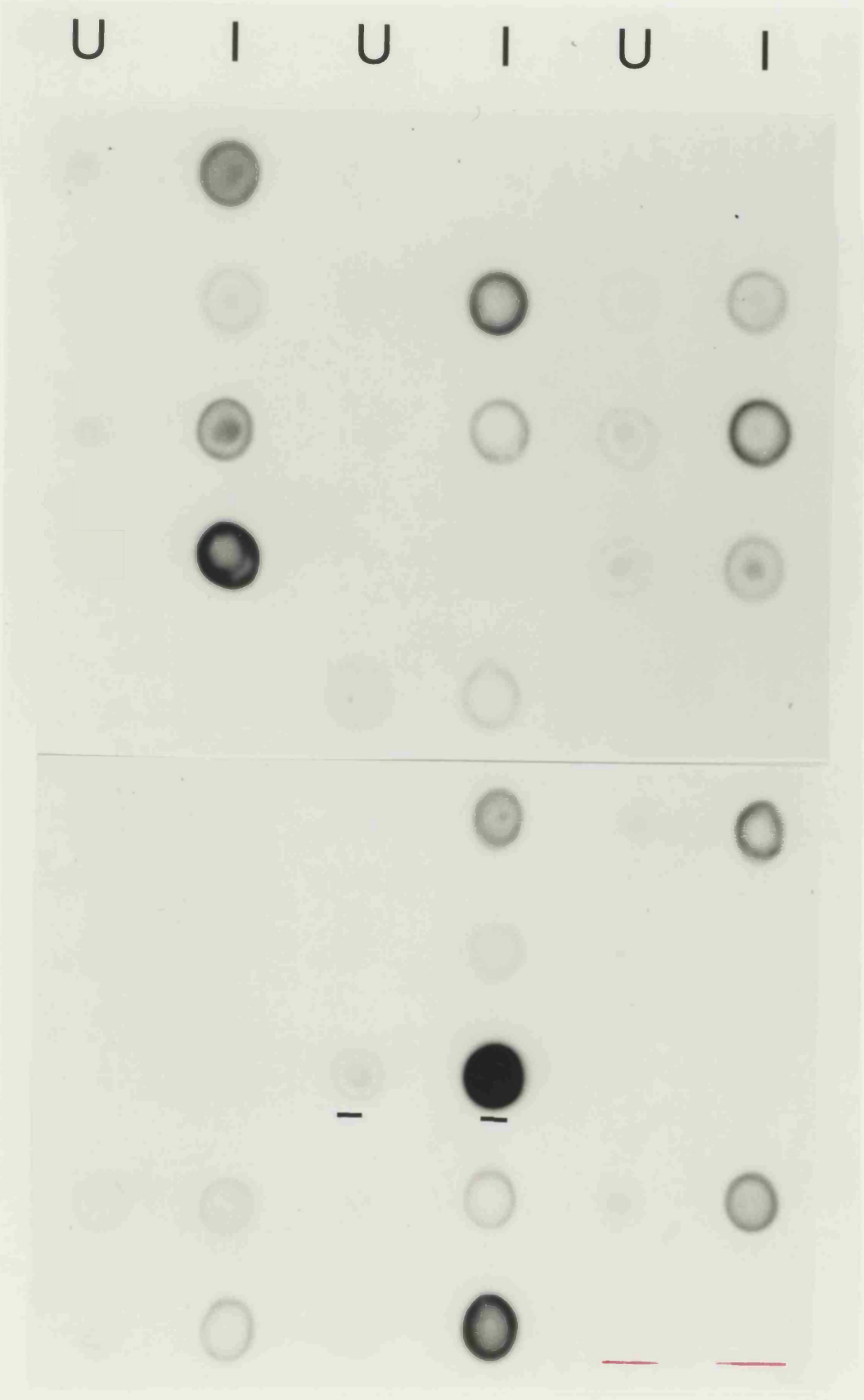
U
I
U
I
U
I

FIGURE 4: **THE DETECTION BY IMMUNOFLUORESCENCE OF M2 PRODUCED IN A G418-RESISTANT POPULATION OF MEL CELLS**

Uninduced (A) and 5 day induced populations of MEL cells (B) attached to poly-L-lysine treated coverslips were fixed with 3.7% paraformaldehyde and the N-terminal anti-M2 polyclonal serum, R53 was applied. M2 was visualized using a secondary goat anti-rabbit antibody conjugated to FITC (GAR-FITC). The cells were viewed under an Ortholux Leitz microscope equipped for epifluorescence.

Negligible levels of background fluorescence were obtained with untransformed MEL-C88 control cells (data not shown).

A

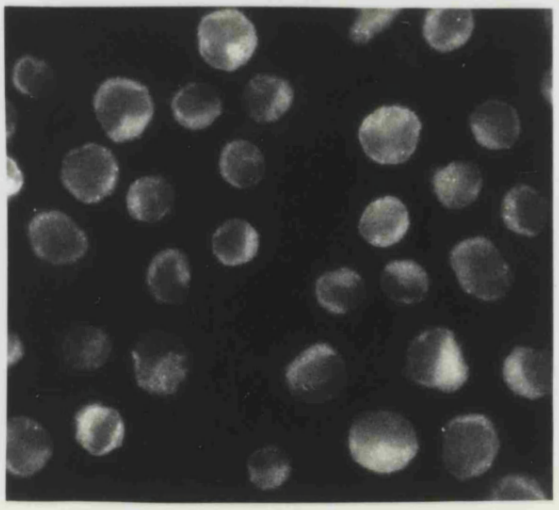

B

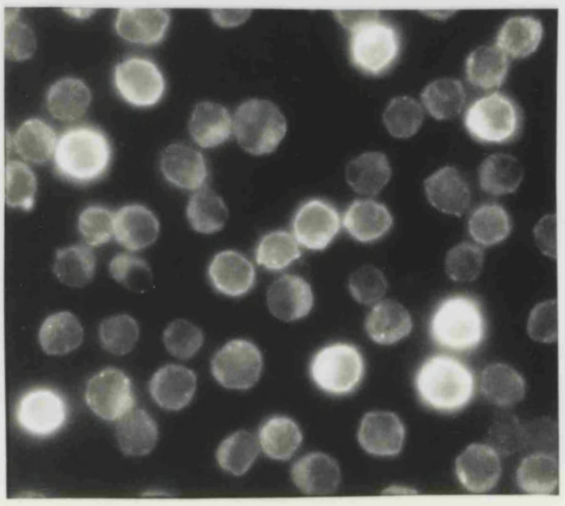

FIGURE 5: **AN INDUCTION TIME COURSE OF THE M2-39 AND R4-B CELL LINES**

A(i) and B(i): After Western blotting equal aliquots of M2-39 (A) and R4-B cells (B) lysed at various days p.i., the M2 protein was detected with a rabbit anti-M2 serum, R54 and the blots developed using a protein A-HRP conjugate and ECL reagent, before exposure to film. Untransformed MEL-C88 cells were used as a negative control.

A(ii) and B(ii): The relative amounts of M2 produced during induction, in arbitrary units, were determined by microdensitometry of the autoradiographs shown in part A and B.

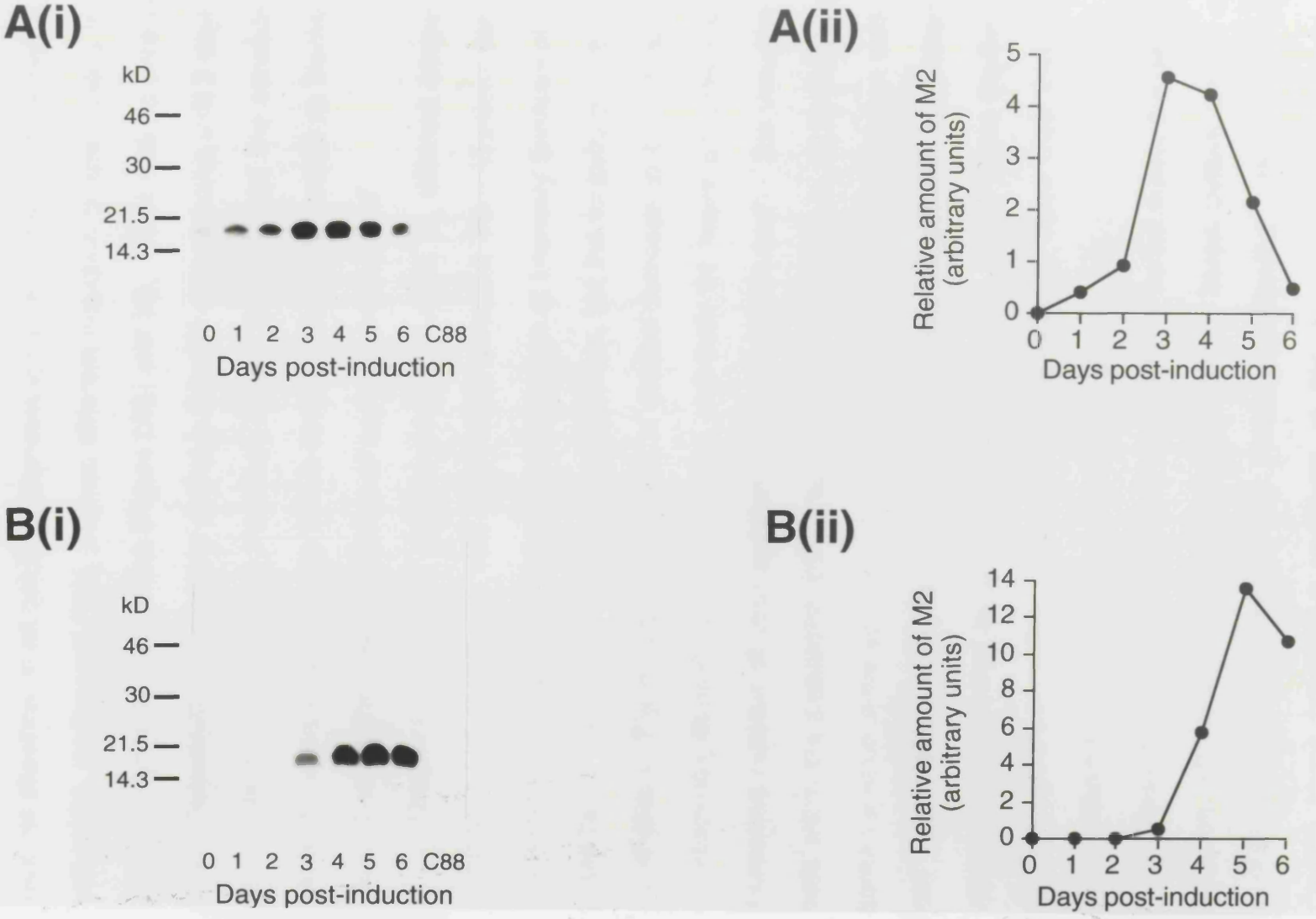
A(i)
kD
46
30
21.5
14.3
0 1 2 3 4 5 6 C88
Days post-induction
A(ii)
Relative amount of M2 (arbitrary units)
0 1 2 3 4 5
0 1 2 3 4 5 6
Days post-induction
B(i)
kD
46
30
21.5
14.3
0 1 2 3 4 5 6 C88
Days post-induction
B(ii)
Relative amount of M2 (arbitrary units)
0 2 4 6 8 10 12 14
0 1 2 3 4 5 6
Days post-induction

effect on the cells.

This gradual increase in the level of M2 accumulation from day 1 p.i. was not observed in all cell lines expressing the M2 protein. The Rostock M2 cell clone, designated R4B, showed different induction characteristics to the M2-39 Weybridge M2 cell line (Figure 5B[i] and [ii]). There was no detectable level of constitutive expression and very little M2 was detected until 3 days p.i. At 5 days p.i. it attained its maximum level. The R4B cell line consistently produced approximately three to five times as much M2 protein as the M2-39 cell line, when the maximum levels of each were compared.

Immunofluorescence studies on M2-39 cells at different stages of induction were consistent with the results obtained from Western blotting experiments (Figure 6). A very low percentage of intensely fluorescent cells could be visualized in the uninduced population, but the majority of cells were as shown in Figure 6A. There was a gradual increase in the intensity of fluorescence throughout the induction and from 24 hours p.i. onwards an increasing number of cells appeared to be "fully induced". The induction of cells within the population did not appear to be synchronous, as by 4 days p.i. some variation in the intensity of fluorescence was apparent between cells. A cell cycle-related event is needed for MEL cells to become committed to differentiate (reviewed by Marks and Rifkind, 1978), which would explain the variation between cells. The cells would need to have their cell cycle synchronized for homogeneous induction to occur.

To determine how the rate of M2 synthesis varied during the period of induction, M2-39 cells were attached to 35mm tissue culture dishes and incubated in the presence of ^{35}S cysteine/methionine. The M2-39 cells showed some constitutive synthesis of M2, followed by an increase in synthesis at 24 hours p.i. (Figure 7). The rate of synthesis remained constant throughout the remainder of the induction period. During induction there may be a change in protein turnover rate, which might account for the differences

FIGURE 6: **THE DETECTION BY IMMUNOFLUORESCENCE OF M2 PRODUCED FOLLOWING INDUCTION**

M2-39 cells attached to 3-APTS treated coverslips were fixed at different stages of induction with 3.7% paraformaldehyde and stained with the anti-M2 polyclonal serum, R7-90. M2 was visualized using a secondary GAR-FITC antibody. Untransformed MEL-C88 cells were used as a negative control. The cells were viewed under an Ortholux Leitz microscope equipped for epifluorescence.

(A) Uninduced cells, (B) 1 day p.i., (C) 2 days p.i., (D) 3 days p.i., (E) 4 days p.i..

Untransformed MEL-C88 control cells gave a negligible level of fluorescence (data not shown).

A

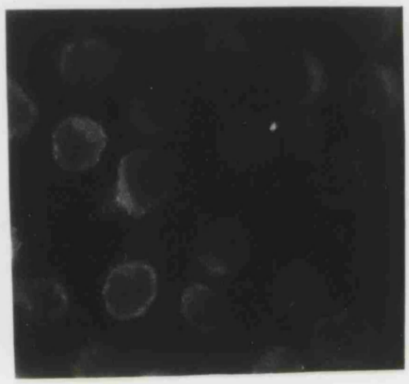

B

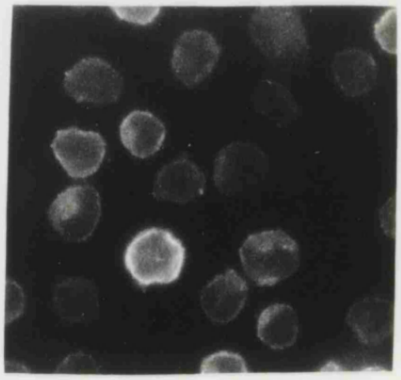

C

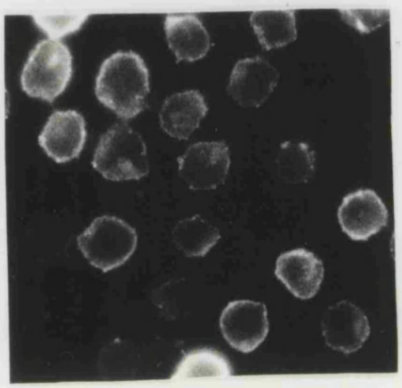

D

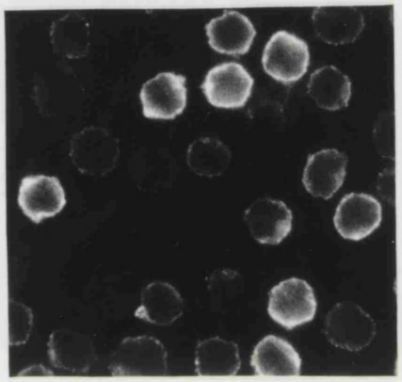

E

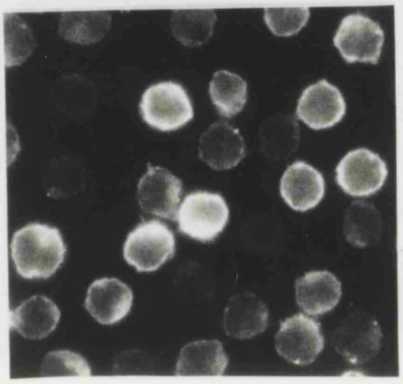

FIGURE 7: **THE SYNTHESIS OF M2 FOLLOWING INDUCTION**

M2-39 cells attached to 3-APTS treated 35mm tissue culture dishes were labelled with 10μCi [^{35}-S] cysteine/methionine for 1 hour at 37°C at different times p.i.. After lysis of the cells, the M2 protein was immuneprecipitated with the anti-M2 polyclonal antibody R7-90. Following SDS-PAGE the M2 immune-precipitates were detected by fluorography.

Uninduced cells are designated U and 1-5 represent the number of days p.i.. Untransformed 4 day induced MEL-C88 cells were used as a negative control.

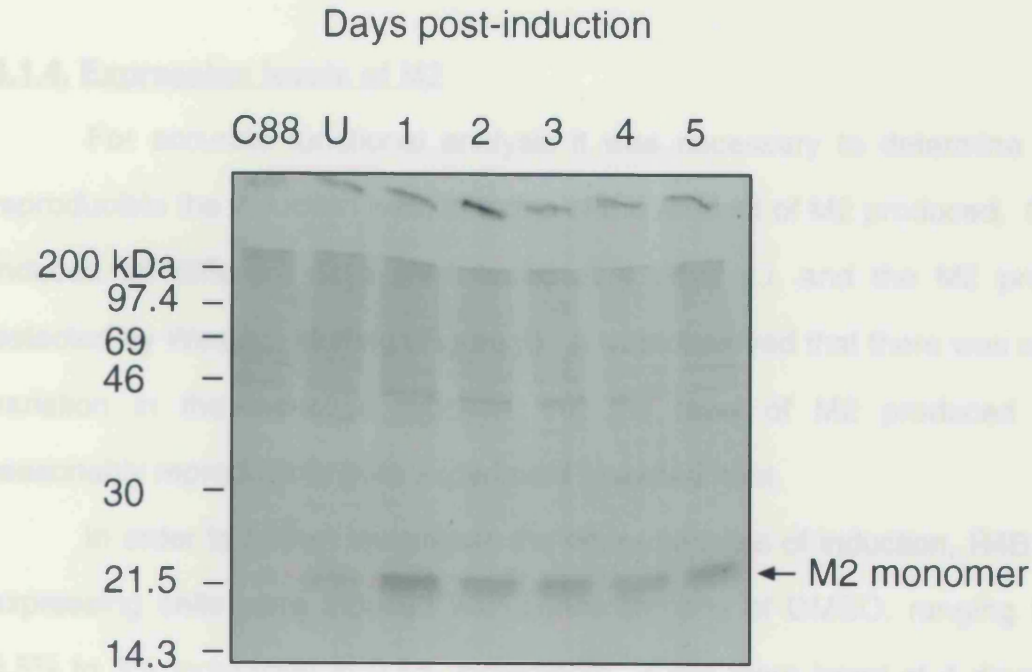

observed between the levels of protein synthesis and accumulation.

3.1.4. Expression levels of M2

For accurate functional analysis it was necessary to determine how reproducible the induction was, in terms of the amount of M2 produced. Cells induced on different days were lysed at 4 days p.i. and the M2 protein detected by Western blotting (Figure 8). It was observed that there was some variation in the induction process, but the level of M2 produced was reasonably reproducible from experiment to experiment.

In order to further investigate the characteristics of induction, R4B M2-expressing cells were induced with concentrations of DMSO, ranging from 0.5% to 3% increasing in 0.5% increments. Cells were lysed at 4 days p.i. and the M2 detected by Western blotting (Figure 9). A concentration of 0.5% to 1% DMSO resulted in a low level of induction and correspondingly a low level of M2 production. A concentration of 1.5% to 2% DMSO produced approximately equivalent amounts of M2, which were higher than those obtained with 0.5-1.0% DMSO. Maximum M2 production was obtained with 2.5% DMSO, but cell viability was compromised. At a concentration of 3% DMSO, there seemed to be some inhibition of cell growth and by 4 days p.i. cell viability was seriously affected as determined by visual inspection of the cells. In view of these results it was decided to continue using 2% DMSO for the purpose of induction.

M2 has also been expressed in *Spodoptera frugiperda* cells using a recombinant baculovirus. On the addition of 5μM amantadine, the yield of M2 increased by about 10 fold (Black *et al.*, 1993; Schroeder *et al.*, 1994). It is thought that the ion channel activity of the expressed M2 impaired cell viability and the addition of amantadine overcame this effect. Western blot analysis of M2-39 cells induced in the presence and absence of amantadine or rimantadine showed that neither drug had a significant effect on the

FIGURE 8: **THE REPRODUCIBILITY OF INDUCTION**

After Western blotting lysates of 4 day induced R4-B cells, the M2 protein was detected with the polyclonal serum, R54 and the blot developed using a protein A-HRP conjugate and ECL reagent.

Lanes 1-5 show 4 day-induced lysates prepared on different days.

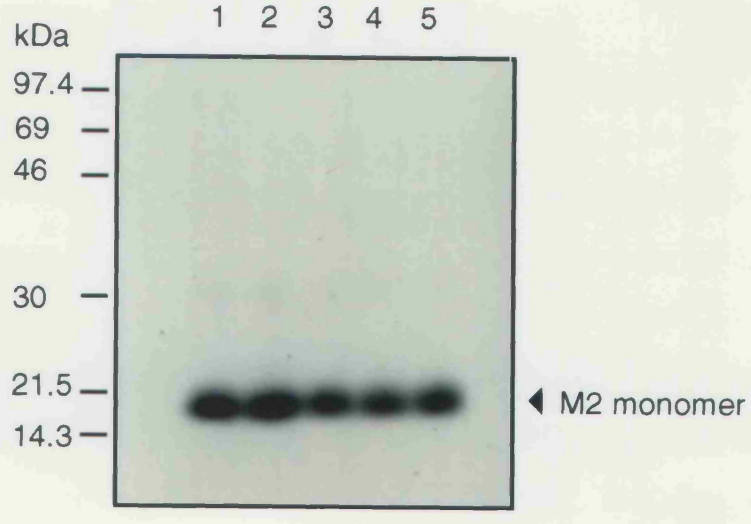

FIGURE 9: **THE EFFECT OF DMSO CONCENTRATION ON M2 PRODUCTION**

R4-B cells were induced with varying concentrations of DMSO and lysed at 4 days p.i.. After Western blotting, the M2 protein was detected using the polyclonal anti-serum, R54 and the blot was developed with a protein A-HRP conjugate and ECL reagent.

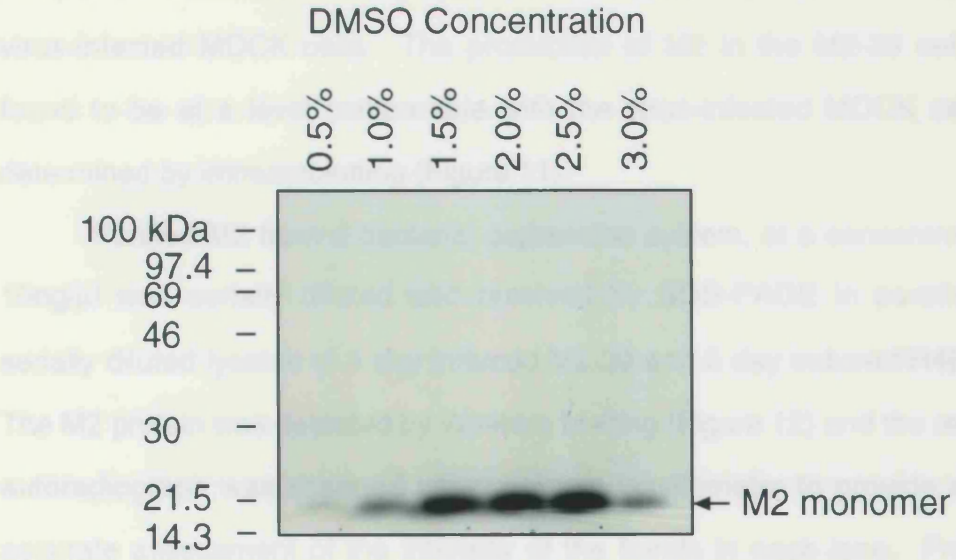

production of M2, even at the higher concentration of 50μM (Figure 10).

In order to estimate the level of M2 production in the M2-39 cells, comparable numbers of 4 day induced cells were compared with Weybridge virus-infected MDCK cells. The production of M2 in the M2-39 cells was found to be at a level comparable with the virus-infected MDCK cells, as determined by immunoblotting (Figure 11).

Purified M2 from a bacterial expression system, at a concentration of 10ng/μl was serially diluted and resolved by SDS-PAGE in parallel with serially diluted lysates of 4 day induced M2-39 and 5 day induced R4B cells. The M2 protein was detected by Western blotting (Figure 12) and the resulting autoradiograph was scanned using a microdensitometer to provide a more accurate assessment of the intensity of the bands in each lane. From the microdensitometer scan, it was possible to estimate the cumulative levels of M2 for each cell line. At 5 days p.i. the R4B cell line produced ~700ng M2 per 10^6 cells and at 4 days p.i. the M2-39 cell line produced ~100ng M2 per 10^6 cells. These results were similar to those obtained by other workers in the laboratory (F.Barr and M. Prudden, personal communication).

3.2.0 CHARACTERISTICS OF THE M2 PROTEIN

3.2.1. Post-translational modifications

M2 produced within virus-infected MDCK cells is modified by the addition of palmitate and phosphate functional groups. It was therefore important to determine whether the M2 expressed in MEL cells possessed these modifications. Metabolic labelling of 4 day induced cells showed that the M2 expressed in MEL cells was both phosphorylated (Figure 13A) and palmitoylated (Figure 13B).

FIGURE 10: **THE EFFECT OF RIMANTADINE AND AMANTADINE ON M2 PRODUCTION**

M2-39 cells were induced with 2% DMSO in the presence of rimantadine or amantadine or in the absence of either drug. After Western blotting cell lysates obtained from 4 day induced cells, the M2 protein was detected using the anti-M2 polyclonal serum R54 and the blot developed with a protein A-HRP conjugate and ECL reagent.

FIGURE 11: **A COMPARISON BY WESTERN BLOTTING OF M2 PRODUCED IN MEL CELLS AND VIRUS-INFECTED MDCK CELLS**

Uninduced and 4 day induced M2-39 cells attached to 35mm poly-L-lysine coated tissue culture dishes were lysed in NP-40 extraction buffer. MDCK cells grown in 35mm tissue culture dishes and infected with Weybridge virus were lysed at 6 hours post-infection. After Western blotting the MEL cell and infected MDCK cell lysates, the M2 protein was detected with the anti-M2 polyclonal serum R54 and a secondary DAR-I^{125}.

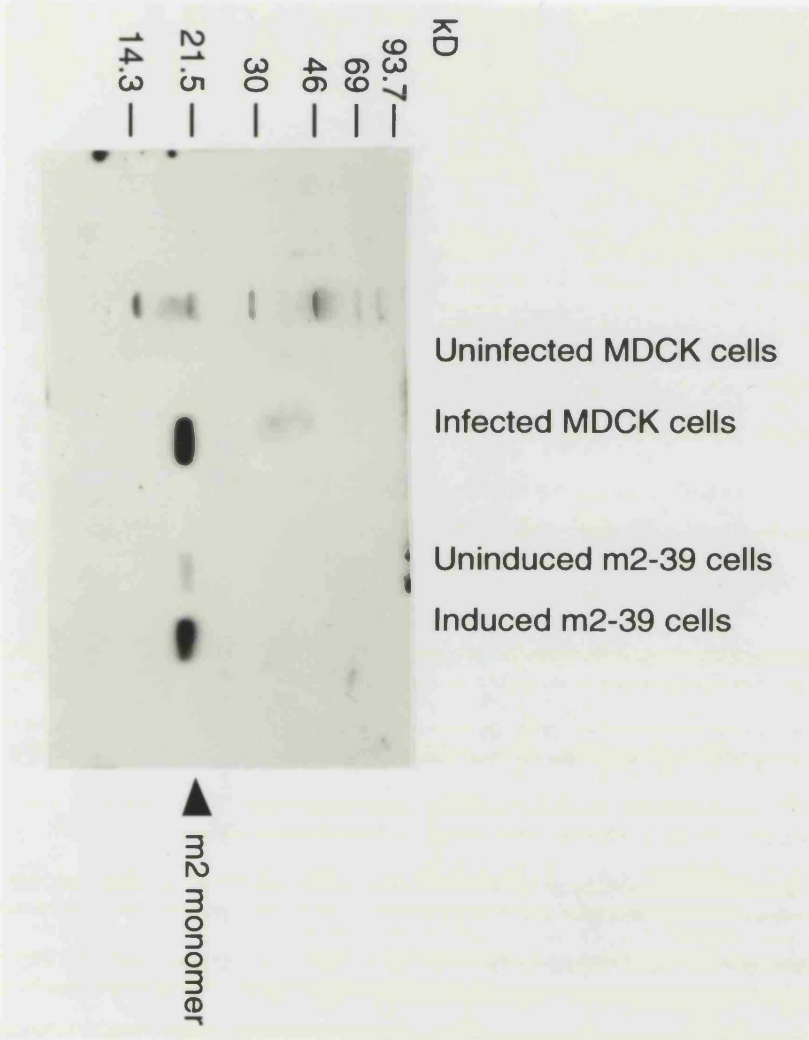
kD
93.7
69
46
30
21.5
14.3
Uninfected MDCK cells
Infected MDCK cells
Uninduced m2-39 cells
Induced m2-39 cells
m2 monomer

FIGURE 12: **QUANTITATION OF M2 EXPRESSION LEVELS IN THE M2-39 AND R4-B CELL LINES**

Purified M2 produced from a bacterial expression system (A.Hayhurst, unpublished results) was serially diluted from 50ng to 6.25ng (panel A) and the samples were subject to Western blotting. Serially diluted lysates of 4 day induced M2-39 cells (panel B) and 5 day induced R4-B cells (panel C) were also Western blotted and the M2 protein was detected using an anti-M2 polyclonal serum, R54. The blots were developed using a protein A-HRP conjugate and ECL reagent. The relative amounts of M2 were determined by microdensitometry of the autoradiographs.

A

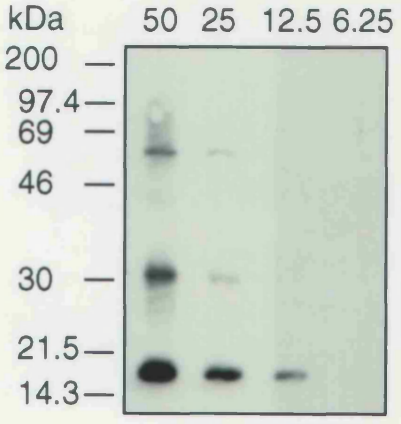

B

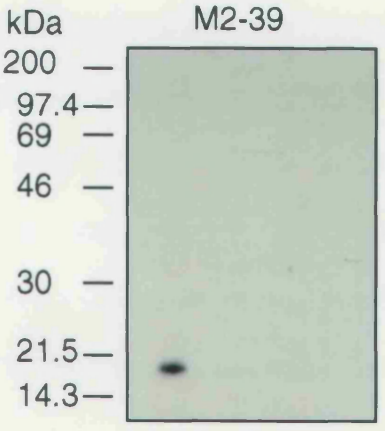

C

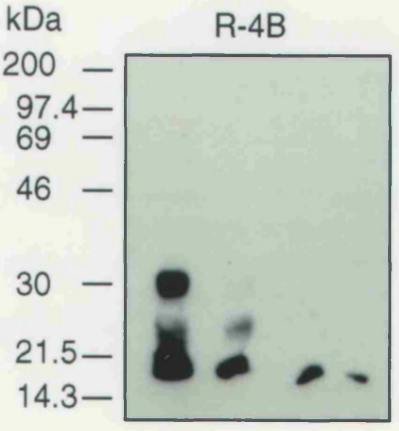

FIGURE 13: **POST-TRANSLATIONAL MODIFICATIONS OF THE EXPRESSED M2**

A: MEL cells at 4 days p.i. were attached to 3-APTS-treated 35mm tissue culture dishes and incubated for 4 hours in MEM- lacking phosphate to deplete intracellular phosphate stores. 0.25mCi of [^{32}P] orthophosphate was added to the cells in 0.5ml of phosphate-free MEM- and the cells incubated for a further 4 hours at 37°C. After lysis of the cells, the M2 was immuneprecipitated from the samples using the anti-M2 polyclonal serum, R7-90. The samples were heated to 100°C before SDS-PAGE on a 20% gel. The gel was subsequently dried under vacuum overnight and then exposed to film. Untransformed MEL-C88 cells were used as a negative control.

B: MEL cells at 4 days p.i. were attached to 3-APTS-treated tissue culture dishes and incubated in MEM- containing 5mM sodium pyruvate with 0.25mCi of [^{3}H]- [9,10 (n)]-palmitic acid for 4 hours at 37°C. The cells were then lysed and the M2 immuneprecipitated with the anti-M2 polyclonal serum, R7-90. After SDS-PAGE on a 20% gel, the M2 immuneprecipitates were detected by fluorography. Untransformed MEL-C88 cells were used as a negative control.

A

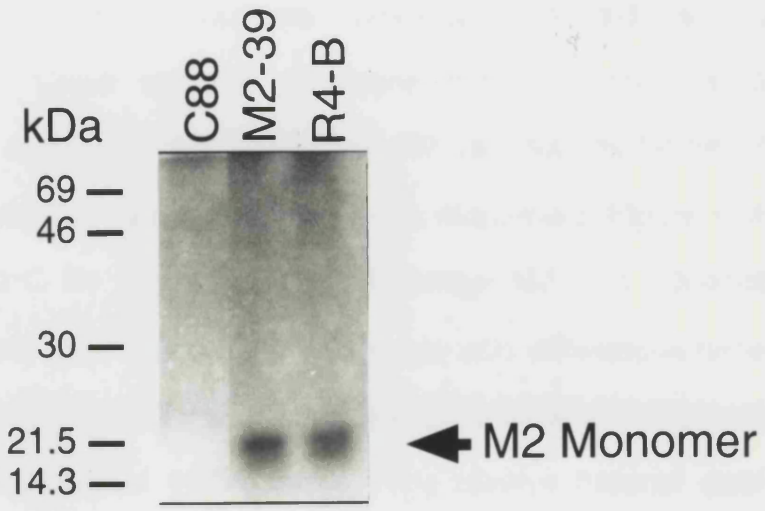
kDa
C88
M2-39
R4-B
69
46
30
21.5
14.3
M2 Monomer

B

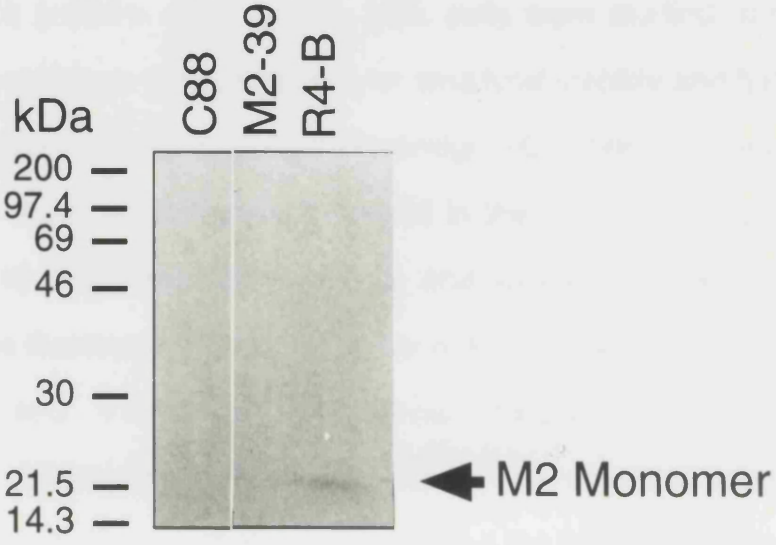
kDa
C88
M2-39
R4-B
200
97.4
69
46
30
21.5
14.3
M2 Monomer

3.2.2 Structural characteristics of M2 expressed in MEL cells

It has been shown previously that Rostock and Weybridge M2 tetramers have distinct structural properties (A.Hayhurst, personal communication). Under reducing conditions in the presence of SDS, but without heating at 100°C, the Weybridge M2 retained its tetrameric form, whereas the Rostock tetramer dissociated into monomers (Figure 14A). After treatment at 100°C for 2 minutes, the Weybridge M2 also dissociated into monomers. These data suggest that the amino acid differences between the Rostock and Weybridge M2 proteins appear to have some differential effect on the thermal stability of the tetramer. The relative thermal stabilities of Rostock and Weybridge M2 expressed in MEL cells were found to correlate with M2 produced in virus-infected cells (Figure 14B). Under reducing conditions at RT Weybridge tetramer was observed, whereas the Rostock tetramer dissociated into monomers. Under reducing conditions, the Weybridge tetramer was stable at 25°C, however heating at 100°C resulted in dissociation of the tetramer to monomer.

3.2.3. Structural characteristics of M2 mutants

Mutant M2 proteins expressed in MEL cells were studied to try and determine which residues were important for structural stability and functional differences between the Rostock and Weybridge M2 proteins. Two amino acid differences occur at positions 18 and 20 in the external domain of the protein. Serine 18 is replaced with arginine and serine 20 is replaced with asparagine in the Rostock M2 protein. Under reducing conditions M2 mutant proteins S20N and S18R/S20N had similar thermal stabilities to the Weybridge form of the protein (Figure 15A and B), indicating that residues 18 and 20 do not play an important role in determining the thermal stability of the Weybridge M2 tetramer. Tetrameric M2 protein was observed at 25°C and began to dissociate at 55°C.

FIGURE 14: **STRUCTURAL CHARACTERISTICS OF M2 PRODUCED IN VIRUS-INFECTED MDCK CELLS AND M2 EXPRESSED IN MEL CELLS**

A: MDCK cells infected with either a reassortant Weybridge (15B) or Rostock (BR02A) virus were lysed at 6 hours post-infection. 50mM DTT was added to the samples and they were either left at 25°C or heated at 100°C for two minutes. After Western blotting the M2 protein was labelled with the anti-M2 polyclonal serum, R54 and the blot developed using a protein-HRP conjugate and ECL reagent.

B: M2-expressing MEL cells were lysed at 4 days p.i. in NP-40 extraction buffer. Reducing agent was added to the samples which were then left at 25°C. or heated at 100°C for two minutes. After Western blotting the M2 protein was labelled using the polyclonal serum, R54 and the blot developed with a protein A-HRP conjugate and ECL reagent.

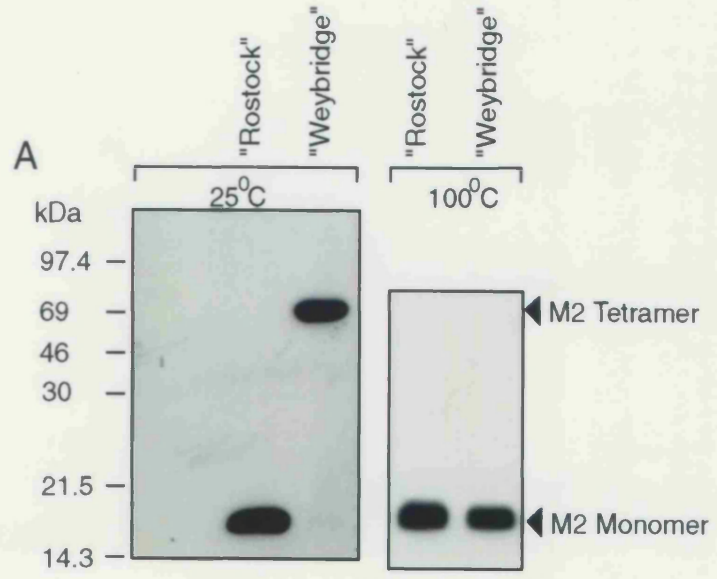
A
"Rostock"
"Weybridge"
"Rostock"
"Weybridge"
25°C
100°C
kDa
97.4
69
46
30
21.5
14.3
M2 Tetramer
M2 Monomer

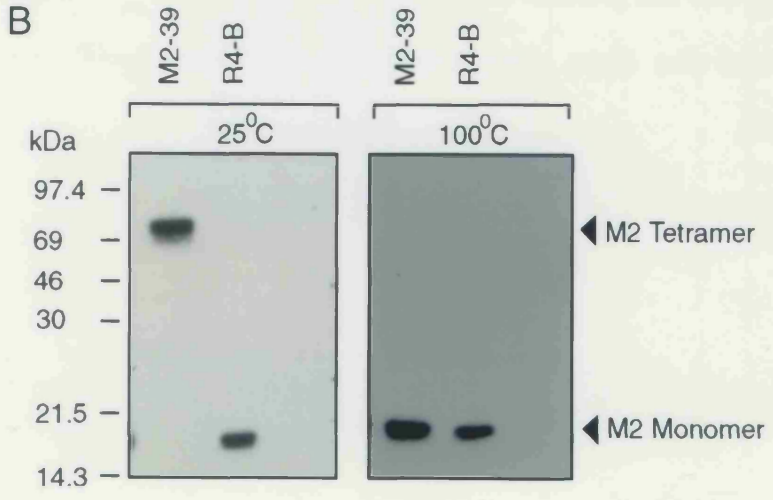
B
M2-39
R4-B
M2-39
R4-B
25°C
100°C
kDa
97.4
69
46
30
21.5
14.3
M2 Tetramer
M2 Monomer

FIGURE 15: **TEMPERATURE DEPENDENCE CHARACTERISTICS OF M2 MUTANT PROTEINS S20N AND S18R/S20N**

Lysates of 4 day induced M2-expressing MEL cells were heated to different temperatures for 3 minutes in the presence of reducing agent. After Western blotting the M2 protein was labelled with the anti-M2 polyclonal rabbit serum, R54 and the blots developed with a protein A-HRP conjugate and ECL reagent.

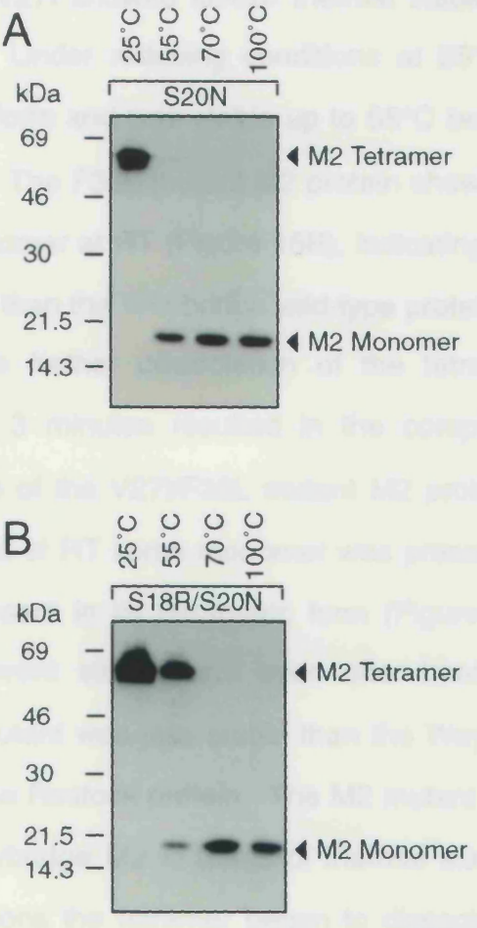

N.I.M.R. London, NW7 1AA.

Three differences in amino acid sequence between Rostock and Weybridge M2 proteins occur within the transmembrane domain of the protein. Valine 27 is replaced with isoleucine, phenylalanine 38 with leucine and aspartic acid 44 with asparagine in the Rostock M2 protein. Weybridge M2 with the mutation V27I showed similar thermal stability to the wild-type protein (Figure 16A). Under reducing conditions at 25°C, the M2 protein retained its tetrameric form and was stable up to 55°C before dissociation of the tetramer occurred. The F38L mutant M2 protein showed the presence of both tetramer and monomer at RT (Figure 16B), indicating that this particular mutant was less stable than the Weybridge wild-type protein. Upon heating to 55°C there was some further dissociation of the tetramer to monomer. Heating to 100°C for 3 minutes resulted in the complete breakdown of tetramer. Investigation of the V27I/F38L mutant M2 protein under reducing conditions revealed that at RT some monomer was present, but the majority of the protein was present in its tetrameric form (Figure 16C). Significant amounts of tetramer were still present even after heating to 70°C for 3 minutes. Again this mutant was less stable than the Weybridge M2 protein, but more stable than the Rostock protein. The M2 mutant protein V27I/D44N was similar to the Weybridge M2 in terms of thermal stability (Figure 16D). Under reducing conditions the tetramer began to dissociate to monomer at about 55°C and upon heating to 70°C, monomer was the predominant species detected. Substitution of all three amino acids to the Rostock transmembrane domain sequence i.e. V27I/F38L/D44N resulted in complete destabilization of the tetramer at 25°C under reducing conditions (Figure 16E). Therefore, substitution of the Weybridge transmembrane domain with the Rostock sequence converted the protein structurally from the Weybridge to the Rostock form.

FIGURE 16: **TEMPERATURE DEPENDENCE CHARACTERISTICS OF WEYBRIDGE M2 PROTEINS WITH MUTATIONS WITHIN THE TRANSMEMBRANE DOMAIN**

Aliquots of cells expressing the mutant M2 proteins V27I (panel A), F38L (panel B), V27I/F38L (panel C), V27I/D44N (panel D) and V27I/F38L/D44N (panel E) were lysed in NP-40 extraction buffer containing 50mM DTT. The samples were left at RT or heated to different temperatures for 3 minutes. After Western blotting the M2 protein was labelled with the anti-M2 polyclonal rabbit serum, R54 and the blots developed with a protein A-HRP conjugate and ECL reagent.

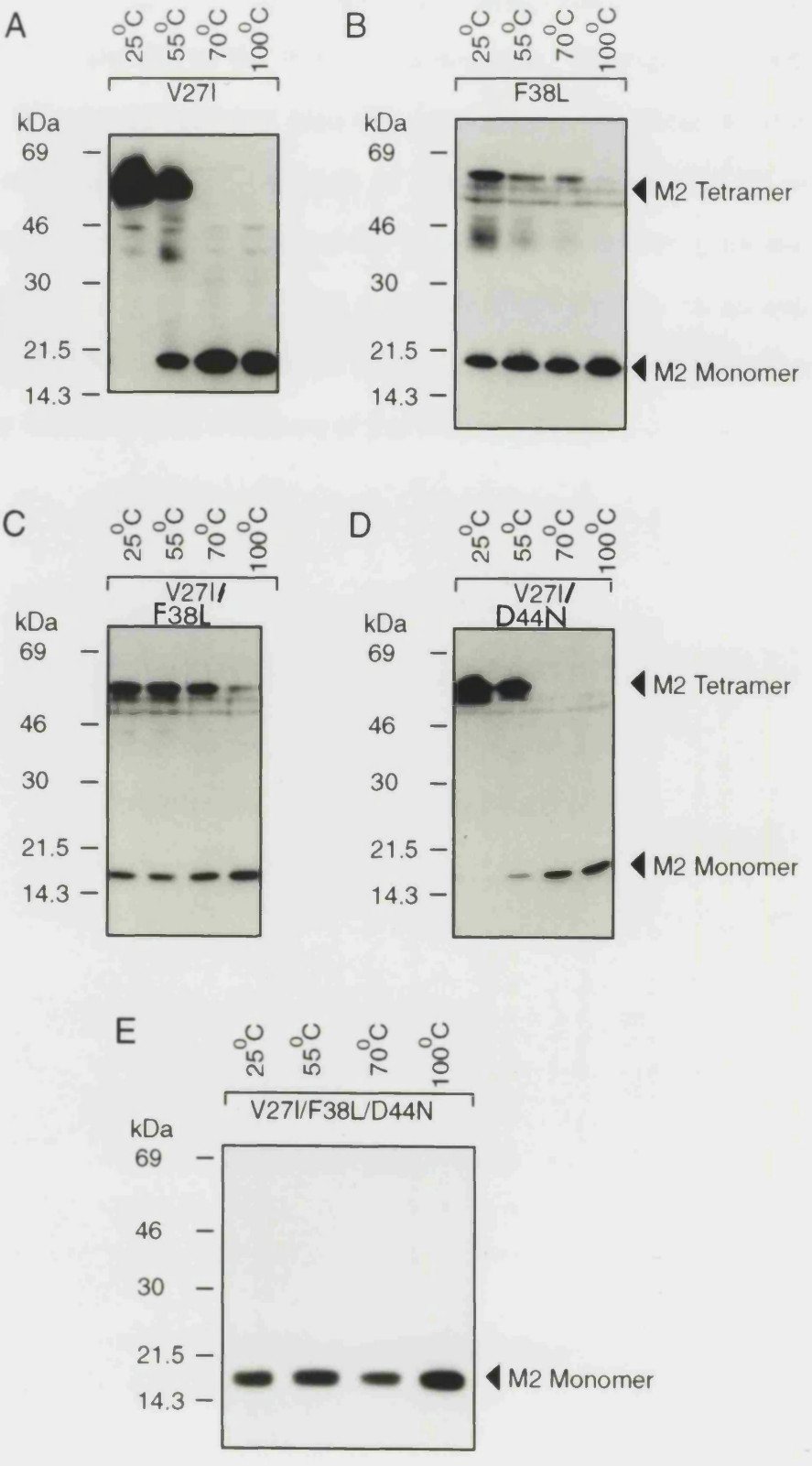
A
25°C
55°C
70°C
100°C
V27I
kDa
69
46
30
21.5
14.3
B
25°C
55°C
70°C
100°C
F38L
kDa
69
46
30
21.5
14.3
M2 Tetramer
M2 Monomer
C
25°C
55°C
70°C
100°C
V27I/
F38L
kDa
69
46
30
21.5
14.3
D
25°C
55°C
70°C
100°C
V27I/
D44N
kDa
69
46
30
21.5
14.3
M2 Tetramer
M2 Monomer
E
25°C
55°C
70°C
100°C
V27I/F38L/D44N
kDa
69
46
30
21.5
14.3
M2 Monomer

The results of the thermal stability experiments are summarized in Table 1. To conclude, altering the external domain residues 18 and 20 had no effect on the stability of the Weybridge tetramer. Changes at position 27 alone and 27 and 44 together also did not seem to significantly affect the tetramer stability, however, changes at position 38 alone and 27 and 38 together did influence the stability of the tetramer, both acting to cause some destabilization. As the change V27I does not affect stability on its own, this suggests that the phenylalanine at position 38 plays an important role in maintaining the tetrameric structure of the Weybridge M2.

TABLE 1: **STRUCTURAL PROPERTIES OF MUTANT M2 PROTEIN TETRAMERS**

Weybridge mutant M2 protein	Thermal stability of M2 mutant
S20N	Weybridge
S18R/S20N	Weybridge
V27I	Weybridge
F38L	Intermediate
V27I/F38L	Intermediate
V27I/D44N	Weybridge
V27I/F38L/D44N	Rostock

A summary of the thermal stability properties of mutant M2 protein tetramers. M2-expressing MEL cells were lysed at 4 days p.i. and the lysates treated at various temperatures before the proteins were resolved by SDS-PAGE on 12% gels. Following transfer onto Immobilon-P, the M2 protein was detected using the anti-M2 polyclonal rabbit serum, R54 and the blot developed with a protein A-HRP conjugate and ECL reagent.

This table is based on the data shown in Figures 15 and 16.

4.0 FUNCTIONAL STUDIES ON M2

4.1.0 Introduction

Previous studies have shown that production of HA in the native conformation is dependent on the pH regulatory function of the M2 protein (Grambas and Hay, 1992; Grambas *et al.*, 1992). Due to the acid-sensitive nature of HA, conformational changes in the HA glycoprotein can be utilized as a probe to provide an indication of M2 activity. MEL cells were investigated to determine whether they had the potential to be used to provide an environment for M2-dependent HA expression, in order to study M2 activity in both the wild type and mutant proteins.

4.1.1 The production of influenza virus proteins in infected MEL cells

MEL cells and CEF were infected with a reassortant virus designated BR02A, which contained the Rostock HA and M genes and labelled with ^{35}S-cysteine/methionine at various time intervals post-infection. The infection of MEL cells proceeded more slowly than that of CEF (Figure 17A and B). Viral proteins could be visualized from 2 hours post-infection in the CEF, in contrast to MEL cells where they were not detectable until 6 hours post-infection. The three polymerase proteins PB1, PB2 and PA, HA0, NP and NS proteins could be seen in both cell types. The matrix protein was difficult to detect in the MEL cells, in contrast to the CEF, where it could be clearly seen at 6 hours post-infection. This result is similar to other cell types such as L cells which are non-permissive to influenza A virus infection (Bosch *et al.*, 1978; Lohmeyer *et al.*, 1979).

M2 and HA were immuneprecipitated using a polyclonal serum, R53 and a monoclonal antibody HC2 respectively. The MEL cells produced a similar amount of HA to the CEF (Figure 17C). There was less HA0 present in the CEF, in contrast with the MEL cells. This could have been due to a

FIGURE 17: **THE PRODUCTION OF VIRAL PROTEINS IN MEL AND CEF CELLS DURING AN INFLUENZA A VIRUS INFECTION**

A and B: Uninfected (U) and BR02A infected CEF (A) and C88 cells (B) were labelled for one hour with 10μCi/200μl [^{35}S]-cysteine/methionine trans label. Infected cells were labelled at 2, 6, 10 and 25 hours post-infection. After washing, the cells were lysed with NP-40 extraction buffer and the proteins resolved by SDS-PAGE on 12% gels. The labelled proteins were detected by fluorography.

C: Cell lysates made at 6 hours post-infection were incubated with R53, an anti-M2 polyclonal serum or HC2, an anti-HA monoclonal antibody which recognizes most forms of HA. After incubation with protein-A Sepharose, immuneprecipitates were washed and loaded onto a 12% polyacrylamide gel, and detected by fluorography.

Left to right the lanes show uninfected CEF R53 immuneprecipitate (1), uninfected MEL cell R53 immuneprecipitate (2), uninfected CEF HC2 immuneprecipitate (3), uninfected MEL cell HC2 immuneprecipitate (4), infected CEF R53 immuneprecipitate (5), infected MEL cell R53 immuneprecipitate (6), infected CEF HC2 immuneprecipitate (7) and infected MEL cell HC2 immuneprecipitate (8).

A

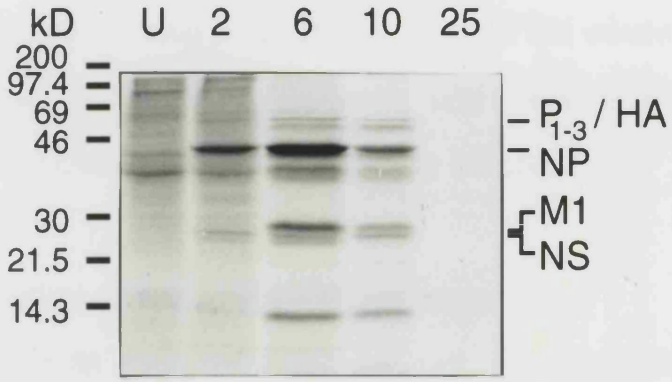
kD
U
2
6
10
25
200
97.4
69
46
30
21.5
14.3
P1-3 / HA
NP
M1
NS

B

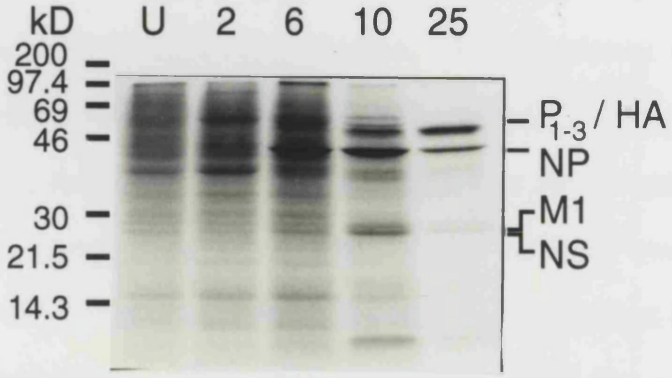
kD
U
2
6
10
25
200
97.4
69
46
30
21.5
14.3
P1-3 / HA
NP
M1
NS

C

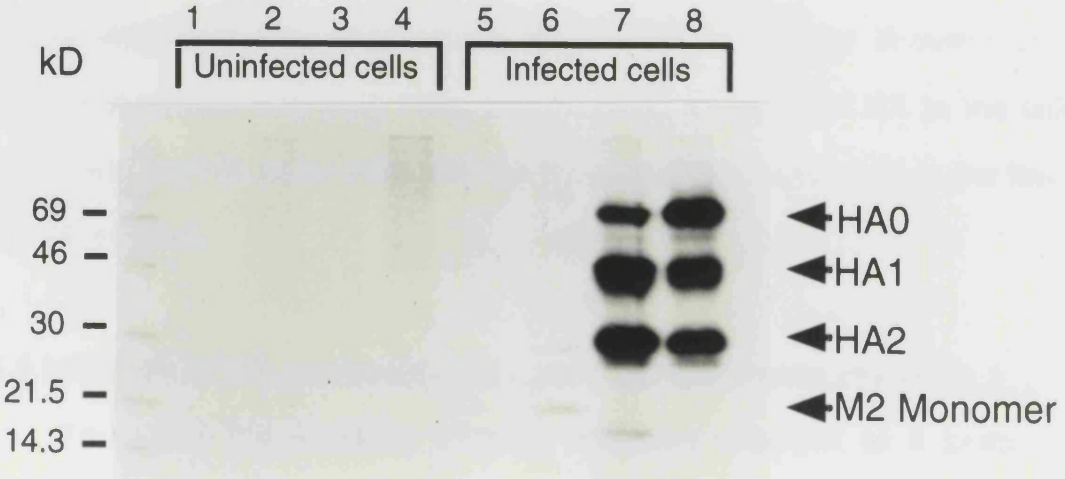
1
2
3
4
5
6
7
8
kD
Uninfected cells
Infected cells
69
46
30
21.5
14.3
HA0
HA1
HA2
M2 Monomer

slower rate of cleavage of HA0 to HA1 and HA2 in the MEL cells or a different control of cleavage. The HA produced in the infected MEL cells may also have been transported more slowly to the TGN where proteolytic cleavage occurs than in the CEF. An extra band was observed in the CEF M2 immuneprecipitate, the origin of which is obscure.

4.1.2 Infection of MEL cells with influenza virus

MEL-C88 cells were infected with the recombinant virus BR02A in order to determine their usefulness for co-expression studies of HA and M2. Monoclonal antibodies HC58 and H9 were used to locate the native and low-pH conformations respectively of HA and a polyclonal serum, R53, was used for the detection of M2. Native HA was located on the cell surface and also within the Golgi complex (Figure 18A). In accordance with studies on other cells infected with this virus (Ciampor *et al.*, 1992b), inhibition of M2 by amantadine resulted in altered expression of HA. Native HA was localized within the Golgi complex and there was minimal staining of surface HA (Figure 18B). The low pH form detected by H9 caused little surface staining, but resulted in the appearance of vesicles within the cell cytoplasm (Figure 18D). This is consistent with results obtained using virus-infected MDCK cells where inhibition of M2 by amantadine resulted in a similar pattern of HA expression (Ciampor *et al.*, 1992b). H9 produced low levels of fluorescence in cells untreated with amantadine (Figure 18C), thereby showing that following treatment with drug there was reduced transport of HA to the cell surface and the HA associated with the cytoplasmic vesicles was in the low-pH conformation.

4.1.3 Infection of M2-expressing MEL cells with influenza virus

To assess the feasibility of using influenza virus HA as a probe to measure the activity of M2 produced in M2-expressing MEL cells, C88 cells

FIGURE 18: **DETECTION OF HA BY IMMUNOFLUORESCENCE IN INFLUENZA A VIRUS-INFECTED MEL CELLS**

C88 cells attached to poly-L-lysine coated coverslips were fixed at 6 hours post-infection with methanol for 5 minutes at -20C which had been shown previously not to affect cell surface antibody staining (Ciampor *et al.*, 1992) and labelled with antibodies HC58 (panel A and B), specific for native HA and H9 (panel C and D), specific for the low pH conformation of HA. Amantadine (5μM) was added (panel B and D) from 1 hour post-infection.

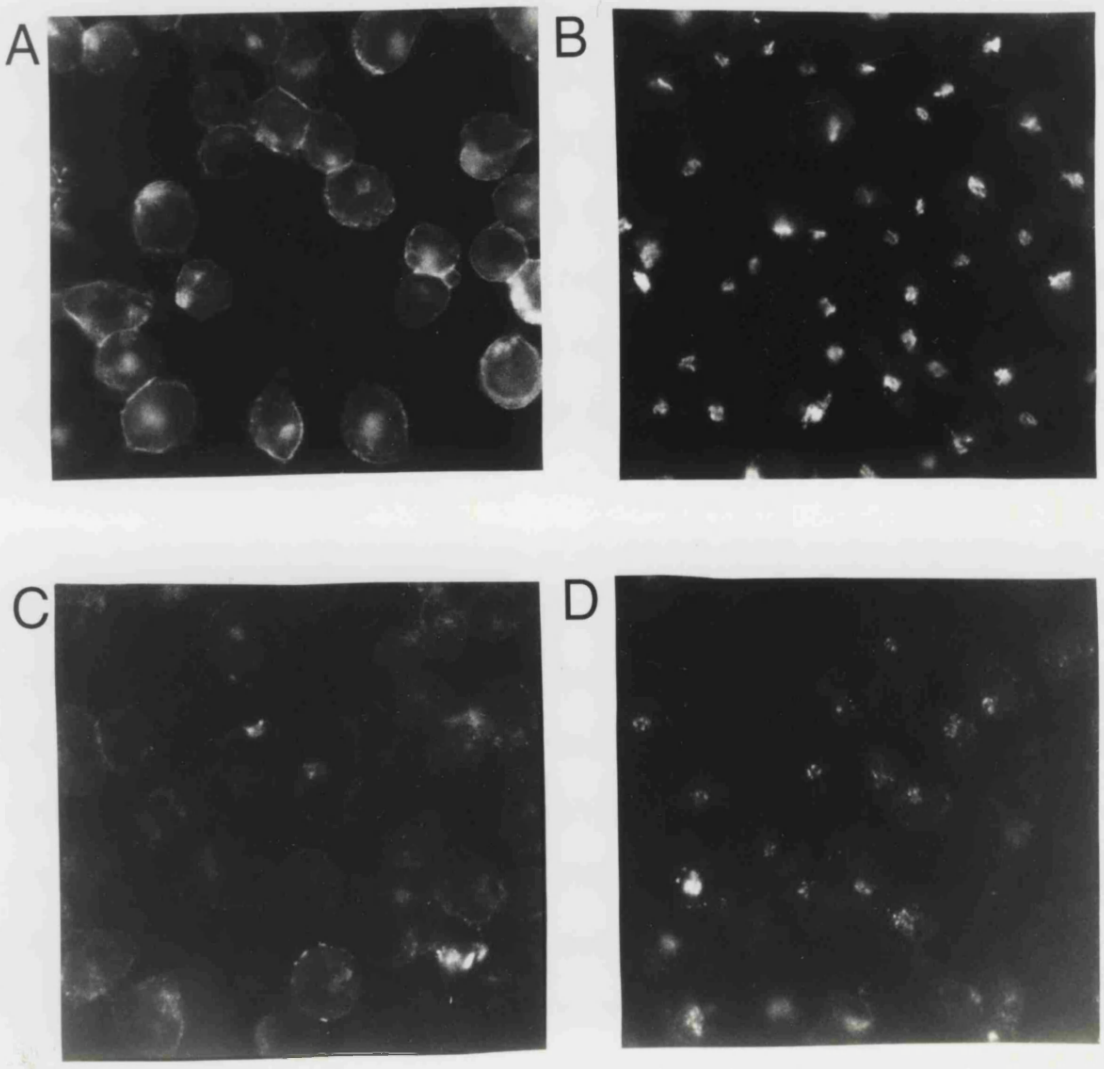
A
B
C
D

were first of all infected with the recombinant virus BR02A to determine the expression level of HA. Expression levels were determined by an ELISA assay. At 8 hours post-infection the C88 cells produced comparable amounts of both HA, as detected by HC2 and M2, detected by R54 (data not shown) as the MDCK cells. Enough HA was produced to be easily detectable, so C88 cells were then infected with either BR02A virus or an amantadine-resistant mutant virus, designated 08 virus. The 08 virus encodes an M2 protein with the mutation A30T, which renders it resistant to amantadine. This M2 is understood to be less active than the corresponding Rostock wild-type M2 protein, based on the proportions of the low-pH form of HA produced in CEF and MDCK cells, which were 74% and 50% respectively (Grambas *et al.*, 1992). Infection of C88 cells with 08 virus did not result in the production of a high proportion of low-pH HA (Table 2). Approximately 80% of the HA produced was in the native conformation, with 20% of HA present in the low-pH conformation. Addition of amantadine had no effect on the relative amounts of native and low-pH HA, which is as expected with a drug resistant virus. Infection of the C88 cells with BR02A virus confirmed the sensitivity of HA due to the action of amantadine as detected by the H9 antibody.

When 4 day induced R4-B cells were infected with either 08 virus or the reassortant BR02A virus, it was observed that the R4-B cells produced approximately twice as much HA as the infected C88 control cells (Table 3). Addition of amantadine to 08 virus-infected R4-B cells, resulted in a doubling of the relative amount of the low-pH form of HA. This phenomenon was not observed in control C88 cells and suggested that the sensitivity of HA to amantadine in this case, was due to inhibition of the expressed M2. Therefore, it is possible that the expressed M2 was helping to maintain the structural integrity of the viral HA.

Infection of 4 day induced R4-B cells with BR02A virus resulted in the conversion of the majority of the HA produced to the low-pH conformation in

TABLE 2: **THE EFFECT OF RIMANTADINE ON HA PRODUCED IN VIRUS-INFECTED MEL CELLS**

Antibody	Relative amount of HA (O.D.@ 450nm x 100)
HC2 -A	67
HC58 -A	43
HC58 +A	35
H9 -A	12
H9 +A	8

C88 cells were infected with the Rostock mutant 08 virus at a m.o.i. of ~50 p.f.u. Amantadine (5μM) was added at 1 hour post-infection. At 8 hours post-infection the cells were fixed with 0.05% glutaraldehyde and the relative amounts of native and low-pH HA detected with the monoclonal antibodies HC58 and H9 respectively. The ELISA was developed with a protein A-HRP conjugate and TMB in citrate buffer and the amounts of HA assessed by measuring the O.D. at 450nm.

TABLE 3: **INFECTION OF C88 AND R4-B CELLS WITH 08 OR BR02A INFLUENZA VIRUS**

Virus	C88 cells				R4-B cells			
	HC58		H9		HC58		H9	
	-	+	-	+	-	+	-	+
08	27	30	12	14	75	77	13	25
BR02A	40	19	6	23	76	24	10	67

C88 and 4 day induced R4-B cells were attached to 3-APTS treated microtitre plates and infected with either the mutant 08 virus or the Rostock/Bel reassortant virus, BR02A at a m.o.i. of ~50 p.f.u. Amantadine (5μM) was added (+) at 1 hour post-infection. The cells were fixed at 8 hours post-infection with 0.05% glutaraldehyde and the native and low-pH form of HA detected with the monoclonal antibodies HC58 and H9 respectively. The ELISA was developed with TMB and the O.D. measured at 450nm. The values shown in the table correspond to the O.D. at 450nm x100.

the presence of amantadine. Addition of amantadine to infected C88 cells resulted in approximately 50% of the HA being converted to its low-pH form, in contrast to the R4-B cells where 76% was converted.

Cells expressing the Weybridge wild-type protein (M2-39) and a rimantadine resistant M2 (G34E) were also infected with 08 virus. Higher values for HA production were obtained in the G34E cells (Table 4), but these could have been due to a larger number cells adhering to the microtitre plate. Although equal numbers of cells were attached to the microtitre plates, a proportion did detach during the washing process, however this was less of a problem after the cells had been fixed. Addition of amantadine resulted in the proportion of native conformation HA decreasing to 30% in the M2-39 cells and decreasing to 11% in the G34E cells, indicating that the G34E and wild-type Weybridge protein were unable to maintain the structural integrity of the viral HA in the presence of amantadine.

4.1.4 Transient expression of HA using a recombinant vaccinia virus

As influenza virus infection showed that the MEL cells were able to provide a suitable environment whereby conformational changes in HA could be used as a probe to monitor M2 activity, transient expression of HA in MEL cells was investigated. X-31 HA has been successfully expressed in CV-1 cells using a recombinant vaccinia virus, so vaccinia virus infection of MEL cells was studied. MEL cells attached to 3-APTS treated tissue culture dishes were infected with a recombinant vaccinia virus expressing the X-31 HA, in parallel with CV-1 cells as a positive control. At about 48 hours post-infection heterokaryon formation was clearly visible in the CV-1 cells, whereas the MEL cells continued to divide and showed no cytopathic effect. Western blotting of the infected cell lysates showed that the recombinant virus had productively infected the CV-1 cells. The MEL cells however, showed no production of HA and therefore appeared to be resistant to vaccinia virus infection (Figure 19).

TABLE 4: **INFECTION OF M2-39 AND G34E CELLS WITH 08 OR BR02A INFLUENZA VIRUS**

Virus	M2-39 cells				G34E cells			
	HC58		H9		HC58		H9	
	-	+	-	+	-	+	-	+
08	18	18	0	1	47	43	4	7
BR02A	27	8	0	6	53	6	0	22

M2-39 and G34E cells were attached to 3-APTS treated microtitre plates at 4 days p.i. and infected with either the mutant 08 virus or the Rostock/Bel reassortant virus, BR02A at a m.o.i. of ~50 p.f.u. Amantadine (5μM) was added (+) at 1 hour post-infection. The cells were fixed at 8 hours post-infection with 0.05% glutaraldehyde and the native and low-pH form of HA detected with the monoclonal antibodies HC58 and H9 respectively. The ELISA was developed with TMB and the O.D. measured at 450nm. The values shown in the table correspond to the O.D. at 450nm x100.

FIGURE 19: **PRODUCTION OF HA IN MEL AND CV1 CELLS INFECTED WITH A RECOMBINANT VACCINIA VIRUS**

C88 cells and CV1 cells were infected with a recombinant vaccinia virus expressing the X31 HA. The cells were lysed at about 48 hours post-infection in 2x sample buffer (Laemmli, 1970) and boiled for 2 minutes. The proteins were then resolved by SDS-PAGE on a 12% gel. After transfer onto Immobilon-P the HA was detected using a rabbit polyclonal serum and the blot was developed with a protein A-HRP conjugate and ECL reagent.

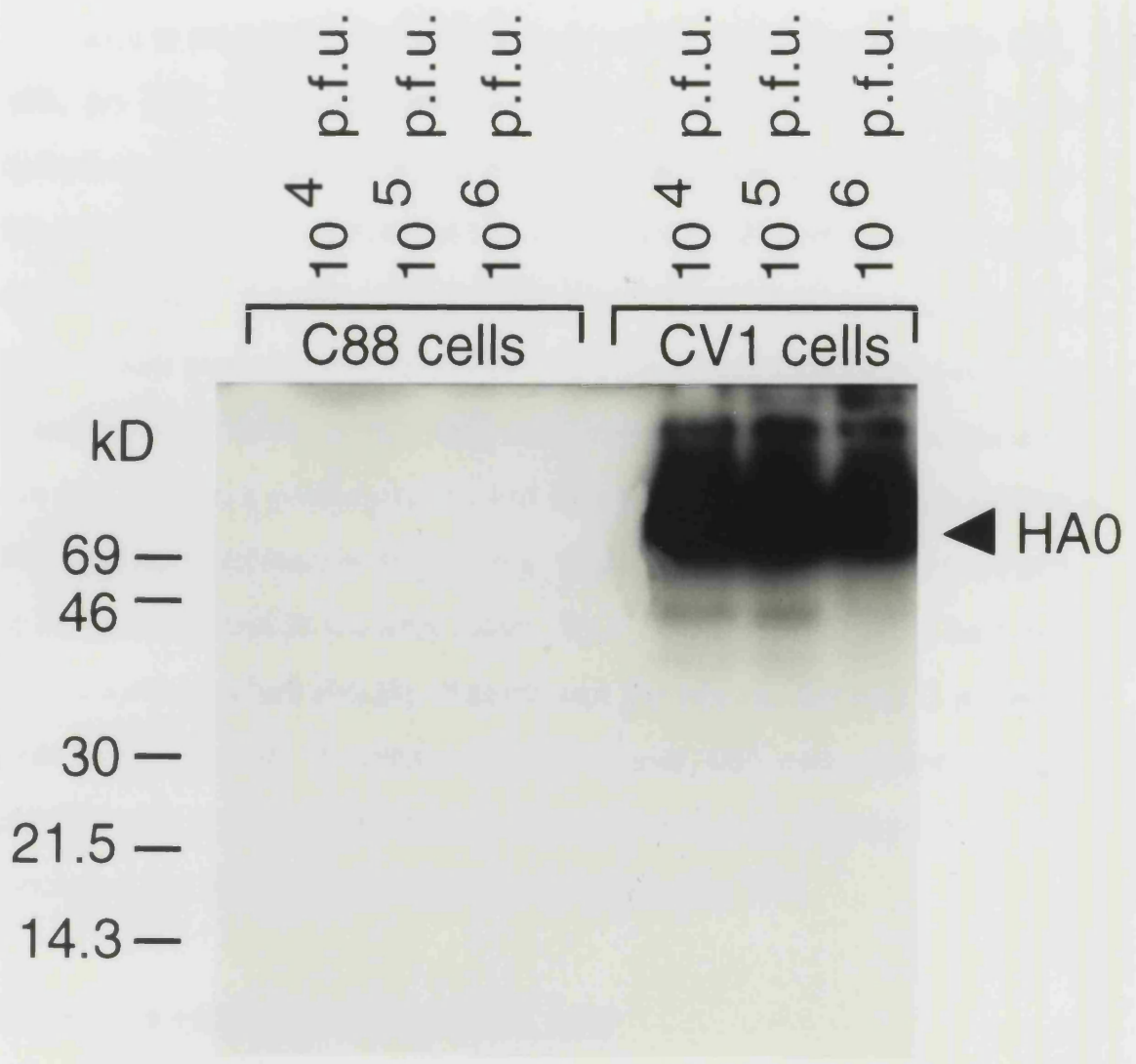
10^4 p.f.u.
10^5 p.f.u.
10^6 p.f.u.
10^4 p.f.u.
10^5 p.f.u.
10^6 p.f.u.
C88 cells
CV1 cells
kD
69
46
30
21.5
14.3
HA0

4.1.5 Transient expression of HA using Semliki Forest Virus

Due to the failure of vaccinia virus to infect and produce HA in the MEL cells, an SFV virus expression system was investigated. SFV is an alphavirus, with a single-stranded RNA genome of positive polarity. This is able to function as an mRNA and has the capability of infecting a wide range of animal cells. Infection with an SFV recombinant virus can result in the infected cells producing the heterologous protein up to 75 hours post-infection (Liljeström and Garoff, 1991). MEL cells were infected with SFV in parallel with BHK cells as a positive control and the cells were radiolabelled at various time intervals post-infection (Figure 20). Viral proteins could be visualized at 3 hours post-infection in the BHK cells. By 7 hours post-infection, host cell protein synthesis had virtually stopped and the p62, E1/E2 and C proteins could be clearly seen. In contrast to the BHK cells, MEL cells did not produce any SFV viral protein products even after 24 hours post-infection. It can be concluded that MEL cells are refractory to infection by SFV.

4.1.6 Stable expression of HA in MEL cells

C88 cells were transfected with the Rostock HA cDNA cloned into pEV3 as an *Eco*RI-*Bgl*.II fragment. G418 resistant populations and clones were screened for HA expression by ELISA using the anti-HA monoclonal antibodies HC2, which recognizes most forms of HA, HC58, specific for the native conformation and H9, specific for the low pH conformation of HA. Very low levels of HA expression were detected, which barely exceeded the background control values (data not shown). Other workers have been able to express HA in the absence of the M2 protein in HeLa and CV-1 cells (Takeuchi and Lamb, 1994; Ohuchi *et al.*, 1994). When HA was expressed without a corresponding M2, the low pH form of the glycoprotein was detected. In total, the MEL cells were transfected three times with the HA cDNA and negative results were obtained on each occasion.

FIGURE 20: **PRODUCTION OF SEMLIKI FOREST VIRUS PROTEINS IN MEL AND BHK CELLS**

C88 cells attached to 3-APTS treated 35mm tissue culture dishes and BHK cells were infected with SFV A7(74) supplied as a BHK cell supernatant at a m.o.i. of 27 p.f.u. per cell. Uninfected and infected cells were labelled with 10μCi/200μl of [^{35}S]-cysteine/methionine trans label for 1 hour at 3, 7, and 23 hours post-infection. After labelling the cells were lysed in NP-40 extraction buffer and boiled in the presence of reducing agent for 2 minutes. The proteins were resolved by SDS-PAGE on a 12% gel and detected by fluorography.

The P62, E1/E2 and C proteins can be visualized in the BHK cell lysates at 69, 46 and 30 kDa respectively.

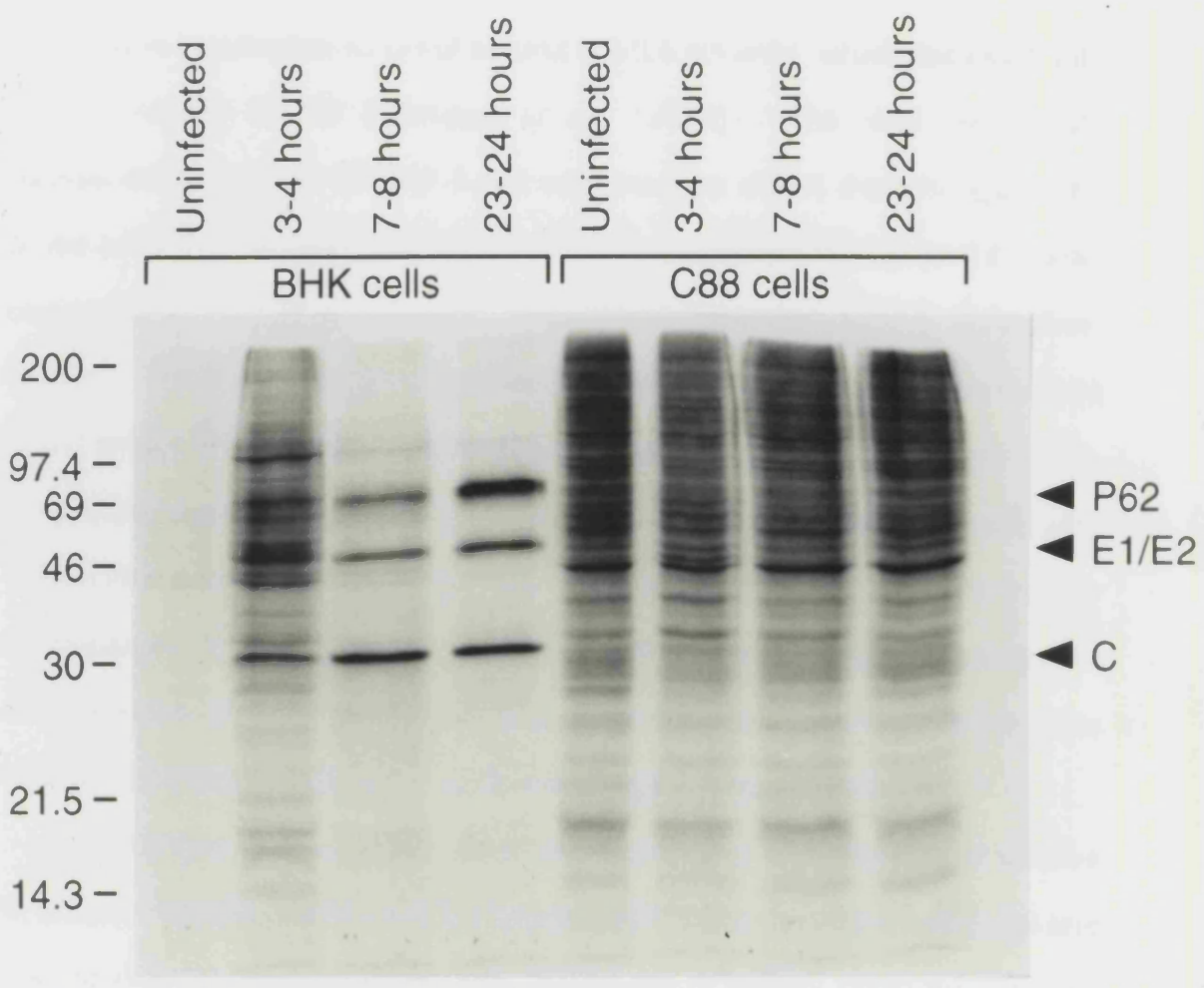
Uninfected
3-4 hours
7-8 hours
23-24 hours
Uninfected
3-4 hours
7-8 hours
23-24 hours
BHK cells
C88 cells
200
97.4
69
46
30
21.5
14.3
P62
E1/E2
C

4.2.0 CYTOPLASMIC pH CHANGES WITHIN MEL CELLS

It has been shown previously that virus infection of MDCK cells causes a decrease in cytoplasmic pH of around 0.3-0.4 pH units, which coincides with the production of M2 (Ciampor *et al.*, 1992b). The dual wavelength fluorescent pH probe SNARF-1-AM was used to detect this change. The probe is loaded into the cells in the form of a cell permeant ester and it is then converted to a cell-impermeant, fluorescent form by cellular esterases. Changes in intracellular pH are reflected by changes in the emission spectra of the probe (Thomas *et al.*, 1979; Bassnett *et al.*, 1990; Seksek *et al.*, 1991). Excitation occurs at 534nm and readings at two emission wavelengths (634/604nm) are taken and the ratio calculated. The ratio eliminates any discrepancies in the results due to non-uniform dye loading and differences in cell thickness and number. Problems associated with probe bleaching are also avoided as the intensity at both wavelengths is equally affected.

Changes in intracellular pH of M2-expressing MEL cells were studied in order to assess whether the M2 expressed in MEL cells was functional and also to determine whether discrete differences in activity could be detected between different M2 proteins. Fluorescence spectra obtained for unloaded C88 cells incubated in Gey's medium showed negligible levels of auto-fluorescence. The leakage of dye from loaded cells was also monitored, as this may cause inconsistencies in the results. SNARF-1 has higher levels of fluorescence in free solution than in the cellular environment due to the effects of quenching in the cell cytoplasm. SNARF-1-AM which had been converted to its pH-sensitive fluorescent form by the addition of hog liver esterase was found to be more fluorescent than that loaded into cells and the emission ratio of the free probe was shifted from the cell-associated form. This is consistent with observations from other workers (Bassnett *et al.*, 1990; Blank *et al.*, 1992; Owen, 1992). Dye leakage was found to vary from experiment to experiment (data not shown). Loading conditions were altered

from those stated previously (Hay *et al.*, 1993) in order to try and minimize the problems of probe leakage. Where loading conditions of 10μM SNARF-1-AM for 1 hour had been used for MEL cells attached to coverslips, this was reduced to 5μM SNARF-1-AM for 15 minutes, in order to alleviate problems due to gross leakage of the fluorescent probe from the cells. However, problems were still encountered with dye leaking from the cells. One explanation is that incubation with DMSO may have affected the integrity of the cell membrane. Alternatively, attaching MEL cells to glass coverslips may alter the properties of the plasma membrane, so that less leakage occurs.

Changes in the emission spectra of the probe were related to intracellular pH by means of a calibration curve (Figure 21). Nigericin is a K^+-H^+ antiporter and under conditions where the internal and external concentrations of K^+ are equal, it allows the intracellular pH to equilibrate with external pH (Thomas *et al.*, 1979). In order to relate the emission ratio to a known pH, cells were incubated with 10μM nigericin in high KCl buffer (115mM KCl, 1mM $MgCl_2$ and 20mM HEPES) adjusted to various pH values.

A decrease in intracellular pH of 0.2-0.25 pH units similar to that obtained with virus-infected MDCK cells occurs in induced M2-39 cells in comparison with uninduced and C88 control cells (Table 5), confirming that it is indeed the M2 protein alone which is responsible for the decrease in internal pH during virus infection. The pH change was specifically reversed on the addition of 5μM rimantadine. Addition of 10μM nigericin reduced the intracellular pH to that obtained with induced cells, confirming that M2 was acting to dissipate the membrane pH gradient. The M2 rimantadine-resistant mutant G34E provided further evidence that the decrease in pH was M2 specific. No change was observed in the cytoplasmic pH of the G34E cell line on the addition of 5μM rimantadine.

The Rostock M2 is understood to be more active than the Weybridge M2 protein, however using this assay to monitor cytoplasmic pH it was not

FIGURE 21: **CALIBRATION CURVE FOR SNARF-1 IN MEL CELLS**

C88 cells were loaded with 5μM SNARF-1 AM for 15 minutes at 37°C and transferred to a cuvette containing Guy's medium buffered with 20mM HEPES adjusted to various pH values. The 634/604nm emission ratio was determined at each pH after the addition of 10μM nigericin (10 minutes) to the cuvette.

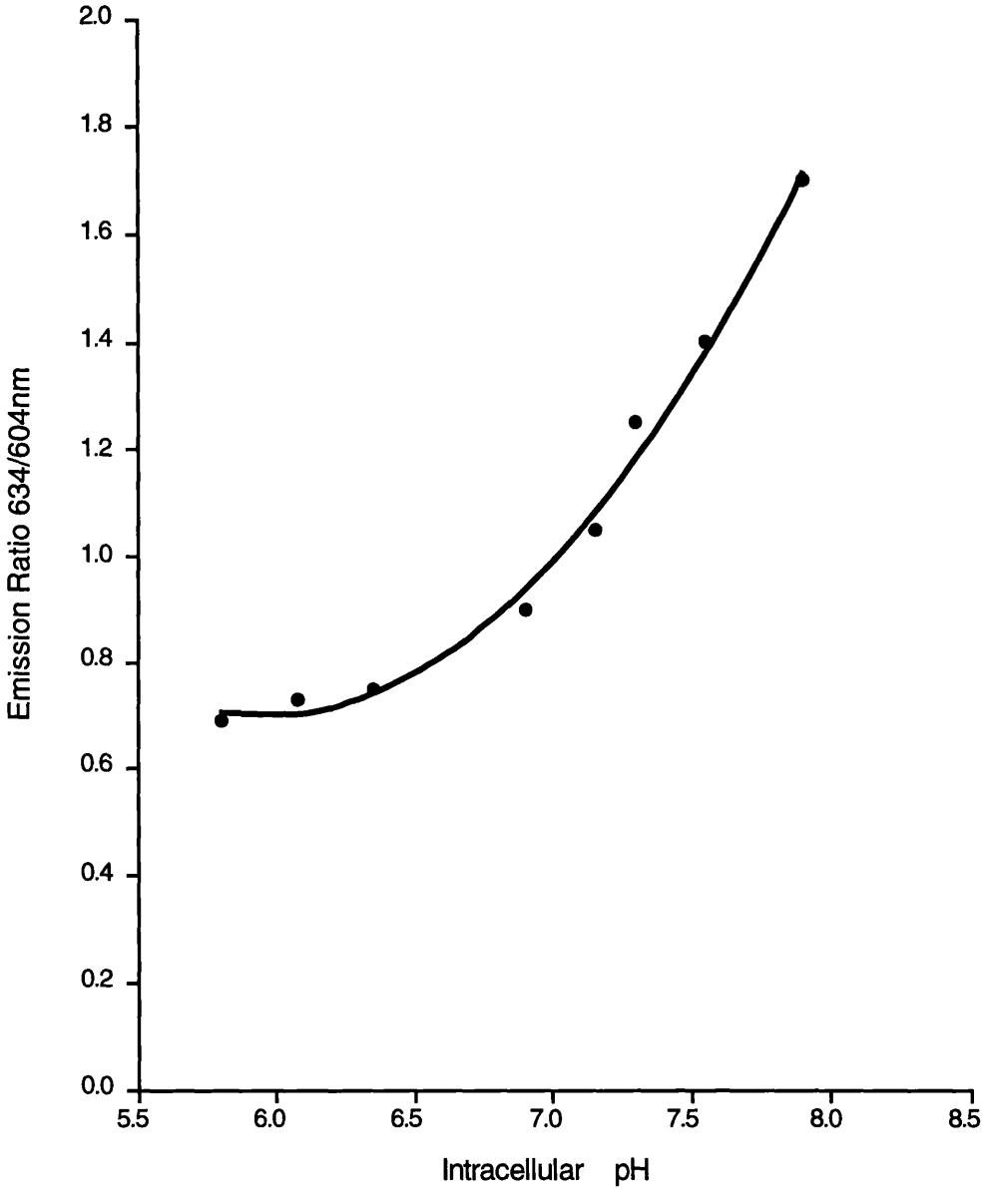
2.0
1.8
1.6
1.4
1.2
1.0
0.8
0.6
0.4
0.2
0.0
Emission Ratio 634/604nm
5.5
6.0
6.5
7.0
7.5
8.0
8.5
Intracellular pH

TABLE 5: **THE EFFECTS OF RIMANTADINE AND NIGERICIN ON THE CYTOPLASMIC pH OF MEL CELLS**

Cell	Cytoplasmic pH		
	No addition	Rimantadine	Nigericin
Control C88	7.30	7.30	7.05
Uninduced M2-39	7.30	7.30	7.10
Induced M2-39	7.10	7.30	7.10
Induced G34E	7.10	7.10	N.D.

Uninduced and 4 day induced MEL cells were loaded with SNARF-1-AM for 15 minutes and incubated in Gey's medium + 20mM HEPES, pH7.10. Emission spectra were obtained before and after the addition of 5μM rimantadine (15 minutes), or 10μM nigericin (10 minutes) to the cuvette.
N.D.= Not done.

possible to detect such a difference in activity between the two M2 types (Table 6). Expression of the Weybridge or Rostock M2 resulted in a similar decrease in intracellular pH. This functional assay lacks the sensitivity to discriminate between discrete differences in activity and is more useful for determining whether a particular mutant M2 protein is functional.

MEL cells expressing some of the mutant M2 proteins were studied using SNARF-1 to determine if these proteins were functional. Cells expressing the Rostock M2 protein with the T65A mutation were metabolically labelled with orthophosphate to verify that the protein was not phosphorylated. In fact, this protein was found to be phosphorylated, indicating that the adjacent serine residue may be phosphorylated instead (Figure 22A). The Weybridge mutant M2 C50S was shown to have had the site of palmitoylation removed (Figure 22B). Intracellular pH measurements showed that both mutants were functional and could be specifically inhibited with either 5μM amantadine or rimantadine (Table 7).

Finally, two other mutant M2 proteins were studied, namely the amantadine-resistant mutant $M2\Delta_{28\text{-}31}$ and the first Weybridge to Rostock transmembrane conversion, V27I. Mutant V27I was observed to be functional and on addition of 5μM rimantadine the decrease in intracellular pH was fully reversed (Table 7). The deletion mutant $M2\Delta_{28\text{-}31}$ showed slightly different characteristics. Although this M2 mutant is amantadine-resistant, a slight increase in pH was noticed after incubation for 15 minutes with the drug. This could have been due to a slight drift in the measurements, or leakage of SNARF-1 from the cells. Another possibility is that the mutant is not completely resistant to the effects of amantadine.

TABLE 6: A COMPARISON OF THE M2-MEDIATED pH CHANGE IN ROSTOCK AND WEYBRIDGE M2-EXPRESSING CELLS

Cell	Cytoplasmic pH	
	No addition	Amantadine/ Rimantadine
Control C88	7.30	7.30
Uninduced M2-39	7.30	7.25
Induced M2-39	7.10	7.30
Uninduced R4-B	7.30	7.30
Induced R4-B	7.10	7.30

Uninduced and 4 day induced MEL cells were loaded with SNARF-1-AM for 15 minutes at 37°C and incubated in Gey's medium + 20mM HEPES, pH7.10. Emission spectra were obtained before and after the addition of 5μM amantadine or rimantadine (15 minutes) to the cuvette.

FIGURE 22: **METABOLIC LABELLING OF T65A AND C50S MUTANT M2 PROTEINS**

A: MEL cells at 4 days p.i. were attached to 3-APTS treated 35mm tissue culture dishes and incubated for 4 hours in MEM- lacking phosphate to deplete intracellular phosphate stores. 0.25mCi of [^{32}P] orthophosphate was added to the cells in 0.5ml of phosphate-free MEM- and the cells incubated for a further 4 hours at 37°C. After lysis of the cells, the M2 was immunoprecipitated from the samples using the anti-M2 polyclonal serum, R7-90. The samples were heated to 100°C before SDS-PAGE on a 20% gel. The gel was subsequently dried under vacuum overnight and then exposed to film.

B: MEL cells at 4 days p.i. were attached to 3-APTS treated tissue culture dishes and incubated in MEM- containing 5mM sodium pyruvate with 0.25mCi of [^{3}H]- [9,10 (n)]-palmitic acid for 4 hours at 37°C. The cells were then lysed and the M2 immunoprecipitated with the anti-M2 polyclonal serum, R7-90. The samples were heated to 100°C for 2 minutes before SDS-PAGE on a 20% gel. M2 immunoprecipitates were detected by fluorography.

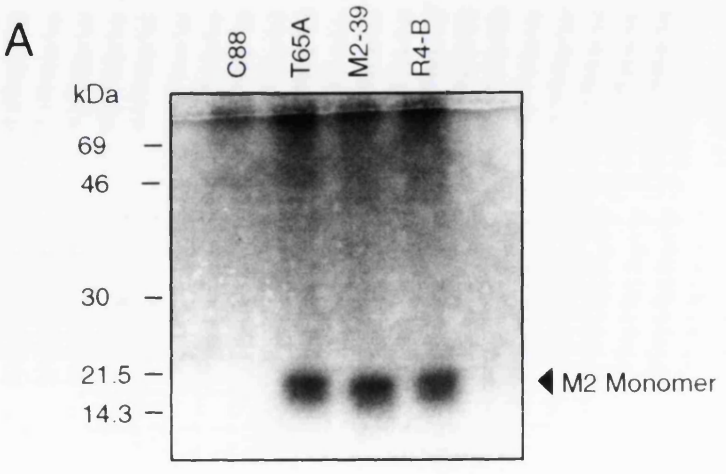
A
C88
T65A
M2-39
R4-B
kDa
69
46
30
21.5
14.3
M2 Monomer

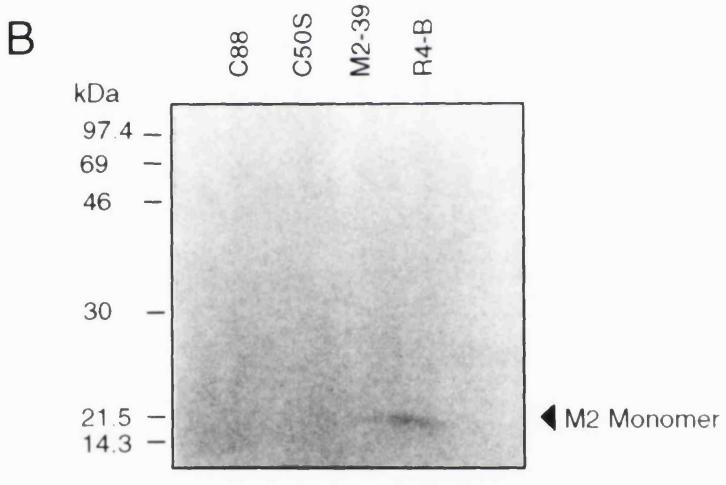
B
C88
C50S
M2-39
R4-B
kDa
97.4
69
46
30
21.5
14.3
M2 Monomer

TABLE 7: A COMPARISON OF THE pH CHANGE PRODUCED IN MEL CELLS EXPRESSING MUTANT M2 PROTEINS

Cell	Cytoplasmic pH	
	No addition	Amantadine/ Rimantadine
Control C88	7.30	7.35
Uninduced C50S	N.D.	N.D.
Induced C50S	7.10	7.30
Uninduced T65A	7.30	N.D.
Induced T65A	7.05	7.25
Uninduced V27I	N.D.	N.D.
Induced V27I	7.10	7.30
Uninduced $M2\Delta_{28-31}$	7.35	N.D.
Induced $M2\Delta_{28-31}$	7.10	7.15

Uninduced and 4 day induced MEL cells were loaded with SNARF-1-AM for 15 minutes at 37°C and incubated in Gey's medium + 20mM HEPES, pH7.10. Emission spectra were obtained before and after the addition of 5μM amantadine or rimantadine (15 minutes) to the cuvette.

N.D. = not done

5.0 ION CONDUCTANCE PROPERTIES OF M2

5.1 Introduction

Previous evidence (Sugrue *et al.,* 1990b; Pinto *et al.,* 1992) suggested that the M2 protein has ion channel activity which plays an important role in both the acid-induced uncoating of the virus and in the modulation of pH in the exocytic pathway. In particular, M2 is involved in maintaining the structural integrity of HA during its transport through the TGN to the plasma membrane. Results from voltage-clamp experiments on M2-expressing MEL cells indicate that the protein forms a proton-activated, proton selective channel.

5.2 Voltage-clamp technique

M2 channel function was studied using a voltage clamp technique which allows the potential to be controlled across the plasma membrane. A voltage is applied across the cell membrane and the resulting current is measured. Voltage clamp measurements were carried out on MEL cells by Dr I Chizhmakov, N.I.M.R. and the cells were subject to the voltage clamp technique in the whole-cell configuration (Figure 23). The patch pipette was pressed against an intact cell to form a giga-ohm seal between the pipette and the membrane. Gentle suction was then applied so that the patch pipette ruptured the cell membrane and became continuous with the inside of the whole cell, permitting exchange of molecules between the cell cytoplasm and the pipette. The volume of the patch pipette was much greater than that of the cell (approximately 10µl compared with 1pl) thereby allowing the cell interior to equilibrate with the solution in the pipette. The solution in the patch pipette was composed of the large impermeant cation e ($NMDG^+$ 90mM) and the anion $HEPES^-$ or MES^- depending on the required pH of the solution. These ions maintain the osmolarity of the cell and allow currents due to

FIGURE 23: **DIAGRAMMATIC REPRESENTATION OF THE VOLTAGE-CLAMP APPARATUS**

A simplified schematic diagram of the whole cell voltage clamp appartus. The pipette forms a tight, high electrical resistance seal with the cell membrane, which then allows the patch of membrane at the pipette tip to be removed following gentle suction. Consequently the cell interior equilibrates rapidly with the solution in the patch pipette. The medium bathing the cell can be changed by fast perfusion with another pipette (not shown).

Voltage - Clamp Apparatus

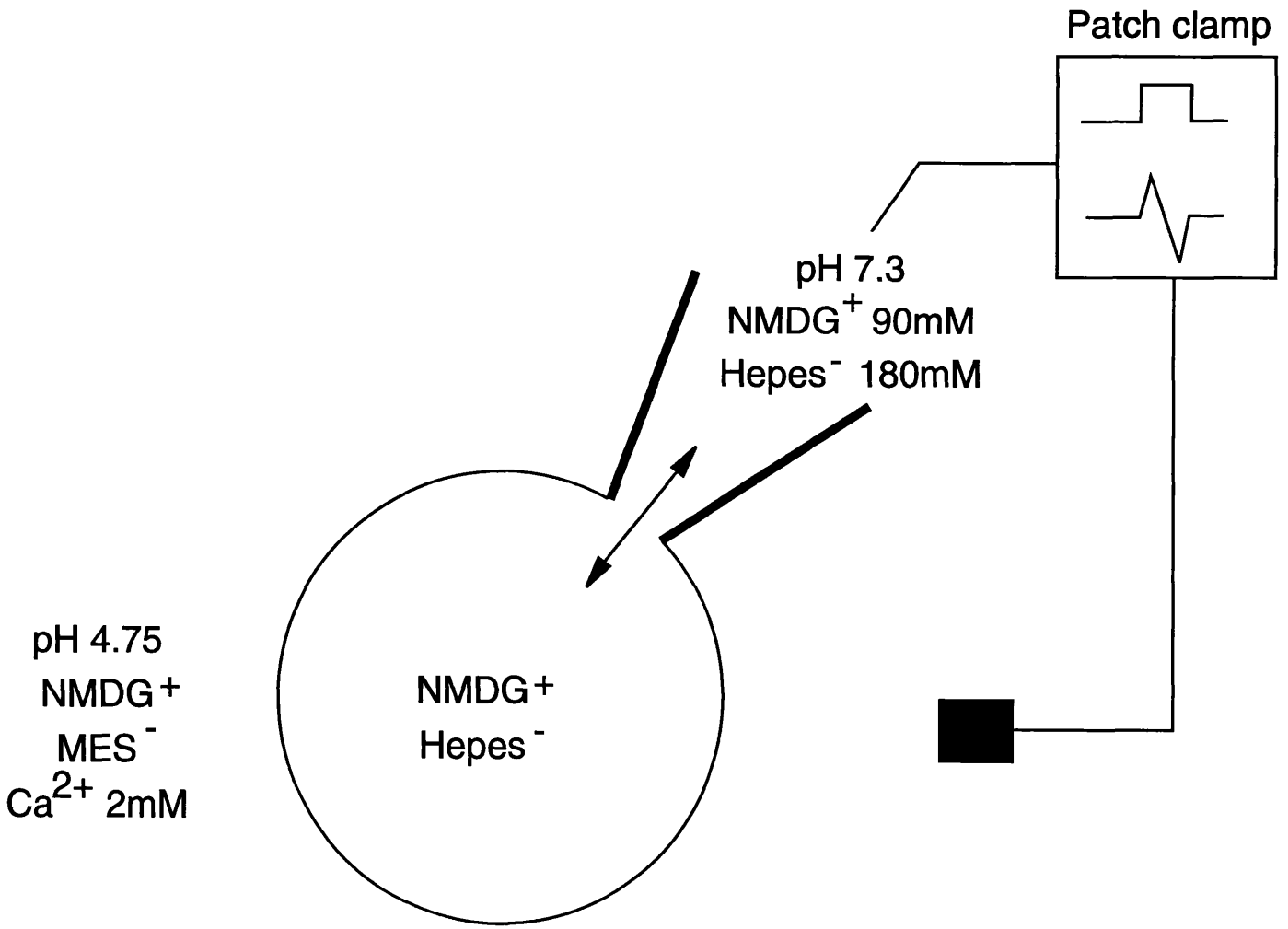

protons to be distinguished from those due to other small ions such as K^+, Na^+ or Cl^-. Both the internal and external environments of the cell are controlled, so effectively all the small permeant ions are diluted out. A perfusion pipette was used to pulse the cells with solutions of $NMDG^+$, MES^- and Ca^{2+} 2mM at varying pH values to provide a proton gradient.

5.3 Inward proton currents due to M2

The current voltage relationship was determined for control C88 cells which do not express the M2 protein. A voltage was applied across the membrane of the cell in the range -80mV to +80mV and the resulting current measured after fast perfusion of the cell exterior with $NMDG^+/MES^-$ buffer at pH5.2. The cell was then re-equilibrated with the original bath solution before re-perfusion at a different holding potential (Figure 24A). The electrode trace shows small currents obtained in the order of ~ 20pA at +80mV. The current was not affected by changes in external pH. Graphical representation of this data (Figure 24B) shows that the current obtained was proportional to the applied voltage and had a reversal potential, i.e. the potential around which the current changes sign, at ~0mV. This current is known as a "leakage current" and is a background conductance of undetermined ionic basis.

Induced M2-expressing cells showed similar current-voltage characteristics at pH7 in the absence of a proton gradient. Addition of 5μM rimantadine to the bath solution had no detectable effect on the current obtained (data not shown). This confirmed that an M2 dependent current was not being produced. Perfusion of 4 day induced M2-expressing cells with a solution at pH4.5 induced an inward current (Figure 25). The magnitude of the current was dependent on the holding potential, with a current of ~100pA obtained at a membrane potential of -90mV. The inward current was also dependent on the magnitude of the proton gradient (Figure 26A). An increase in the proton gradient was followed by a corresponding increase in the

FIGURE 24: **CURRENT/VOLTAGE RELATIONSHIP FOR C88 CELLS**

A: Inward currents obtained for the same cell in response to a decrease in external pH from pH7.4 to pH5.2 during a 1 second pulse (indicated above the trace) at several holding potentials (V_h). The current was allowed to return to baseline values between each pulse.

B: Current/voltage relationship for membrane currents obtained at different V_h values.

■ - pH7.4

▲ - pH5.2

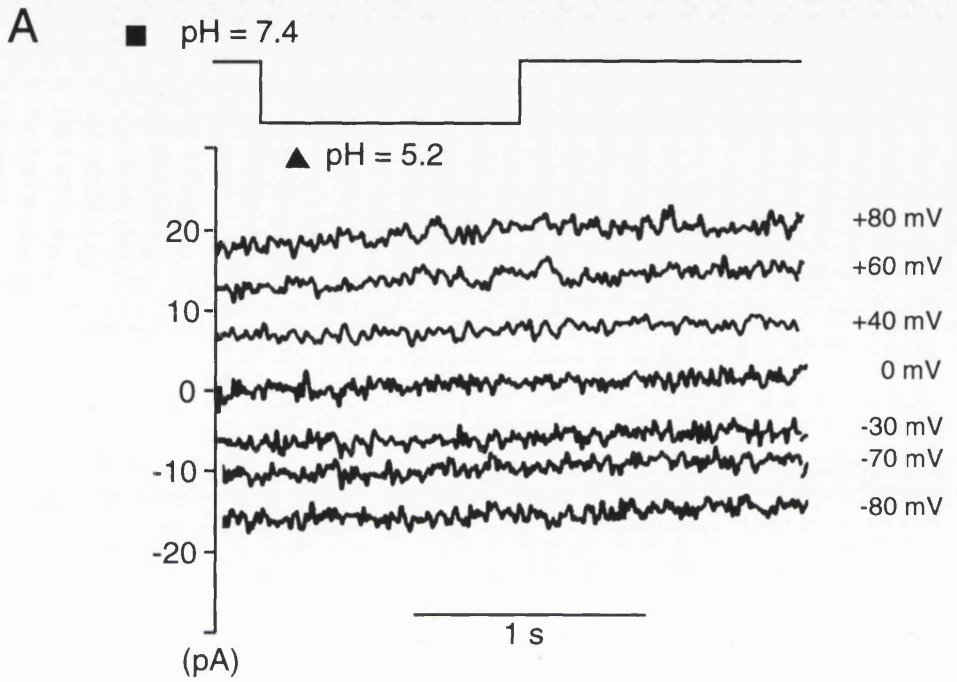
A
pH = 7.4
pH = 5.2
20
10
0
-10
-20
(pA)
+80 mV
+60 mV
+40 mV
0 mV
-30 mV
-70 mV
-80 mV
1 s

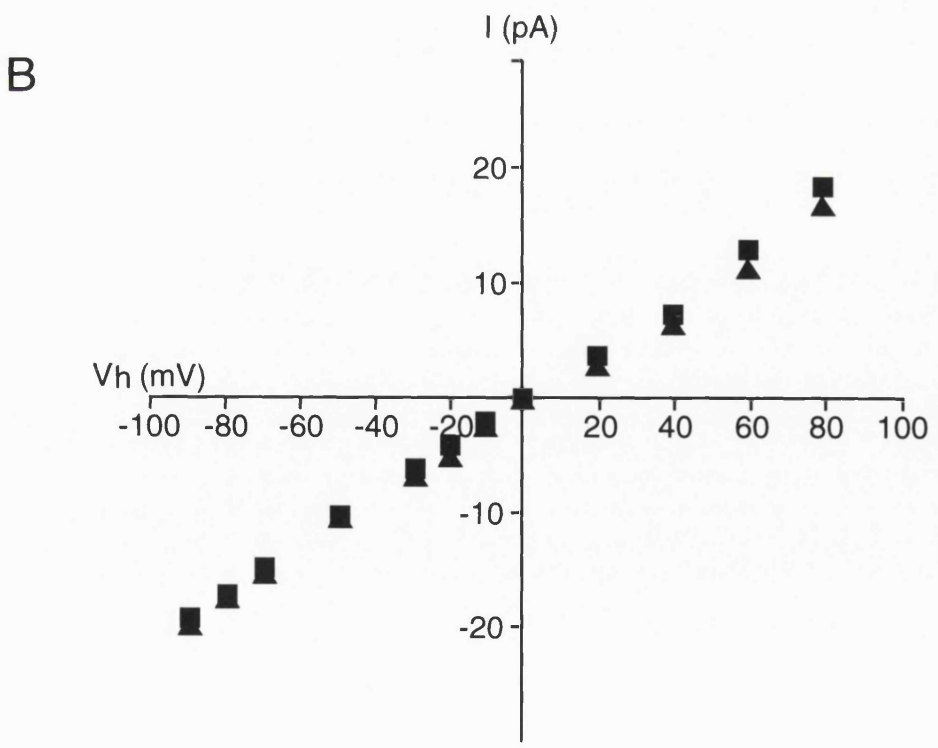
B
I (pA)
20
10
Vh (mV)
-100 -80 -60 -40 -20
20 40 60 80 100
-10
-20

FIGURE 25: **CURRENT/VOLTAGE RELATIONSHIP FOR M2-39 M2-EXPRESSING CELLS**

Inward currents obtained in M2-expressing MEL cells on reduction of the external pH from pH7.4 to pH4.5 during a 1 second pulse (indicated on the trace) at different V_h values. The current was allowed to return to its baseline level between each pulse.

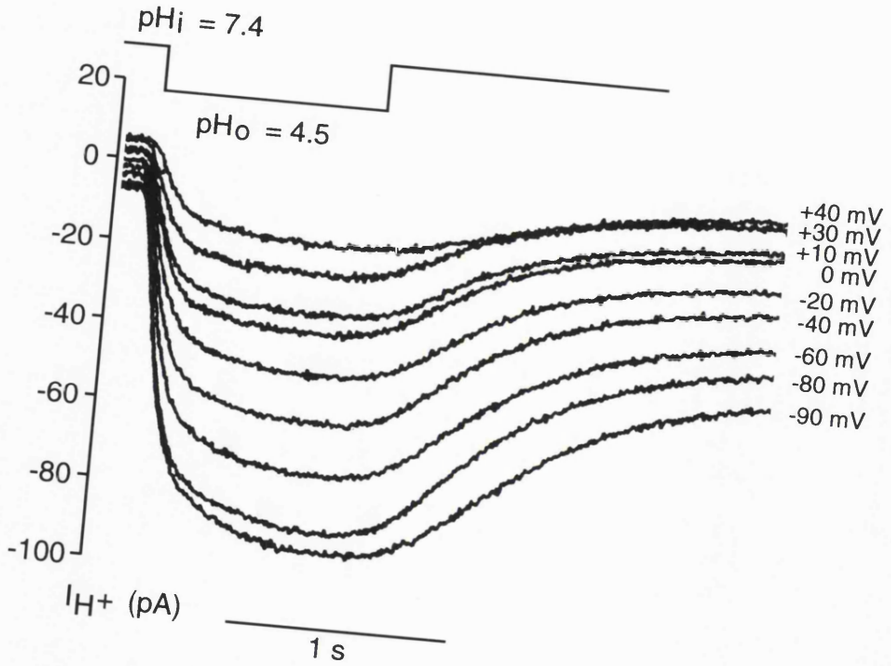

FIGURE 26: **THE DEPENDENCE OF INWARD CURRENT ON PROTON CONCENTRATION**

A: Current/voltage relationship for membrane currents produced in the same cell at different external pH values.

B: Effect of proton concentration on saturation of the inward current at different V_h values.

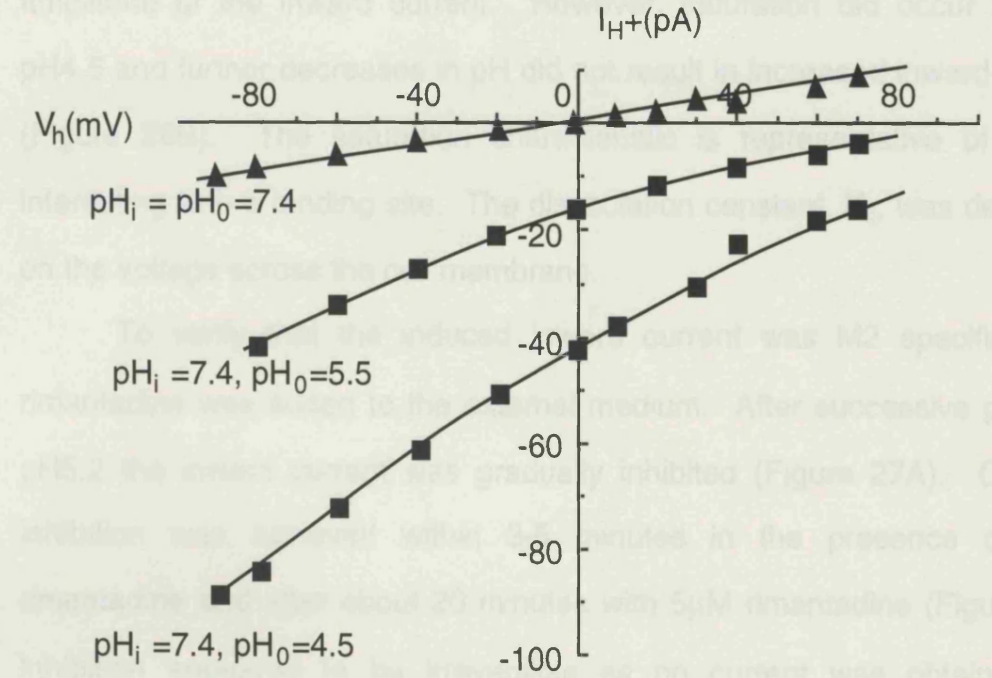

B

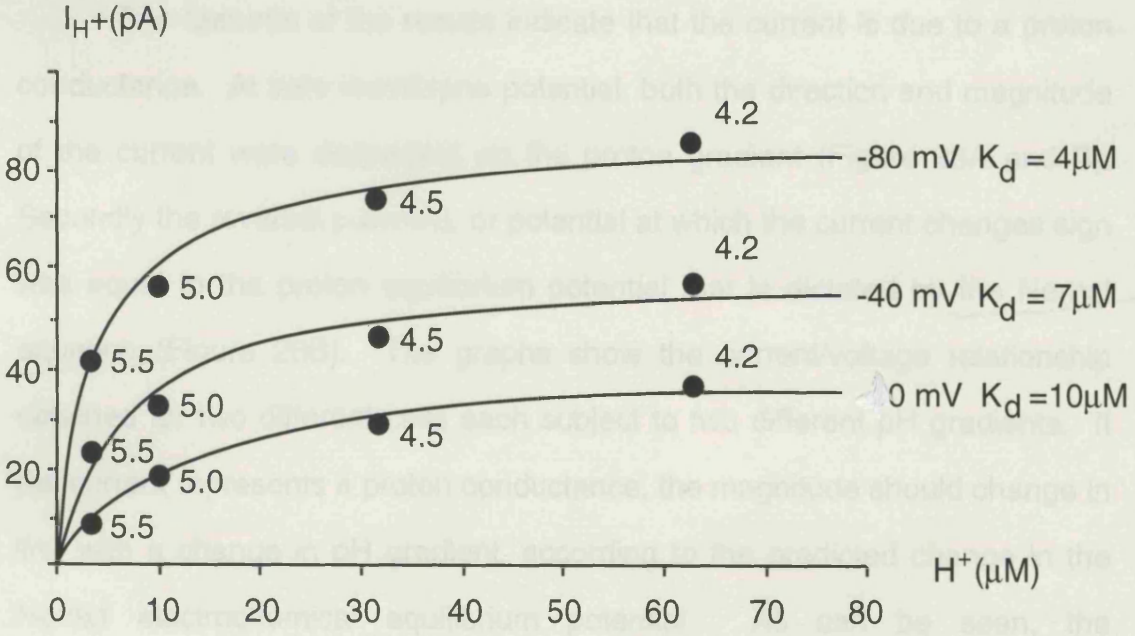

amplitude of the inward current. However, saturation did occur at about pH4.5 and further decreases in pH did not result in increased inward currents (Figure 26B). The saturation characteristic is representative of protons interacting with a binding site. The dissociation constant, K_d, was dependent on the voltage across the cell membrane.

To verify that the induced inward current was M2 specific, 50μM rimantadine was added to the external medium. After successive pulses at pH5.2 the inward current was gradually inhibited (Figure 27A). Complete inhibition was achieved within 3-5 minutes in the presence of 50μM rimantadine and after about 20 minutes with 5μM rimantadine (Figure 27B). Inhibition appeared to be irreversible as no current was obtained after incubation of the cell for 1 hour in drug-free medium (data not shown). These results are reminiscent of those obtained from pH measurements of M2-expressing cells, in terms of the length of time needed to achieve complete inhibition of the M2 protein (Hay *et al.*, 1993). Specific inhibition has also been confirmed by similar studies on cells expressing the Weybridge rimantadine-resistant mutant M2 protein, G34E. In the presence of 50μM rimantadine the inward M2-specific current was not blocked (data not shown).

Two features of the results indicate that the current is due to a proton conductance. At zero membrane potential, both the direction and magnitude of the current were dependent on the proton gradient (Figure 28A and B). Secondly the reversal potential, or potential at which the current changes sign was equal to the proton equilibrium potential that is dictated by the Nernst equation (Figure 28B). The graphs show the current/voltage relationship obtained for two different cells each subject to two different pH gradients. If the current represents a proton conductance, the magnitude should change in line with a change in pH gradient, according to the predicted change in the Nernst electrochemical equilibrium potential. As can be seen, the experimental values obtained for the reversal potential were close to those

FIGURE 27: **THE EFFECT OF RIMANTADINE ON INWARD CURRENT**

A: Trace of inward current obtained on the same M2-39 cell in response to a reduction in external pH from pH7.2 to pH5.2 during a 1 second pulse. 50μM rimantadine was added to the external medium as indicated on the trace.

B: A time course of inhibition of inward currents by rimantadine in two M2-39 cells (Δ 5μM, ▲ 50μM). The amplitude of the inward current (I) is shown as a fraction of the amplitude of the total current (I_{max}) prior to the addition of rimantadine.

A

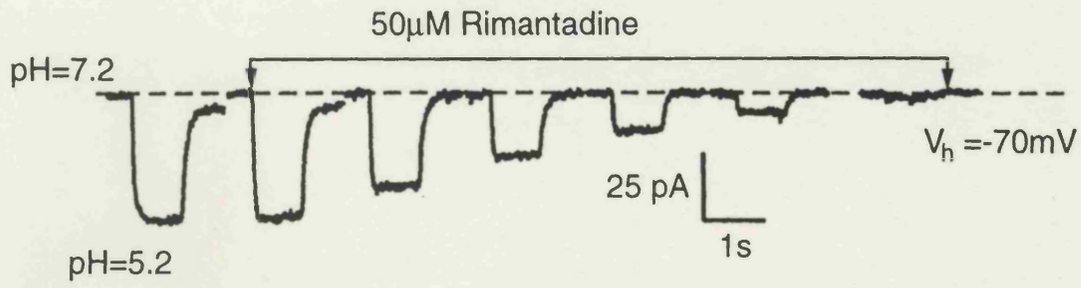

B

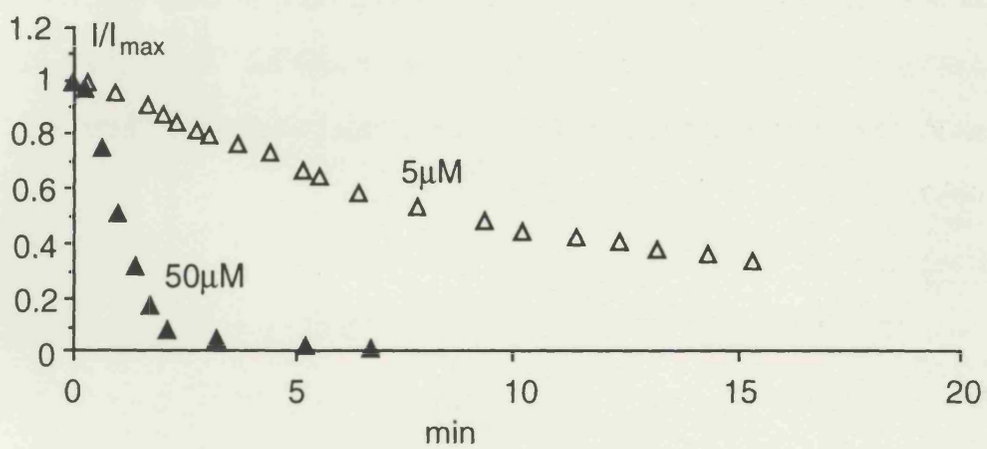

FIGURE 28: **DETERMINATION OF THE REVERSAL POTENTIAL**

A and B: Current/voltage relationships obtained for different cells indicating the reversal potential for four different pH gradients. The lines indicate the theoretical equilibrium potentials for the respective proton gradients as dictated by the Nernst equation, where $E_{rev} = RT/Z_sF \ln [S]_2/[S]_1$

$Z_s = 1.602 \times 10^{-19}$ C

s= Arbitrary ion

$R = 8.315$ $JK^{-1}mol^{-1}$

$F = 9.684 \times 10^4$ C mol^{-1}

T= Absolute temperature

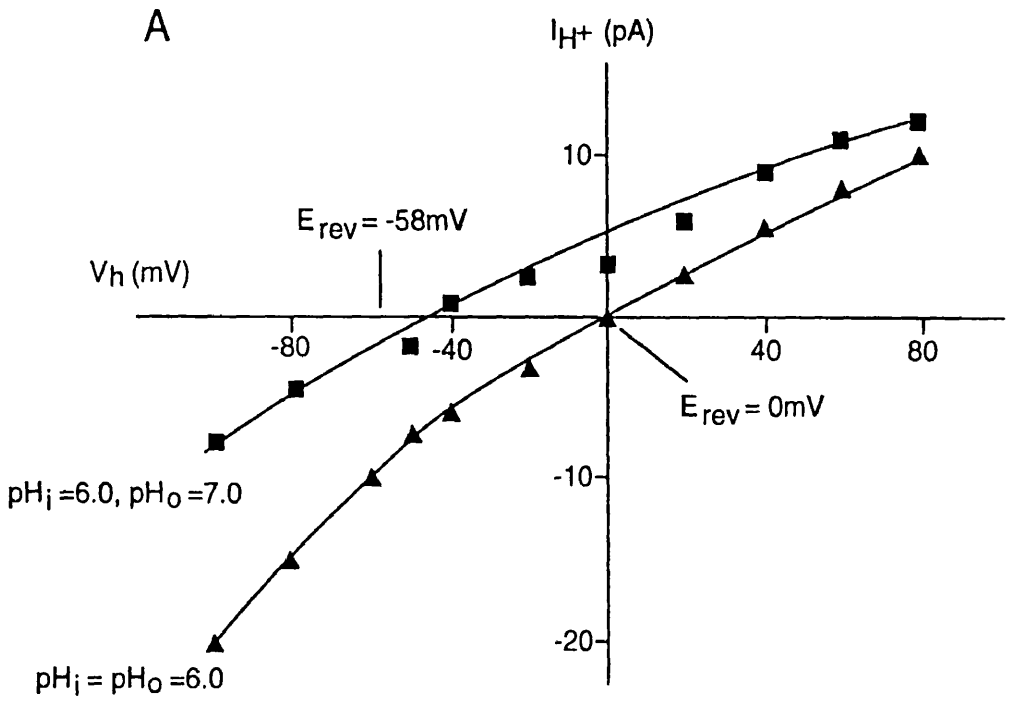
A
I_{H^+} (pA)
10
E_{rev} = -58mV
V_h (mV)
-80
-40
40
80
E_{rev} = 0mV
-10
pH_i =6.0, pH_o =7.0
-20
pH_i = pH_o =6.0

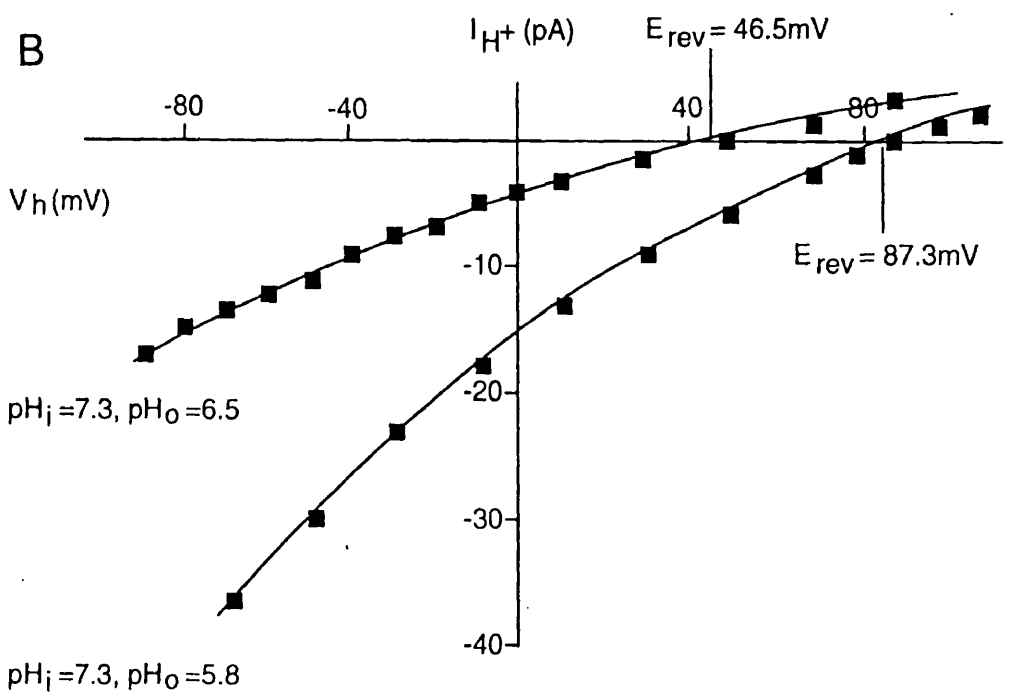
B
I_{H^+} (pA)
E_{rev} = 46.5mV
-80
-40
40
80
V_h (mV)
-10
E_{rev} = 87.3mV
-20
pH_i =7.3, pH_o =6.5
-30
-40
pH_i =7.3, pH_o =5.8

predicted by the Nernst equation for the proton gradient, indicating a proton conductance.

Other workers (Pinto *et al.*, 1992) have reported that M2 may be permeable to cations, such as Na^+. To determine the effect of small ions on the permeability of M2, inward currents were obtained on the same cell in response to a decrease in external pH from pH7.4 to pH4.75. Initially the cells were perfused with normal Ringers solution (120mM NaCl, 2mM KCl, 2mM $CaCl_2$, $MgCl_2$ and 20mM $HEPES^-$), followed by $NMDG^+/MES^-$ buffer. The solution in the patch pipette was composed of 90mM $NMDG^+$ and 180mM $HEPES^-$. The amplitude of the inward current was the same whether the cell was pulsed with Ringers solution, or the $NMDG^+/MES^-$ buffer (Figure 29). There was a difference in the length of time needed for the cells to re-equilibrate, however, this can be explained by the different buffering capacities of the two solutions. Inclusion of other ions in the internal or external solution had no significant effect on the characteristics of the currents observed, indicating that protons were the predominant permeant ion.

5.4 Activation of the M2 protein

When the M2-39 cell interior was held at pH6.0 and the exterior pulsed with $NMDG^+/HEPES^-$ buffer at pH7.0, an outward current was observed (Figure 30A). In the absence of a proton gradient, when both the internal and external pH values were held at pH6.0, the current produced consisted of the pH-independent "leak" and the current due to the action of M2. When the external pH was raised to pH8.0, instead of observing an increase in the outward current at a membrane potential greater than 0mV as a result of the increased proton gradient, the current actually decreased to a level equal to the leak current in untransformed control C88 cells (Figure 30B). Additionally, no current was detectable at zero membrane potential indicating that the proton-dependent current had been abolished. This decrease in outward

FIGURE 29: **THE EFFECT OF SMALL IONS ON THE MAGNITUDE OF THE INWARD CURRENT**

Inward currents were obtained in response to a reduction in external pH from pH7.4 to pH4.75, in normal Ringers (NR) solution (left trace) and in NMDG-MES solution (middle trace). The right hand trace shows the two currents superimposed.

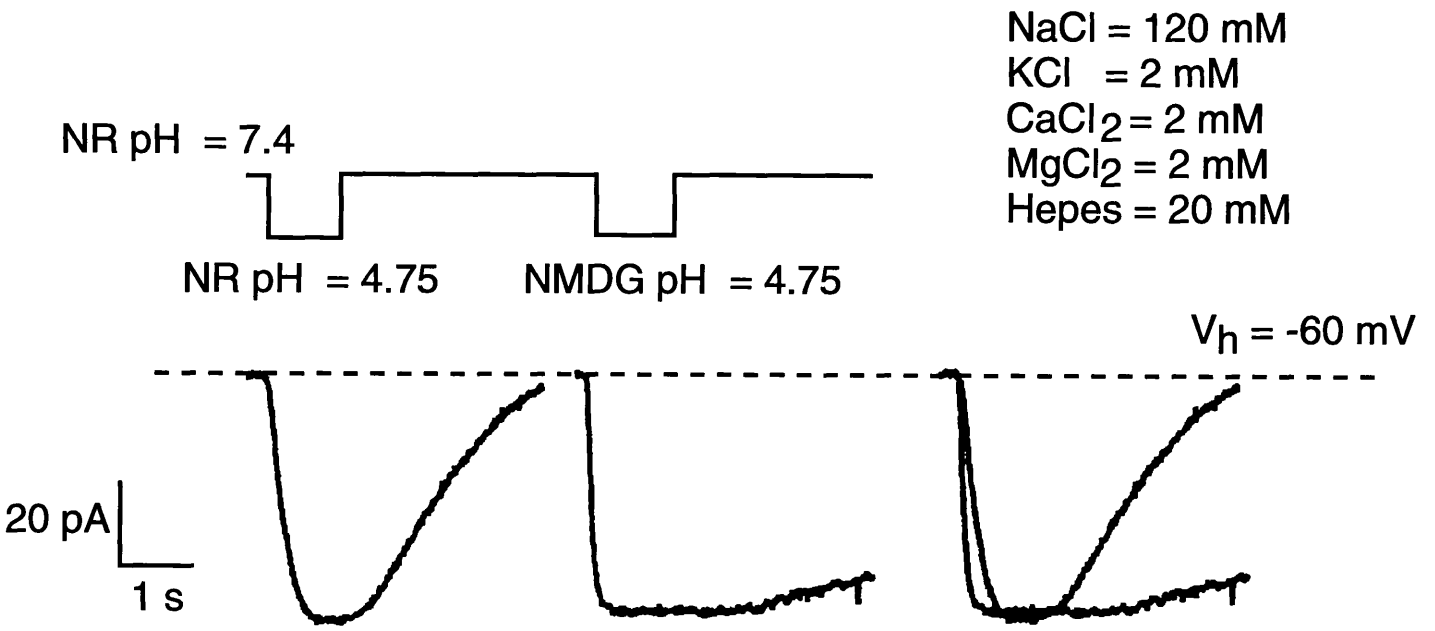
NaCl = 120 mM
KCl = 2 mM
CaCl2 = 2 mM
MgCl2 = 2 mM
Hepes = 20 mM
NR pH = 7.4
NR pH = 4.75
NMDG pH = 4.75
Vh = -60 mV
20 pA
1 s

FIGURE 30: **PRODUCTION OF OUTWARD CURRENTS**

Current/voltage relationships obtained for different cells showing the production of outward currents upon the application of a lowered internal pH and raised external pH.

A

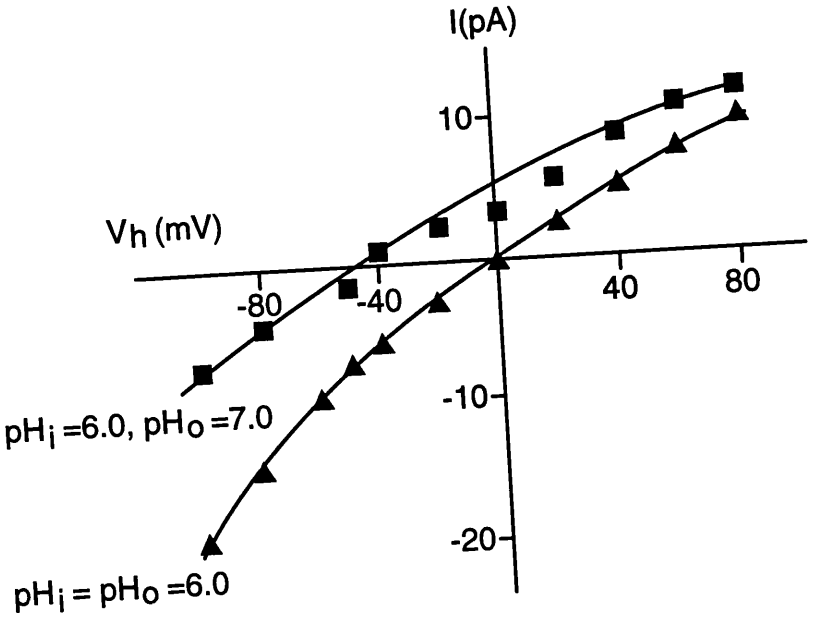
I(pA)
10
Vh (mV)
-80
-40
40
80
-10
-20
pHi =6.0, pHo =7.0
pHi = pHo =6.0

B

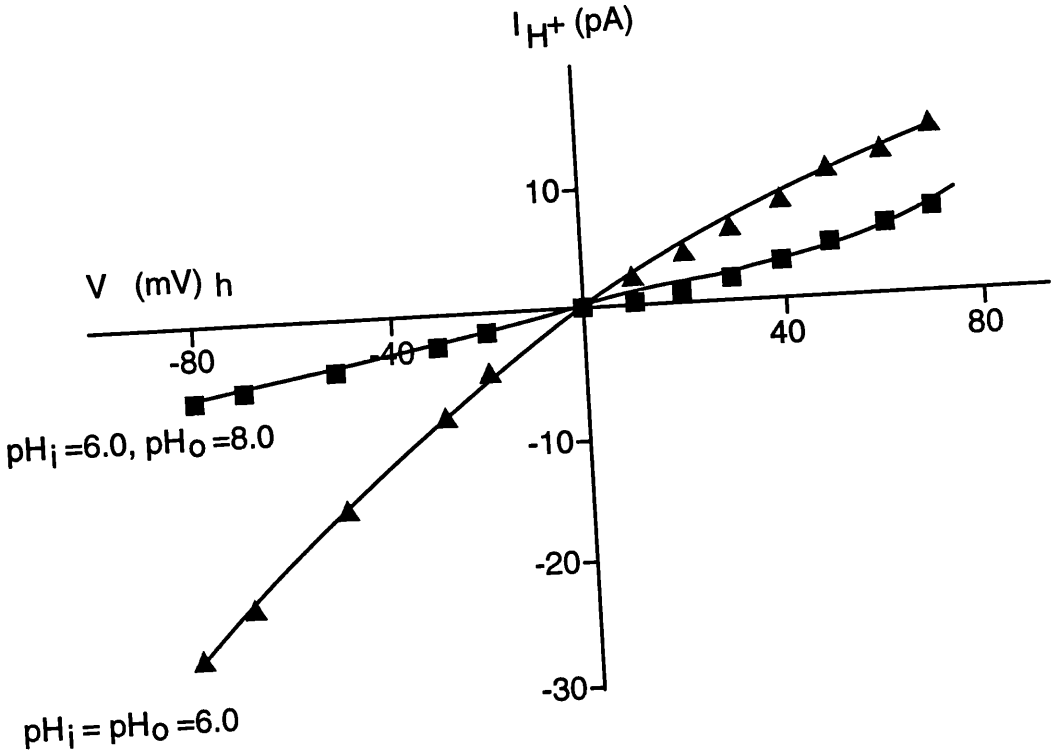
I H+ (pA)
10
V (mV) h
-80
-40
40
80
-10
-20
-30
pHi =6.0, pHo =8.0
pHi = pHo =6.0

current on increasing proton gradient was observed in cells expressing the Weybridge M2 protein. R4-B cells expressing the Rostock M2 protein, produced outward currents which increased in relation to the greater proton gradient (Figure 31).

5.5 Characterization of mutant M2 proteins

The distinct differences in activation between the Weybridge and Rostock M2 proteins, constitutes a useful assay for characterizing the ion conductance properties of MEL cells expressing mutant M2 proteins. The M2 mutants T65A and C50S were both found to be functional proton channels. The mutation T65A in the Rostock M2 did not affect the activation property of the protein and the mutant was indistinguishable from the Rostock wild type M2 (Table 8). Preliminary results indicated that replacement of cysteine 50 with serine in the Weybridge M2 protein did result in altered activation properties. This mutant was activated at a lower pH than the wild-type protein and the significance of this is as yet unknown.

The Weybridge to Rostock transmembrane conversions were also studied (see section 3.2.3. pp86). The mutations V27I/F38L and V27I/D44N showed activation properties which were very close to the Weybridge wild type protein. However it was observed that conversion of all three transmembrane residues from the Weybridge to Rostock sequence, resulted in a protein which had identical activation characteristics to the Rostock wild-type M2. The data indicates that the three transmembrane residues together are responsible for determining the differences in activity observed between the Rostock and Weybridge M2 proteins.

In summary, the work reported shows that M2 forms a proton-selective channel, which is activated by external pH. This is consistent with the role M2 is perceived to play in virus uncoating and HA maturation.

FIGURE 31: **DIFFERENCES IN ACTIVATION BETWEEN THE ROSTOCK AND WEYBRIDGE M2 PROTEINS**

Production of inward and outward currents by M2-39 and R4-B cells. The cell interior was held at pH6.0 and NMDG-MES/HEPES solutions of various pH values were applied to the cell exterior. The amplitude of the current (I) is shown as a fraction of the amplitude of the total current (I_{max}).

O - M2-39 cell line

▲ - R4-B cell line

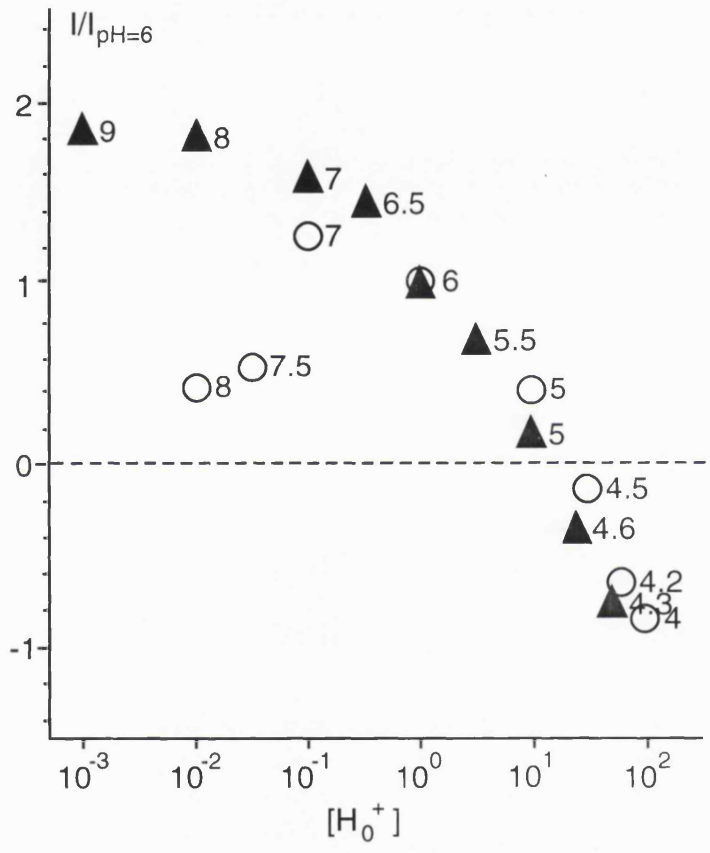
I/I pH=6
2
1
0
-1
9
8
7
6.5
7
6
5.5
8
7.5
5
5
4.5
4.6
4.2
4.3
4
10-3
10-2
10-1
100
101
102
[H0+]

TABLE 8: ACTIVATION PROPERTIES OF M2 MUTANT PROTEINS

M2 Mutant Protein	Activation Property
T65A	Rostock activation
C50S	Activated at a lower pH than Weybridge
V27I/F38L	Weybridge activation
V27I/D44N	Weybridge activation
V27I/F38L/D44N	Rostock activation

The activation properties of M2 mutant proteins were compared with the Rostock and Weybridge wild-type proteins. The cell interior was held at pH6.0 and $NMDG^+$-MES^-/$HEPES^-$ buffer adjusted to various pH values was applied externally and the induced current measured.

DISCUSSION

DISCUSSION

6.1 Introduction

As the M2 protein provides a target for anti-viral therapy, it is of great interest to determine the role of this protein in the influenza A virus replication cycle. The initial intent of this study was to set up an expression system which would both enable the function of M2 to be studied in the absence of viral infection and also be amenable to mutagenesis. It has been shown that it was possible to express the M2 protein in MEL cells and at a level comparable to that in virus-infected MDCK cells. The function of M2 was studied by its effect on intracellular pH using the fluorescent pH probe SNARF-1-AM, its ability to chaperone HA and also its ion conductance properties.

6.2 Expression of the M2 protein in MEL cells

The results show that stable MEL cell lines expressing the influenza A virus M2 protein were produced. Stable chimeric M2/human β-globin mRNA was produced following induction and the mRNA was then translated into M2 protein. Western blot analysis confirmed that the expressed M2 was similar to that produced within the virus-infected MDCK cell, in particular with regard to the formation of dimer and tetramer. M2 protein produced during a viral infection is a palmitoylated phosphoprotein and analysis of the M2 protein expressed in MEL cells confirmed that the protein was post-translationally modified by the addition of palmitate and phosphate. The MEL cell expression system also produced M2 at levels equivalent to that of Weybridge-reassortant virus-infected MDCK cells. Expression of the M2 cDNA increased to a maximum between 4-5 days post-induction and did not seem to have a deleterious effect on MEL cells.

The level of M2 production following induction was not subject to a

significant degree of variation, thereby facilitating reproducible functional analysis of the M2 expressed in MEL cells. Preliminary metabolic [^{35}S] labelling studies revealed that during induction M2 was synthesized at a constant rate. This was surprising as the rate of synthesis of M2 might have been expected to increase during the early stages of induction and to reach a maximum by 3-4 days p.i.. The M2 protein turnover rate may have changed during the induction period which would account for the differences observed between the rates of M2 protein synthesis and accumulation. Pulse-chase studies would therefore be useful to investigate the kinetics of M2 synthesis and breakdown. Inhibition of M2 activity by the addition of 5μM or 50μM amantadine to the cells during induction did not significantly increase the level of M2 production suggesting that expression of M2 was not deleterious to the cells. Adaptation of purification protocols would facilitate the production of purified M2 protein for structural studies e.g. nuclear magnetic resonance (NMR), circular dichroism (CD), crystallization and X-ray studies and incorporation into vesicles for *in vitro* functional analysis of channel activity and ion conductance.

It was therefore concluded that the M2 protein expressed in MEL cells closely resembled the M2 protein produced within a viral infection. This similarity rendered the MEL cell M2 protein suitable for functional studies, including mutagenesis. The expression system was used to study the functional and structural characteristics of a series of transmembrane mutant proteins and also M2 proteins possessing mutations at the sites of post-translational modification.

In addition to structural similarities, the expressed M2 was shown to possess similar functional characteristics to the M2 produced within virus-infected MDCK cells as determined by co-expression of HA and M2 and intracellular pH measurements. Three assays were used to investigate M2 function, namely co-expression of M2 and HA, determination of cytoplasmic pH and

electrophysiological studies on MEL cells expressing M2. These techniques can be used to study aspects of the protein structure which are functionally important and also the structure/activity relationship of M2 in relation to HA transport and maturation.

6.3 Co-expression of HA and M2

Previous experimental evidence (Grambas and Hay, 1992; Grambas *et al.*, 1992) indicated that the Rostock M2 was more active than the Weybridge M2 protein. In addition recombinant viruses have been produced with the Rostock M gene complementing the Weybridge HA gene, but no viable virus has been produced containing the Weybridge M and Rostock HA genes. This suggests that the Weybridge M2 does not have sufficient activity to complement the Rostock HA glycoprotein. As the Weybridge HA undergoes its pH-mediated conformational change some 0.6 pH units lower than the Rostock HA, there is less selective pressure for the Weybridge M2 to be more active. This suggests that co-expression of HA and M2 does provide a system for analysing activity of M2. If the MEL cell expression system could have been used to co-express HA and M2, it would have provided much needed information in respect of the activities of mutant M2 proteins. M2 and HA are co-transported through the TGN (Ciampor *et al.*, 1992b), so mutations within the M2 protein may greatly influence the structural integrity of HA as it progresses through the TGN to the cell surface, in terms of the amount of native and low-pH form of HA produced.

However, MEL cells were successfully infected with influenza virus. Although the cells showed the characteristics of a non-permissive infection, HA was produced at a similar level to virus-infected CEF. There did appear to be some retardation in the rate of cleavage of the HA0 precursor to the HA1 and HA2 polypeptides and very little M1 protein was produced. However influenza virus infection of MEL cells was similar to that of MDCK cells in

terms of the effect of amantadine on HA production. Addition of amantadine to virus-infected MEL cells resulted in HA in the native conformation confined to the TGN whilst the low-pH form of HA was detected on the cell surface. This provides evidence that MEL cells can be used to provide an environment for M2-dependent expression of the HA glycoprotein.

M2-expressing MEL cells were infected with influenza virus to determine whether the expressed M2 was capable of complementing the viral HA. When influenza virus infects cells, a shut-off in host cell protein synthesis occurs. The time taken for this to occur seems to be a feature of both the cell type and the virus type. As MEL cell protein synthesis is not shut-off until a later stage of infection, this is actually of benefit to the co-expression system. If protein synthesis was abolished very early on in infection, the induced M2-expressing MEL cell would be unable to translate its M2/human β-globin mRNA. Although this chimeric mRNA encodes a viral protein, presumably it is recognized as host cell mRNA and will be subject to cleavage of the cap structure and hence degradation in the nucleus. MEL cells in tissue culture do not normally enucleate until the later stages of induction. This would mean that the viral HA could not be co-transported with the MEL cell M2 and no complementation would occur, as the viral HA would be co-transported with its own M2. Further information is required to determine the effect of the MEL cell M2 on the splicing of the viral M gene mRNA. Splicing is normally regulated during the infectious cycle of the virus (Valcárcel *et al.*, 1991; Valcárcel *et al.*, 1993) and is important for virus maturation, as the M1 protein binds to the RNP cores in the infected cell nucleus and inhibits transcription (Hankins *et al.*, 1989; Hankins *et al.*, 1990). If there is a large amount of MEL cell M2 mRNA present in the cytoplasm, or abundant expression of the M2 protein on the cell surface early on in infection, this may interfere with normal splicing events. To investigate the production of viral M2 and the MEL cell expressed M2, the cells could be infected with a recombinant human/avian

virus containing a human M2 protein and an intracellularly cleaved avian HA glycoprotein, from a virus such as Weybridge. Antibodies which do not cross react could then be used to detect both the human and avian forms of M2 to determine the relative amounts of viral and MEL cell M2 produced. [^{35}S] metabolic labelling would also provide an indication of the relative amount of M1 protein produced in M2-expressing MEL cells in comparison with C88 control cells.

MEL cells proved to be non-permissive with respect to vaccinia virus infection. This could be due to lack of the viral receptor on the MEL cell surface. Very little is known about the vaccinia virus receptor, but previously the virus was thought to bind to the epidermal growth factor receptor (Eppstein *et al.*, 1985), as vaccinia virus encodes a protein termed virus growth factor. This viral protein shows structural and functional homology to both epidermal growth factor and transforming growth factor alpha (Blomquist *et al.*, 1984; Stroobant *et al.*, 1985; King *et al.*, 1986). It was thought that after incorporation into the viral membrane, the protein could then target the virus to cellular growth receptors. It has since been reported that this may not now be the case (Hügin and Hauser, 1994). As MEL cells have been transformed with Friend leukaemia virus, this may affect their ability to undergo subsequent infection with other viruses. The lack of productive infection with SFV is probably also due to the reasons mentioned above.

Attempts to produce MEL cell lines which stably expressed HA were unsuccessful. Only very low levels of HA expression were detected. This could have been due to instability of the HA/human β-globin chimeric mRNA and perhaps only a very small proportion was stable enough to undergo translation. During the selection process of transformed cells, there is a possibility that cells which had a higher level of constitutive HA expression were selected against, by the binding of HA to surface sialic acid, resulting in agglutination and cell death. Permeabilization of cells did not increase the

amount of HA detected by ELISA, indicating that the HA glycoprotein was not retained within the transport pathway.

6.4 Intracellular pH measurements

Measurements involving the intracellular fluorescent pH probe SNARF-1-AM confirmed that the M2 protein was responsible for a decrease in intracellular pH. The decrease was comparable to that produced in virus-infected MDCK cells and provided evidence that the expressed M2 was functional. The M2-mediated pH change was similarly inhibitable by 5μM rimantadine or amantadine. Using this assay it was not possible to distinguish differences in activity between different mutant M2 proteins, however a more accurate comparison of M2 activity could perhaps be made by comparing cells at an earlier stage of induction, when only a small amount of M2 has been synthesized. In view of the small pH change produced within MEL cells, this particular approach may not be viable, but the assay was useful for determining whether a particular M2 protein was functional. Leakage of the fluorescent dye from the cells was the main problem encountered during the experiments. Dye leakage has the effect of altering the fluorescence intensity ratio to include the contribution of the external SNARF-1. It is well documented that SNARF-1 is more fluorescent in free solution, as quenching occurs within the cell cytoplasm. One way of circumventing the problem of probe leakage would be to use a microspectrofluorimetry technique. Changes in intracellular pH within murine B lymphocytes have been studied by coupling a microscope with a spectrofluorimeter so that fluorescence spectra can be obtained for single cells (Seksek *et al.*, 1991). This method bypassed the problems of gross probe leakage from a population of cells. FACS analysis of MEL cells loaded with SNARF-1 might also alleviate problems associated with dye leakage from the cells.

6.5 Ion channel activity of the M2 protein

The results reported here provide evidence that the M2 protein is responsible for the decrease in intracellular pH during virus-infection and that it has ion conductance properties consistent with the transfer of protons. Data obtained by Schroeder *et al.*, (1994) using M2 protein purified from *Spodoptera frugiperda* cells and incorporated into vesicles, is consistent with the proposal that M2 forms a proton channel. This provides evidence that the M2 protein expressed in MEL cells is not modifying a cellular channel. On application of a pH gradient a current was induced in MEL cells expressing the M2 protein. The current induced was also specifically inhibited by the anti-M2 drugs amantadine and rimantadine. That the current is due to a proton conductance is confirmed by the fact that at zero membrane potential the direction and amplitude of the current were dependent on the proton concentration gradient and the reversal potential, i.e. the potential around which the current changes sign, was equal to the proton equilibrium potential. The reversal potential also did not change upon the addition of other small ions such as Cl^-, K^+ or Na^+. Other workers have also used this method to determine the ionic specificity of mutants of the acetyl-choline receptor (Galzi *et al.*, 1992). Substitution of chloride ions with gluconate or methane sulphonate resulted in a shift of the reversal potential, indicating that the current was almost exclusively carried by chloride ions.

Studies on M2 expressed in *Xenopus laevis* oocytes (Pinto and Lamb, 1992) suggested that M2 was a pH-activated cation channel, with high permeability for Na^+ ions. Similar conclusions were also obtained when the M2 protein was expressed in CV-1 cells (Wang *et al.*, 1994) and also incorporated into lipid bilayers (Tosteson *et al.*, 1994). The permeability to Na^+ is a little difficult to reconcile in terms of the biological function of M2. There seems to be no immediately obvious reason why there should be a need for permeability to Na^+. Data obtained from MEL cells does not support

such an Na^+ permeability and when both inward and outward currents were measured in either the presence or absence of other small ions, the reversal potential did not change.

6.6 Activation of the M2 protein

The Weybridge and Rostock M2 proteins have been shown to possess different activation characteristics. Outward currents produced by the Rostock M2 increased gradually in response to an increase in external pH (internal pH held at pH6.0). Increasing the external pH from pH4.2 to pH9.0 both changed the direction of and increased the proton gradient, so a concomitant increase in outward current was not unexpected. The maximum current was produced at an external pH between pH9.0-9.5, after which no further increase was detected. In contrast, the outward currents produced by the Weybridge M2 protein, in response to an increased external pH, actually decreased with increasing external pH. This difference in activation allowed MEL cells expressing various mutant M2 protein molecules to be characterized and compared with the Weybridge and Rostock wild types. To make quantitative comparisons between cell lines expressing different M2 proteins the results need to be normalized so that equal numbers of channels are compared. FACS analysis of "beads" with a known number of FITC sites can be used to relate levels of fluorescence to number of antibody molecules bound. This technique would allow an estimation of the number of M2 molecules per MEL cell to be made assuming that the anti-M2 antibody binds to different M2 proteins with the same specificity. Ideally single channel measurements would allow more accurate comparisons to be drawn between cell lines and indeed between different cells expressing a particular M2 protein. Unfortunately, the current obtained was too small to allow single channel measurements to be made.

Preliminary data showed that the Weybridge mutant M2 protein with

the substitution V27I possessed similar activation characteristics to the wild type protein, as did the Weybridge mutant M2 protein with the substitution V27I/F38L. The outward currents decreased in response to an increasing external pH. Only after substitution of all three transmembrane residues did the Weybridge mutant M2 protein, V27I/F38L/D44N, gain activation properties which resembled those associated with the Rostock M2 and showed an increasing outward current in response to an increasing external pH. Three amino acids had to be altered to change the activation property of the M2 protein from Weybridge to Rostock. To change the activation property from Rostock to Weybridge the converse was true and a change in one of the three amino acids was sufficient to convert the activation from that of Rostock to Weybridge. The change in activation property of Rostock to Weybridge following one amino acid substitution also emphasizes the prevalence of the Weybridge wild type.

The activation properties of M2 proteins possessing mutations at the sites of post-translational modification were also studied, to determine the importance of these modifications for channel function. The site of phosphorylation of the Rostock M2 protein had previously been shown to be threonine 65 (R. Sugrue, personal communication), however replacement of threonine 65 with alanine had no effect on the ion conductance properties of the protein and the protein was in fact shown to be phosphorylated. As the adjacent serine residue was determined to be the main site of phosphorylation of the A/Udorn/72 M2 protein (Holsinger *et al.*, 1995) more work is needed to verify that threonine 65 is the site of phosphorylation for the Rostock and Weybridge M2 proteins. In the absence of threonine 65 the adjacent serine residue or another residue may be phosphorylated instead, so an M2 mutant protein with both the threonine and serine residues substituted may need to be produced to determine the role of phosphorylation on channel function. Previously phosphorylation was shown to be unnecessary for

channel function of M2 expressed in *Xenopus laevis* oocytes (Pinto and Lamb, 1992). Preliminary data indicated that the Weybridge mutant C50S lacking a palmitate group was activated at a lower pH than the Weybridge wild type protein. The significance of this is as yet unknown. Not all viruses possess a palmitoylated M2 protein, particularly recent H3N8 equine viruses, so palmitoylation may not be essential for M2 function.

The significance of the activation/deactivation characteristics of the Weybridge virus M2 is as yet unknown. The activation characteristics of the Weybridge M2 protein may serve to protect the virus interior from alkalinization in the event of the virus being subject to an alkaline environment. The RNP core would be protected and hence infectivity of the virus retained. This hypothesis could be tested by exposing influenza virus to a range of solutions with alkaline pH and then measuring the subsequent infectivity of the virus by plaque assay, giving an indication of the susceptibility of the virus to pH. It should be considered that the electrophysiological measurements were performed at room temperature, rather than at 37°C and it is unknown what effect this temperature difference might have on the activity of the M2 protein. It would be useful if data could be acquired at 37°C to investigate the possibility of temperature effects on M2 function.

6.7 Inhibition of M2-specific currents

That the current is M2-specific has been confirmed by the addition of amantadine or rimantadine. M2 activity was shown to be sensitive to amantadine, whereas the inward current induced in MEL cells expressing the drug-resistant mutant G34E was not. Ion conductance measurements on MEL cells did not produce reversible inhibition of M2 function. Inhibition of the M2-specific current was only obtained when amantadine was applied externally and blocking did not occur when the drug was present in the patch

pipette. As yet the mechanism of inhibition of M2 by amantadine and rimantadine is still unknown. Mutations in drug resistant viruses occur between amino acids 26 to 34 and these mutations tend to result in less hydrophobicity within the transmembrane domain of the M2 protein. Binding of drug could occur within the channel pore itself and can be described as a "cork in a bottle". Alternatively, there may be some allosteric mechanism, whereby the binding of the inhibitor stabilizes the closed conformation of the channel and makes opening less likely. Previous work involving the study of a 25 residue peptide incorporating the transmembrane domain of M2 has located the binding site of amantadine to a region between residues 27 to 31 (Duff and Ashley, 1992; Duff, 1994). The 25 residue peptide produced a single channel current of 0.5pA and the current could be inhibited with amantadine present on either side of the membrane. Inhibition of the M2 protein was also shown to be reversible. This is in contrast with results obtained on M2-expressing MEL cells. The results from the peptide measurements may be misleading as they ignore the electrostatic interaction of the transmembrane domain with any other part of the protein. This may affect the overall structure of the protein, which in turn will affect the functional properties of the ion channel. The fact that amantadine inhibits M2 only from the external region, is consistent with data obtained from the study of previously characterized channel blockers. Some calcium channel blockers inhibit only from the intracellular side of the channel (Hille, 1992). As inhibition of M2 by amantadine in MEL cells was shown to be irreversible, this suggests that amantadine is actually interacting with a particular region of the M2 protein and possibly inducing a conformational change, rather than acting as a "passive" channel blocker. If the latter situation was the case, amantadine would be free to diffuse out of the channel and following extensive washing, channel function would be restored.

Sansom and Kerr (1993), postulated that the helices which form the

M2 channel may be tilted. This characteristic would allow amantadine to enter the channel and to interact with residues at the N-terminal region of the pore. If the pore tapered, the drug would not be able to move through to the C-terminal region due to steric inhibition. Cyclo-octylamine has been shown to be an efficient inhibitor of M2 function, whereas cyclo-pentylamine which is a smaller molecule and is presumably free to diffuse out of the channel is not (Hay *et al.*, 1985).

Some of the mutations within the transmembrane domain of the M2 protein which result in drug resistance, increase the activity of the M2 protein relative to the wild type, whereas other mutations result in a decrease in activity (Grambas *et al.*, 1992; Grambas and Hay, 1992). It is possible that the mutations alter the structure of the pore so that amantadine is unable to bind. If amantadine inhibits M2 function by binding to a "pocket", the mutation conferring drug resistance may change the structure so that the binding site no longer remains. Where the activity of the mutant protein is reduced as in the Rostock glycine 34 to glutamate substitution, the structure may be changed so that either there are unfavourable electrostatic interactions within the pore which perhaps cause it to narrow, thus allowing less protons to move through. Alternatively, structural alterations can exert conformational changes which extend over some distance. From the available data, it seems likely that there is a direct interaction of amantadine with the channel itself, rather than an interaction at an external allosteric binding site. However these mechanisms are purely speculative and much work remains to be done before the exact process can be elucidated.

6.8 Structural differences between Weybridge and Rostock M2 proteins

There are six amino acid differences between the Weybridge and Rostock M2 proteins. Three changes occur within the transmembrane domain. Investigation of mutations within the transmembrane domain of the

M2 protein revealed that the three differences in amino acid residues between the Rostock and Weybridge M2 proteins played a role in determining the thermal stability of the tetramer. Converting all three amino acid residues from the Weybridge to Rostock sequence, (V27I/F38L/D44N) resulted in an M2 protein with structural characteristics resembling the Rostock wild type. This mutant M2 protein has also been shown to possess functional properties which are similar to the Rostock wild-type protein. Mutant M2 proteins with the alterations V27I and V27I/D44N were comparable with the Weybridge M2 protein in respect of thermal stability of the tetramer indicating that these substitutions were not sufficient to result in destabilization of the M2 tetramer. However, M2 proteins with the substitutions F38L and V27I/F38L were less stable than the Weybridge wild type protein, suggesting that the phenylalanine residue at position 38 may play a role in stabilizing the Weybridge tetramer. Ion conductance measurements indicated that there was some correlation between structure and activation properties of the M2 mutant proteins.

Mutations in the external N-terminal domain of the Weybridge M2 protein were shown to have little effect on the thermal stability of the tetramer as the mutants exhibited Weybridge wild-type thermal characteristics. These data indicate that the N-terminal region of the M2 protein is less important than the transmembrane domain in maintaining the structural integrity of the tetramer.

If the structures of the amino acids are compared, there are some interesting observations to be made. Valine and isoleucine both have non-polar side chains, with isoleucine possessing an additional CH_2 group. Both amino acids are similar in size and structure, so substitution of valine with isoleucine will probably not result in a gross alteration in tetramer structure. The replacement of aspartic acid with asparagine might be expected to result in some structural alterations, due to the difference in pKa values for the

amino acids (3.86 and 8.80 respectively). Charged residues tend to influence the structure adjacent residues adopt due to electrostatic effects. However, as both amino acids have side chains of a similar size, replacing aspartic acid with asparagine may not disrupt the structure of the α-helix sufficiently to cause tetramer destabilization. The greatest difference in amino acid structure occurs with the mutation F38L. Phenylalanine possesses a bulky phenyl-ring side chain, in contrast with leucine which has a smaller non-polar aliphatic side chain. Therefore, it is quite likely that the difference in size will result in a change in structural properties of the M2 protein. The histidine residue at position 37 has been identified as playing a role in the regulation of M2 ion channel activity (Pinto and Lamb, 1992). It is possible that the charged histidine residue may interact with the adjacent phenylalanine residue. The delocalization of *pi* electrons in the phenyl ring may play a role in stabilizing the charged histidine residue. There may also be an interaction with the tryptophan residue at position 41. Hydrophobic groups are thermodynamically more stable when they are clustered together and Van der Waals bonds between tightly packed hydrophobic side chains can lead to increased stability of a protein. In addition, hydrogen bonding and steric repulsion also contribute to the three-dimensional protein structure. If the structure of the Rostock M2 protein is held together less tightly than the Weybridge protein this may account for the higher activity of the protein and facilitate increased ion transport through the channel pore.

6.9 Conclusions

The work reported here shows that the MEL cell expression system was suitable for the expression and study of the M2 protein of influenza A virus. The expressed M2 was similar to that produced within virus-infected MDCK cells, in respect of its structural and functional characteristics and was inhibited by the action of amantadine or rimantadine. The expressed M2 was

also shown to be responsible for the decrease in intracellular pH during virus infection and in modifying the transmembrane pH gradients of the TGN during virus maturation.

M2 expressed within MEL cells formed a proton-selective channel which was regulated by external pH. The reversal potential did not change upon the addition of other ions confirming that protons were the permeant species. This proton-selectivity of M2 reflects its perceived role in protonating the virion interior during virus uncoating aswell as its physiological role in modifying transmembrane pH gradients of the TGN or the plasma membrane of virus-infected cells. The low intrinsic channel activity of MEL cells makes them particularly suitable for the expression and study of an ion channel and this expression system may also be useful for screening potential anti-viral compounds.

The MEL cell system also proved to be amenable to the expression and characterization of mutant M2 proteins, thus providing a suitable environment for the study of the structural and functional properties of M2. Structure/activity studies identified three amino acids in the transmembrane domain which were important in determining the activation characteristics and structural stability of the tetramer.

REFERENCES

REFERENCES

Apostolov, K. and Flewitt, T.H. (1969). Further observations on the structure of influenza viruses A and C. J. Gen. Virol. **4**, 365-370.

Appleyard, G. (1977). Amantadine-resistance as a genetic marker for influenza viruses. J. Gen. Virol. **36**, 249-255.

Arcangeli, A., Wanke, E., Olivotto, M., Camagni, S., and Ferrona, A. (1987). Three types of ion channels are present on the plasma membrane of Friend erythroleukaemia cells. Biochem. and Biophys. Res. Com. **146**, No. 3: 1450-1457.

Basak, S., Tomana, M. and Compans, R.W. (1985). Sialic acid is incorporated into influenza virus hemagglutinin glycoproteins in the absence of viral neuraminidase. Virus Res. **2**, 61-68.

Bassnet, S., Ranisch, L. and Beebe, D.C. (1990). Intracellular pH measurement using single excitation-dual emission fluorescence ratios. Am. J. Physiol. **258**, C171-178.

Bean, W.J., Threlkeld, S.C. and Webster, R.G. (1989). Biologic potential of amantadine-resistant influenza A virus in an avian model. J. Infect. Dis. **159**, 1050-1056.

Beaton, A.R. and Krug, R.M. (1986). Transcription antitermination during influenza viral template RNA synthesis requires the nucleocapsid protein and the absence of a 5' capped end. Proc. Natl. Acad. Sci. USA **83**, 6282-6286.

Belshe, R.B., Hall-Smith, M., Hall, C.B., Betts, R. and Hay, A.J. (1988). Genetic basis of resistance to rimantadine emerging during treatment of influenza virus infection. J. Virol. **62**, 1508-1512.

Black, R.A., Rota, P.A., Gorodkova, N., Cramer, A., Klenk, H-D. and Kendal, A.P. (1993). Production of the M2 protein of influenza A virus in insect cells is enhanced in the presence of amantadine. J. Gen. Virol. **74**, 1673-1677.

Blank, P.S., Silverman, H.S., Chung, O.Y., Hogue, B.A., Stern, M.D., Hansford, R.G., Lakatta, E.G. and Capogrossi, M.C. (1992). Cytosolic pH measurements in single cardiac myocytes using carboxy-seminapthorhodafluor-1. Am. J. Physiol. **263**, H276-284.

Blok, J., Air, G., Laver, W., Ward, C., Lilley, G., Woods, E., Roxburgh, C. and Inglis, A. (1982). Studies on the size, chemical composition and partial sequence of the neuraminidase (NA) from type A influenza viruses showed that the N-terminal region of the NA is not processed and serves to anchor the NA in the viral membrane. Virology **119**, 109-121.

Blomquist, M.C., Hunt, L.T. and Barker, W.C. (1984). Vaccinia virus 19-kilodalton protein: relationship to several mammalian proteins, including two growth factors. Proc. Natl. Acad. Sci. USA **81**, 7363-7367.

Bosch, F.X., Hay, A.J. and Skehel, J.J. (1978). RNA and protein synthesis in a permissive and an abortive influenza virus infection. In "Negative Strand viruses and the Host Cell" (Mahy, B.W.J. and Barry, R.D. eds) pp465-474, Academic Press, London, New York, San Francisco.

Both, G.W. and Sleigh, M.J. (1981). Conservation and variation in the hemagglutinins of Hong Kong subtype influenza viruses during antigenic drift. J. Virol. **39**, 663-672.

Bouloy, M., Plotch, S.J. and Krug, R.M. (1978). Globin mRNAs are primers for the transcription of influenza viral RNA *in vitro*. Proc. Natl. Acad. Sci. USA **75**, 4886-4890.

Bouloy, M., Morgan, M.A., Shatkin, A.J. and Krug, R.M. (1979). Cap and internal nucleotides of reovirus mRNA primers are incorporated into influenza viral complementary RNA during transcription *in vitro*. J. Virol. **32**, 895-904.

Braam, J., Ulmanen, I. and Krug, R.M. (1983). Molecular model of a eukaryotic transcription complex: functions and movements of influenza P proteins during capped RNA-primed transcription. Cell **34**, 609-618.

Bron, R., Kendal, A.P., Klenk, H-D. and Wilschut, J. (1993). Role of the M2 protein in influenza virus membrane fusion: Effects of amantadine and monensin on fusion kinetics. Virology **195**, 808-811.

Bukrinskaya, A.G., Vorkunova, N.K., Kornilayeva, G.V., Narmanbetova, R.A. and Vorkunova, G.K. (1982). Influenza virus uncoating in infected cells and effects of rimantadine. J. Gen. Virol. **60**, 49-59.

Bullough, P.A., Hughson, F.M., Skehel, J.J. and Wiley, D.C. (1994). Structure of influenza haemagglutinin at the pH of membrane fusion. Nature **371**, 37-43.

Buonaguirio, D.A., Krystal, M., Palese, P., DeBorde, D.C. and Maassab, H.F. (1984). Analysis of an influenza A virus mutant with a deletion in the NS segment. J. Virol. **49**, 418-425.

Castrucci, M.R. and Kawaoka, Y. (1993). Biologic importance of neuraminidase stalk length in influenza A virus. J. Virol. **67**, 759-764.

Ciampor, F., Bayley, P.M., Nermut, M.V., Hirst, E.M.A., Sugrue, R.J. and Hay, A.J. (1992a). Evidence that the amantadine-induced M2 mediated conversion of influenza virus haemaglutinin to the low pH conformation occurs in an acidic *trans* Golgi compartment. Virology **88**, 14-24.

Ciampor, F., Thompson, C.A., Grambas, S., Hay, A.J. (1992b). Regulation of pH by the M2 protein of influenza A viruses. Virus Res. **22**, 247-258.

Compans, R.W. and Dimmock, N.J. (1969). An electron microscopic study of single cycle infection of chick embryo fibroblasts by influenza virus. Virology **39**, 499-515.

Compans, R.W., Klenk, H-D., Caliguiri, L.A. and Choppin, P.W. (1970). Influenza virus proteins. I. Analysis of polypeptides of the virion and identification of spike glycoproteins. Virology **42**, 880-889.

Compans, R.W., Content, J. and Duesberg, P.H. (1972). Structure of the ribonucleoprotein of influenza virus. J. Virol. **10**, 795-800.

Daniels, R.S., Douglas, A.R., Skehel, J.J., Waterfield, M.D., Wilson, I.A. and Wiley, D.C. (1983a). Studies of the influenza virus hemagglutinin in the pH5 conformation. In "The origin of pandemic viruses" (Laver, W.G. ed), pp1-7. Elsevier, New York.

Daniels, R.S., Douglas, A.R., Skehel, J.J. and Wiley, D.C. (1983b). Analysis of the antigenicity of influenza haemagglutinin at the pH optimum for virus-mediated fusion. J. Gen. Virol. **64**, 1657-1661.

Duff, K.C. and Ashley, R.H. (1992). The transmembrane domain of influenza A M2 protein forms amantadine-sensitive proton channels in planar lipid bilayers. Virology **190**, 485-489.

Duff, K.C., Gilchrist, P.J., Saxena, A.M. and Bradshaw, J.P. (1994). Neutron diffraction reveals the site of amantadine blockade in the influenza A M2 ion channel. Virology **202**, 287-292.

Enami, K., Qiao, Y., Fukuda, R. and Enami, M. (1993). An influenza virus temperature-sensitive mutant defective in the nuclear-cytoplasmic transport of the negative-sense viral RNAs. Virology **194**, 822-827.

Eppstein, D.A., Marsh, Y.V., Schreiber, A.B., Newman, S.R., Todaro, G.J. and Nestor Jr., J.J. (1985). Epidermal growth factor occupancy inhibits vaccinia virus infection. Nature **318**, 663-665.

Fields, S., and Winter, G. (1981). Structure of the neuraminidase gene in human influenza virus A/PR/8/34. Nature **290**, 213-217.

Fortes, P., Beloso, A. and Ortin, J. (1994). Influenza virus NS1 protein inhibits pre-mRNA splicing and blocks mRNA nucleocytoplasmic transport. EMBO J. **13**, 704-712.

Fraser, P.J., and Curtis, P.J. (1987). Specific pattern of gene expression during induction of mouse erythroleukemia cells. Genes Dev. **1**, 855-861.

Galzi, J-L., Devillers-Thiéry, A., Hussy, N., Bertrand, S., Changeux, J-P. and Bertrand, D. (1992). Mutations in the channel domain of a neuronal nicotinic receptor convert ion selectivity from cationic to anionic. Nature **359**, 500-505.

Godley, L., Pfeifer, J., Steinhauer, D., Ely, B., Shaw, G., Kaufmann, R., Suchanek, E., Pabo, C., Skehel, J.J., Wiley, D.C. and Wharton, S. (1992). Introduction of intersubunit disulfide bonds in the membrane-distal region of the influenza hemagglutinin abolishes membrane fusion activity. Cell **68**, 635-645.

Gottschalk, A. (1958). Neuraminidase: Its substrate and mode of action. Adv. Enzymol. **20**, 135-145.

Gottschalk, A. (1972). Historical introduction in "glycoproteins, their composition, structure and function" (Gottschalk, A. ed), pp2-3. Elsevier, Amsterdam.

Grambas, S. and Hay A.J. (1992). Maturation of influenza A virus haemagglutinin-Estimates of the pH encountered during transport and its regulation by the M2 protein. Virology **190**, 11-18.

Grambas, S., Bennett, M.S. and Hay, A.J. (1992). Influence of amantadine resistance mutations on the pH regulatory function of the M2 protein of influenza A viruses. Virology **191**, 541-549.

Gregoriades, A. (1973). The membrane protein of influenza virus: extraction from virus and infected cells with acidic chloroform-methanol. Virology **54**, 369-383.

Griffin, J.A. and Compans, R.W. (1979). Effect of cytochalasin B on the maturation of enveloped viruses. J. Exp. Med. **150**, 379-391.

Griffin, J.A., Basak, S. and Compans, R.W. (1983). Effects of hexose starvation and the role of sialic acid in influenza virus release. Virology **125**, 324-334.

Hanahan, D. (1983). Studies on transformation of *Escherichia coli* with plasmids. J. Mol. Biol. **166**, 557-580.

Hankins, R.W., Nagata, K., Buchner, D.J., Popple, S.S. and Ishihama, A. (1989). Monoclonal antibody analysis of influenza virus matrix protein epitopes involved in transcription inhibition. Virus Genes **3**, 111-126.

Hankins, R.W., Nagata, K., Kato, A. and Ishihama, A. (1990). Mechanism of influenza virus transcription inhibition by matrix (M1) protein. Res. Virol. **141**, 305-314.

Haslam, E.A., Hampson, A.W., Radiskevics, I. and White, D.O. (1970). The polypeptides of influenza virus. II. Interruptions of polyacrylamide gel electrophoresis patterns. Virology **42**, 555-565.

Hatada, E., Takizawa, T. and Fukada, R. (1992). Specific binding of influenza A virus NS1 protein to the virus minus-sense RNA *in vitro*. J. Gen. Virol. **73**, 17-25.

Hay, A.J., Abraham, G., Skehel, J.J., Smith, J.J., Smith, J. and Fellner, P. (1977a). Influenza messenger RNAs are incomplete transcripts of genome RNAs. Nucl. Acids Res. **4**, 4197-4209.

Hay, A.J., Lomnizi, B., Bellamy, A. and Skehel, J.J. (1977b). Transcription of the influenza virus genome. Virology **83**, 337-355.

Hay, A.J., Kennedy, N.T.C., Skehel, J.J. and Appleyard, G. (1979). The matrix protein gene determines amantadine-sensitivity of influenza viruses. J. Gen. Virol. **42,** 189-191.

Hay, A.J., Skehel, J.J. and McCauley, J. (1980). Structure and synthesis of complementary RNAs. Philosophical Transactions of the Royal Society of London Biological Sciencies, Series B **288,** 341-348.

Hay, A.J., Skehel, J.J. and McCauley, J. (1982). Characterization of influenza virus complete transcripts. Virology **116,** 517-522.

Hay, A.J., Wolstenholme, A.J., Skehel, J.J. and Smith, M.H. (1985). The molecular basis of the specific anti-influenza action of amantadine. EMBO J. **4,** 3021-3024.

Hay, A.J., Zambon, M.C., Wolstenholme, A.J., Skehel, J.J. and Smith, M.H. (1986). Molecular basis of resistance of influenza A viruses to amantadine. J. Antimicrob. Chem. **18,** (Suppl. B), 19-29.

Hay, A.J. (1989). The mechanism of action of amantadine and rimantadine against influenza viruses. In Concepts in Viral Pathogenesis III, (Notkins, A.L. and Oldstone, M.B.A. eds), pp361-367.

Hay, A.J. (1992). The action of adamantamines against influenza A viruses: inhibition of the M2 ion channel protein. Semin. Virol. **3,** 21-30.

Hay, A.J., Thompson, C.A., Geraghty, F.M., Hayhurst, A., Grambas, S. and Bennett, M, (1993). The role of the M2 protein in influenza A virus infection. In "Options for the control of influenza II" (Hannoun, C., Kendal, A.P., Klenk, H-D. and Ruben, F.C. eds), pp281-288.

Hayden, F.G., Belshe, R.B., Clover, R.D., Hay, A.J., Oakes, M.G. and Soo, W. (1989). Emergence and apparent transmission of rimantadine-resistant influenza A virus in families. N. Engl. J. Med. **321,** 1696-1702.

Hille, B. (1992). Ionic channels of excitable membranes. Sinauer Associates Inc., Sunderland, Mass.

Holland, J., Spindler, K, Horodyski, F., Grabau, E., Nichol, S. and VandePol, S. (1982). Rapid evolution of RNA genomes. Science **215,** 1577-1585.

Holsinger, L.J. and Lamb, R.A. (1991). Influenza virus M2 integral membrane protein is a homotetramer stabilized by formation of disulfide bonds. Virology **183,** 32-43.

Holsinger, L.J., Shaughnessy, M.A., Micko, A., Pinto, L.H. and Lamb, R.A. (1995). Analysis of the post-translational modifications of the influenza virus M2 protein. J. Virol. **69,** 1219-1225.

Horisberger, M.A. (1980). The large P proteins of influenza A viruses are composed of one acidic and two basic polypeptides. Virology **107,** 302-305.

Houck, P., Hemphill, M., LaCroix, S., Hirsch, D. and Cox, N. (1995). Amantadine-resistant influenza A in nursing homes. Arch. Intern. Med. **155,** 533-537.

Hoyle, L. and Davies, S.P. (1961). Amino acid composition of the protein components of influenza virus A. Virology **13,** 53-57.

Hügin, A.W. and Hauser, C. (1994). The epidermal growth factor is not a receptor for vaccinia virus. J. Virol. **68,** 8409-8412.

Inglis, S.C., and Mahy, B.J.W. (1979). Polypeptides specified by the influenza virus genome. III. Control of synthesis in infected cells. Virology **95,** 154-164.

von Itzstein, M., Wu, W-Y., Kok, G.B., Pegg, M.S., Dyason, J.C., Jin, B., van Phan, T., Smythe, M.L., White, H.F., Oliver, S.W., Colman, P.M., Varghese, J.N., Ryan, D.M., Woods, J.M., Bethell, R.C., Hotham, V.J., Cameron, J.M. and Penn, C.R. (1993). Rational design of potent sialidase-based inhibitors of influenza virus replication. Nature **363,** 418-423.

Kawaoka, Y., Krouss, S. and Webster, R.G. (1989). Avian-to-human transmission of the PB1 gene of influenza A viruses in 1957 and 1968 pandemics. J. Virol. **63,** 4603-4608.

Kendal., A.P. and Klenk, H-D. (1991). Amantadine inhibits an early, M2 protein-dependent event in the replication cycle of avian influenza (H7) viruses. Arch. Virol. **119,** 265-273.

King, C.S., Cooper, J.A., Moss, B. and Twardzik, D.R. (1986). Vaccinia virus growth factor stimulates tyrosine protein kinase activity of A431 cell epidermal growth factor receptors. Mol. Cell. Biol. **6,** 332-336.

Klenk, H-D., Rott, R., Orlich, M. and Blödorn, J. (1975). Activation of influenza A viruses by trypsin treatment. Virology **68,** 426-439.

Kollias, G., Wrighton, N., Hurst, J., and Grosveld, F. (1986). Regulated expression of human $^{A}\gamma$-, β-, and hybrid γβ-globin genes in transgenic mice: manipulation of the developmental expression patterns. Cell **46,** 89-94.

Krishtal, O.A. and Pidoplichko, V.I. (1980). A receptor for protons in the nerve cell membrane. Neuroscience **5,** 2325-2327.

Krug, R.M., Broni, B.B and Bouloy, M. (1979). Are the 5' ends of influenza viral mRNAs synthesized *in vivo* donated by host mRNAs? Cell **18,** 329-334.

Laemmli, U.K. (1970). Cleavage of structural proteins during the assembly of the head of bacteriophage T4. Nature **227,** 680-685.

Lamb, R.A., Lai, C-J. and Choppin, P.W. (1981). Sequences of mRNAs derived from genome RNA segment 7 of influenza virus: colinear and interrupted mRNA's code for overlapping proteins. Proc. Natl. Acad. Sci. USA **78,** 4170-4174.

Lamb, R.A., Zebedee, S.L. and Richardson, R.D. (1985). Influenza virus M2 protein is an integral membrane protein expressed on the infected-cell surface. Cell **40,** 627-633.

Laver, W.G. and Valentine, R.C. (1969). Morphology of the isolated hemagglutinin and neuraminidase subunits of influenza viruses. Virology **38,** 105-119.

Lazarowitz, S.G., Compans, R.W. and Choppin, P.W. (1973). Proteolytic cleavage of the hemagglutinin polypeptide of influenza virus. Function of the uncleaved polypeptide HA. Virology **52,** 199-212.

Liljeström, P. and Garoff, H. (1991). A new generation of animal cell expression vectors based on the Semliki Forest virus replicon. Biotechnology Vol **9,** 1356-1361.

Lohmeyer, J., Talens, L.T. and Klenk, H-D. (1979). The molecular basis of influenza virus pathogenicity. Adv. Virus Res. **34,** 247-281.

Lubeck, M.D., Schulman, J.L. and Palese, P. (1978). Susceptibility of influenza A viruses to amantadine is influenced by the gene coding for M protein. J. Virol. **28,** 710-716.

Marks, P.A. and Rifkind, R.A. (1978). Erythroleukemic differentiation. Ann. Rev. Biochem. **47,** 419-448.

Martin, K. and Helenius, A. (1991a). Transport of incoming influenza virus nucleocapsids into the nucleus. J. Virol. **65,** 232-244.

Martin, K. and Helenius, A. (1991b). Nuclear transport of influenza virus ribonucleoproteins: the viral matrix protein (M1) promotes export and inhibits import. Cell **67,** 117-130.

Mast, E.E., Harmon, M.W., Gravenstein, S., Ping Wu, S., Arden, N.H., Circo, R., Tyszka, G., Kendal, A.P. and Davis, J.P. (1991). Emergence and possible transmission of amantadine resistant viruses during nursing home outbreaks of influenza A (H3N2). Am. J. Epidem. **134,** 988-997.

Meiklejohn, G., Eickhoff, T.C., Graves, P. and Josephine, I. (1978). Antigenic drift and efficacy of influenza virus vaccines, 1976-1977. J. Infect. Dis. **138,** 618-624.

Meyer, H.M., Hepps, H.E., Parkman, P.D. and Ennis, F.A. (1978). A review of existing vaccines for influenza. Am J. Clinical Path. **70,** 146-152.

Murti, K.G., Webster, R.G. and Jones, I.M. (1988). Localization of RNA polymerases on influenza viral ribonucleoproteins by immunogold labelling. Virology **164,** 562-566.

Naeve, C.W. and Williams, D. (1990). Fatty acids on the A/Japan/305/57 influenza virus hemagglutinin have a role in membrane fusion. EMBO J. **9,** 3857-3866.

Needham, M., Gooding, C., Hudson, K., Antoniou, M., Grosveld, F., and Hollis, M. (1992). LCR/MEL : A versatile system for high-level expression of heterologous proteins in erythroid cells. Nucl. Acids Res. **20,** No. 5, 997-1003.

Ohuchi, M., Cramer, A., Vey, M., Ohuchi, R., Garten, W. and Klenk, H-D. (1994). Rescue of vector-expressed fowl plague virus hemagglutinin in biologically active form by acidotropic agents and co-expressed M2 protein. J. Virol. **68,** 920-926.

Owen, C.S. (1992). Comparison of spectrum shifting intracellular pH probes 5'(and 6')-carboxy-10-dimethylamino-3-hydroxyspiro[7h-benzo[c]xanthene-7, 1'(3'H)-isobenzafuran]-3'-one and 2', 7'-biscarboxyethyl-5(and 6)-carboxyfluorescein. Anal. Biochem. **204,** 65-71.

Palese, P., Tobita, K. and Ueda, M. (1974). Characterization of temperature sensitive influenza virus mutants defective in neuraminidase. Virology **61,** 397-410.

Pinto, L.H., Holsinger, L.J. and Lamb, R.A. (1992). Influenza virus M2 protein has ion channel activity. Cell **69,** 517-528.

Plotch, S.J., Bouloy, M. and Krug, R.M. (1979). Transfer of 5' terminal cap of globin mRNA to influenza viral complementary RNA during transcription *in vitro*. Proc. Natl. Acad. Sci. USA **76,** 1618-1622.

Plotch, S.J., Bouloy, M., Ulmanen, I. and Krug, R.M. (1981). A unique cap(m7GpppXm)-dependent influenza virion endonuclease cleaves capped RNA's to generate the primers that initiate viral RNA transcription. Cell **23,** 847-858.

Pons, M.W. (1975). Influenza virus messenger ribonucleoprotein. Virology **67,** 209-218.

Porterfield, J. (1960). A simple plaque-inhibition test for the study of arthropod-borne viruses. Bulletin of the World Health Organization **22,** 373-380.

Qiu, Y. and Krug, R.M. (1994). The influenza virus NS1 protein is a poly(A)-binding protein that inhibits nuclear export of mRNAs containing poly(A). J. Virol. **68,** 2425-2432.

Richardson, J.C. and Akkina, R.K. (1992). NS2 protein of influenza virus is found in purified virus and phosphorylated in infected cells. Arch. Virol. **116,** 69-80.

Robertson, J.S., Schubert, M. and Lazzarini, R.A. (1981). Polyadenylation sites for influenza virus mRNA. J. Virol. **38,** 157-163.

Rodriguez-Boulan, E. and Sabatini, D.D. (1978). Asymmetric budding of viruses in epithelial monolayers: a model system for study of epithelial polarity. Proc. Natl. Acad. Sci. USA **75,** 5071-5075.

Rodriguez-Boulan, E. and Prendergast, M. (1980). Polarized distribution of viral envelope proteins in the plasma membrane of infected epithelial cells. Cell **20**, 45-54.

Roth, M.G. and Compans, R.W. (1981). Delayed appearance of pseudotypes between vesicular stomatitis virus and influenza virus during mixed infection of MDCK cells. J. Virol. **40**, 848-860.

Roth, M.G., Srinivas, R.V. and Compans, R.W. (1983). Basolateral maturation of retroviruses in polarized epithelial cells. J. Virol. **45**, 1065-1073.

Roth, M.G., Gething, M.J. and Sambrook, J. (1989). Membrane insertion and intracellular transport of influenza virus glycoproteins. In "The influenza viruses" (Krug, R.M. ed), pp219-269. Plenum publishing, New York.

Ruben, F.L. (1987). Prevention and control of influenza: role of vaccine. Am J. Med. **82**, Suppl. 6A, 31-34.

Ruigrok, R.W.H., Aitken, A., Calder, L.J., Martin, S.R., Skehel, J.J., Wharton, S.A., Weis, W. and Wiley, D.C. (1988). Studies on the structure of the influenza virus haemagglutinin at the pH of membrane fusion. J. Gen. Virol. **69**, 2785-2795.

Ruigrok, R.W.H., Hirst, E.M.A. and Hay, A.J. (1991). The specific inhibition of influenza A virus maturation by amantadine: an electron microscopic examination. J. Gen. Virol. **72**, 191-194.

Sansome, M. S. P. and Kerr, I.D. (1993). Influenza virus M2 protein: a molecular modelling study of the ion channel. Prot. Eng. **6**, 65-74.

Schild, G.C., Oxford, J.S. and Newman, R.W. (1979). Evidence for antigenic variation in influenza A nucleoprotein. Virology **93**, 569-573.

Scholtissek, C., Burger, H., Kistner, O. and Shortridge, K.F. (1985). The nucleoprotein as a possible major factor in determining host specificity of influenza H3N2 viruses. Virology **147**, 287-294.

Schroeder, C., Ford, C. M., Wharton, S.A., and Hay, A.J. (1994). Functional reconstitution in lipid vesicles of influenza virus M2 protein expressed by baculovirus: evidence for proton transfer activity. J. Gen. Virol. **75**, 3477-3484.

Schulze, I.T. (1970). The structure of influenza virus. I. The polypeptides of the virion. Virology **42**, 890-904.

Seksek, O., Henry-Toulmé, N., Sureau, F. and Bolard, J. (1991). SNARF-1 as an intracellular pH indicator in laser microspectrofluorometry: a critical assessment. Anal. Biochem. **193**, 49-54.

Shapiro, G.I. and Krug, R.M. (1988). Influenza virus RNA replication *in vitro*: synthesis of viral template RNA's and virion RNA's in the absence of added primer. J. Virol. **62**, 2285-2290.

Shi, L., Summers, D.F., Peng, Q. and Galarza, J.M. (1995). Influenza A virus RNA polymerase subunit PB2 is the endonuclease which cleaves host cell mRNA and functions only as the trimeric enzyme. Virology **208,** 38-47.

Skehel, J.J. and Schild, G.C. (1971). The polypeptide composition of influenza A viruses. Virology **44,** 396-408.

Skehel, J.J. (1972). Polypeptide synthesis in influenza virus-infected cells. Virology **49,** 23-36.

Skehel, J.J., Bayley, P.M., Brown, E.B., Martin, S.R., Waterfield, M.D., White, J.M., Wilson, I.A. and Wiley, D.C. (1982). Changes in the conformation of influenza virus hemagglutinin at the pH optimum of virus-mediated fusion. Proc. Natl. Acad. Sci. USA **79,** 968-972.

Snyder, M.H., Buckler-White, A.J., London, W.T., Tierney, E.L. and Murphy, B.R. (1987). The avian influenza virus nucleoprotein gene and a specific constellation of avian and human virus polymerase genes each specify attenuation of avian-human influenza A/Pintail/79 reassortant viruses for monkeys. J. Virol. **61,** 2857-2863.

Steinhauer, D, A. and Holland, J.J. (1987). Rapid evolution of RNA viruses. Ann. Rev. Microbiol. **41,** 409-433.

Steinhauer, D.A., Wharton, S.A., Skehel, J.J., Wiley, D.C and Hay, A.J. (1991). Amantadine selection of a mutant influenza virus containing an acid-stable hemagglutinin glycoprotein: Evidence for virus-specific regulation of the pH of glycoprotein transport vesicles. Proc. Natl. Acad. Sci. USA **88,** 11525-11529.

Stroobant, P., Rice, A.P., Gullick, W.J., Cheng, D.J., Kerr, I.M. and Waterfield, M.D. (1985). Purification and characterization of vaccina virus growth factor. Cell **42,** 383-393.

Sugrue, R.J., Bahadur, G., Zambon, M.C., Hall-Smith, M., Douglas, A.R. and Hay, A.J. (1990a). Specific structural alteration of the influenza haemagglutinin by amantadine. EMBO J. **9,** 3469-3476.

Sugrue, R.J., Belshe, B.B., and Hay, A.J. (1990b). Palmitoylation of the influenza A virus M2 protein. Virol. **179,** 51-56.

Sugrue, R.J., and Hay, A.J., (1991). Structural characteristics of the M2 protein of influenza A viruses: evidence that it forms a tetrameric channel. Virol. **180,** 617-624.

Takeuchi, K. and Lamb, R.A. (1994). Influenza virus M2 protein ion channel activity stabilizes the native form of fowl plague virus hemagglutinin during intracellular transport. J. Virol. **68,** 911-919.

Thomas, J.A., Bucksbaum, R.N., Zimniak, A. and Racker, E. (1979). Intracellular pH measurement in Ehrlich ascites tumour cells utilizing spectroscopic probes generated in situ. Biochemistry **18,** 2210-2218.

Tian, S.F., Buckler-White, A.J., London, W.T., Reck, L.J., Chanock, R.M. and Murphy, B.R. (1985). Nucleoprotein and membrane protein genes are associated with restriction of replication of influenza A/Mallard/NY/78 virus and its reassortants in squirrel monkey respiratory tract. J. Virol. **53**, 771-775.

Tosteson, M.T., Pinto, L.H., Holsinger, L.J. and Lamb, R.A. (1994). Reconstitution of the influenza virus M2 ion channel in lipid bilayers. J. Membrane Biol. **142**, 117-126.

Ulmanen, I., Broni, B.A. and Krug, R.M. (1981). The role of two of the influenza virus core P proteins in recognizing cap I structures (m7GpppNm) on RNA's and initiating viral RNA transcription. Proc. Natl. Acad. Sci. USA **78**, 7355-7359.

Valcárcel, J., Portela, A. and Ortin, J. (1991). Regulated M1 splicing in influenza virus-infected cells. J. Gen. Virol. **72**, 1301-1308.

Valcárcel, J., Fortes, P. and Ortin, J. (1993). Splicing of influenza virus matrix protein mRNA expressed from a simian virus 40 recombinant. J. Gen. Virol. **74**, 1317-1326.

Van Wyke, K., Hishaw, S., Bean, W. and Webster, R. (1980). Antigenic variation of influenza nucleoprotein detected with monoclonal antibodies. J. Virol. **35**, 24-30.

Varghese, J.N., Laver, W.G. and Colman, P.M. (1983). Structure of the influenza virus glycoprotein antigen neuraminidase at 2.9Å resolution. Nature **303**, 35-40.

Varghese, J.N. and Colman, P.M. (1991). Three dimensional structure of the neuraminidase of influenza virus A/Tokyo/3/67 at 2.2Å resolution. J. Mol. Biol. **221**, 473-486.

Veit, M., Kretzschmar, E., Kuroda, K., Garten, W., Schmidt, M.F.G., Klenk, H-D. and Rott, R. (1990). Site-specific mutagenesis identifies three cysteine residues in the cytoplasmic tail as acylation sites of influenza virus hemagglutinin. J. Virol. **65**, 2491-2500.

Veit, M., Klenk, H-D., Kendal, A., and Rott, R. (1991). The M2 protein of influenza A virus is acylated. J. Gen. Virol. **72**, 1461-1465.

Wang, C., Lamb, R.A. and Pinto, L.H. (1994). Direct measurement of the influenza A virus M2 protein ion channel activity in mammalian cells. Virology **205**, 133-140.

Watowich, S.J., Skehel, J.J. and Wiley, D.C. (1994). Crystal structures of influenza virus hemagglutinin in complex with high affinity receptor analogs. Structure **2**, 719-731.

Webster, R.G., Brown, L.E. and Jackson, D.C. (1983). Changes in the antigenicity of the haemagglutinin molecule of H3 influenza virus at acidic pH. Virology **126**, 587-599.

Weis, W., Brown, J.H., Cusack, S., Paulson, J.C., Skehel, J.J. and Wiley, D.C. (1988). Structure of the influenza virus haemagglutinin complexed with its receptor, sialic acid. Nature **333**, 426-431.

Weis, W.I., Brünger, A.T., Skehel, J.J. and Wiley, D.C. (1990). Refinement of the influenza virus hemagglutinin by simulated annealing. J. Mol. Biol. **212**,: 737-761.

Wharton, S.A., Ruigrok, R.W.H., Martin, S.R., Skehel, J.J., Bayley, P.M., Weis, W. and Wiley, D.C. (1988). Conformational aspects of the acid-induced fusion mechanism of influenza virus hemaglutinin. J. Biol. Chem. **263**, 4474-4480.

Wharton, S.A., Hay, A.J., Sugrue, R.J., Skehel, J.J., Weis, W.I. and Wiley, D.C. (1990). Membrane fusion by influenza viruses and the mechanism of action of amantadine. In "Use of X-ray crystallography in the design of antiviral agents" (Laver, W.G. and Air, G.M. eds), pp1-12, Academic Press, Orlando, FL, USA.

Wharton, S.A., Belshe, R.B., Skehel, J.J. and Hay, A.J. (1994). Role of virion M2 protein in influenza virus uncoating: Specific reduction in the rate of membrane fusion between virus and liposomes by amantadine. J. Gen. Virol. **75**, 945-948.

Wharton, S.A., Calder, L.J., Ruigrok, R.W.H., Skehel, J.J., Steinhauer, D.A. and Wiley, D.C. (1995). Electron microscopy of antibody complexes of influenza virus haemagglutinin in the fusion pH conformation. EMBO J. **14**, 240-246.

White, J.M. and Wilson, I.A. (1987). Anti-peptide antibodies detect steps in a protein conformational change: low-pH activation of the influenza virus hemagglutinin. J. Cell. Biol. **105**, 2887-2896.

Wiley, D.C., Skehel, J.J. and Waterfield, M. (1977). Evidence from studies with a cross-linking reagent that the haemagglutinin of influenza virus is a trimer. Virology **79**, 446-448.

Wiley, D.C. and Skehel, J.J. (1987). The structure and function of the hemagglutinin membrane glycoprotein of the influenza virus. Ann. Rev. Biochem. **56**, 365-394.

Wilson, I.A., Skehel, J.J. and Wiley, D.C. (1981). Structure of the haemagglutinin membrane glycoprotein of influenza virus at 3Å resolution. Nature **289**, 366-373.

Wrigley, N.G., Laver, W.G. and Downie, J.C. (1977). Binding of antibodies to isolated haemagglutinin and neuramindase molecules of influenza virus observed in the electron microscope. J. Mol. Biol. **109**, 405-421.

Yasuda, J., Nakada, S., Kato, A., Toyoda, T. and Ishihama, A. (1993). Molecular assembly of influenza virus: Association of the NS2 protein with virion matrix. Virology **196**, 249-255.

Ye, Z., Pal, R., Fox, J.W. and Wagner, R.R. (1987). Functional and antigenic domains of the matrix (M1) protein of influenza A virus. J. Virol. **61,** 239-246.

Yewdell, J.W., Gerhard, W. and Bachi, T. (1983). Monoclonal anti-haemagglutinin antibodies detect irreversible antigenic alterations that coincide with the acid activation of influenza virus A/PR/8/34-mediated haemolysis. J. Virol. **48,** 239-248.

Zebedee, S.L., Richardson, C.D. and Lamb, R.A. (1985). Characterization of the influenza virus M2 integral membrane protein and expression at the infected cell surface from cloned cDNA. J. Virol. **56,** 502-511.

Zebedee, S.L. and Lamb, R.A. (1988). Influenza A virus M2 protein: monoclonal antibody restriction of virus growth and detection of M2 in virions. J. Virol. **62,** 2762-2772.

Zhirnov, O.P. (1990). Solubilization of matrix protein M1/M from virions occurs at different pH for orthomyxo and paramyxoviruses. Virology **176,** 274-279.

Zlydnikov, D.M., Kubar, O.I., Kovaleva, T.P. and Kamforin, L.E. (1981). Study of rimantadine in the USSR: a review of the literature. Rev. Infect. Dis. **3,** 408-421.

APPENDIX I

M2 proteins

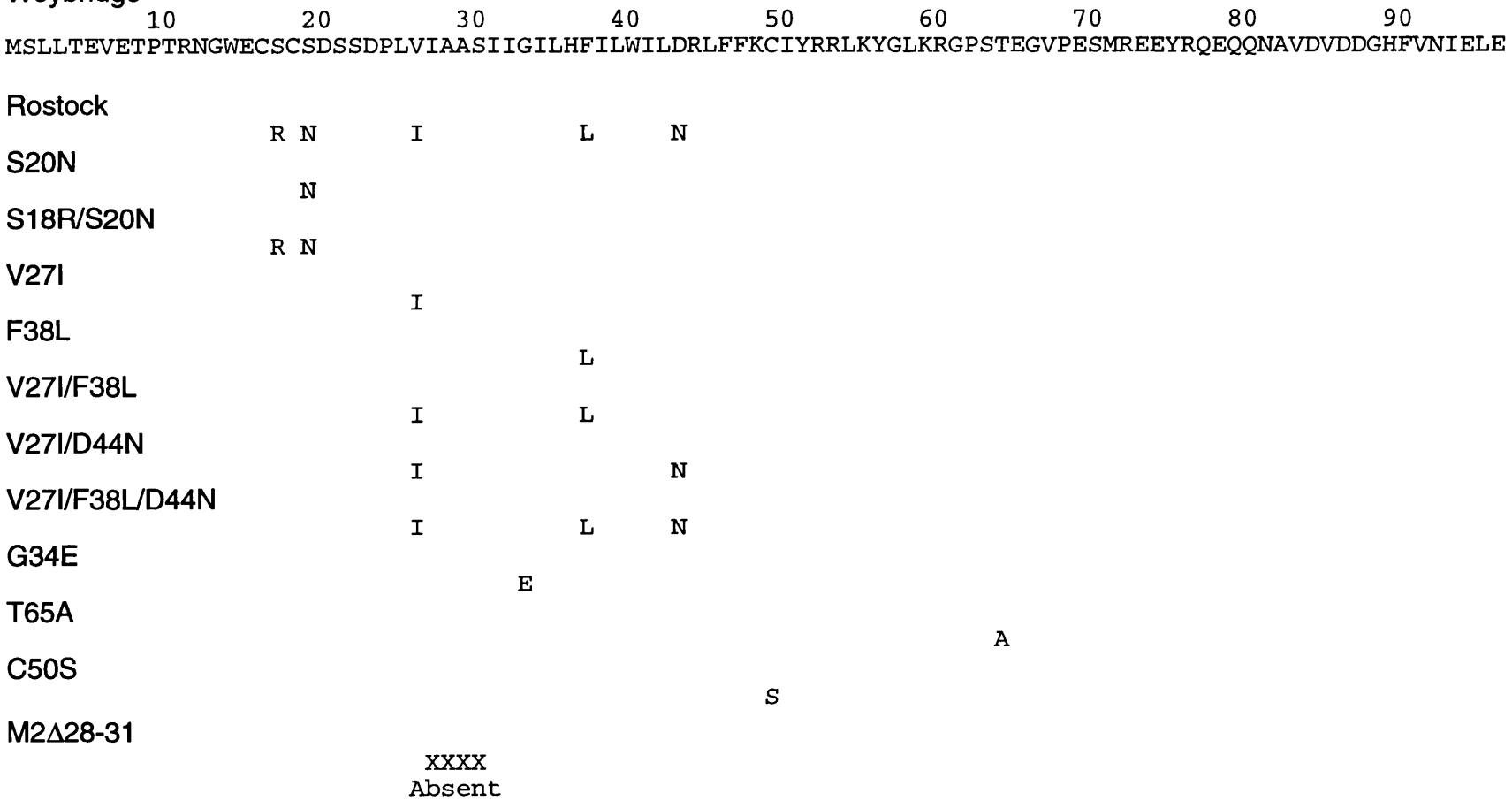

APPENDIX II

Plasmids

1) pEV3 (Needham *et al.*, 1992)
2) pTU.M2W - Weybridge M2 cDNA cloned into a pUC based vector (A.Hayhurst, Thesis, 1995)
3) pUTL.7p1 - Rostock M2 cDNA
4) pUTL.7p2 - S20N mutant
5) pUTL.7p3 - S18R/S20N mutant
6) pUTL.7p4 - V27I mutant
7) pUTL.7p5 - F38L mutant
8) pUTL.7p6 - V27I/F38I mutant
9) pUTL.7p7 - V27I/D44N mutant
10) pUTL.7p8 - V27I/F38L/D44N mutant
11) pUTL.7p9 - G34E mutant
12) pUTL.7p10- T65A mutant
13) pUTL.7p11- C50S mutant
14) pCS - A derivative of pVLM2 (Schroeder *et al.*, 1994)
15) pmal.pntr - Bacterial expression plasmid (A.Hayhurst, unpublished results)
16) pHAr - pUC based plasmid containg Rostock HA cDNA. The cDNA was obtained following RT-PCR of virus-infected CEF.